Nonlinear Interaction of an Intense Ultra-short Pulse Laser with Magnetized Plasma

A thesis

submitted for the award of the

Doctor of Philosophy

Degree in

Physics

(Faculty of Science)

to the

University of Kota, Kota

by

Ramesh Chand

Under the supervision of

Prof. N. K. Jaiman

Department of Pure and Applied Physics

University of Kota, Kota-324005(India)

2018

C E R T I F I C A T E

I feel great pleasure in certifying that the thesis entitled **'Nonlinear interaction of an intense ultra-short pulse laser with magnetized plasma'** by **Ramesh Chand** under my guidance. He has completed the following requirements as per Ph. D. regulations of the University.

(a) Course work as per the university rules.
(b) Residential requirements of the university (200 days)
(c) Regularly submitted annual progress report.
(d) Presented his work in the departmental committee.
(e) Published/accepted minimum of one research paper in a referred research journal,

I recommend the submission of thesis.

Date:

(N. K. Jaiman)
Professor
Department of Pure and Applied Physics,
University of Kota, Kota-324005

Abstract

The nonlinear interaction of the linearly and circularly polarized Laguerre-Gaussian (LG) laser pulse with an inhomogeneous parabolic plasma channel is studied. We consider the transfer of the orbital angular momentum (OAM) associated with the LG mode of the laser photon to the plasma electron. This results in the excitation of the magnetic field. The governing equations for the transfer of orbital angular momentum and the effective mass of photons in a plasma are derived. The analysis of the generation of magnetic fields B_z and B_φ for the different azimuthal angles and the laser beam intensities has been carried out. The results are analyzed numerically and compared with the results of 2D particle-in-cell (PIC) simulation of the Laguerre-Gaussian mode of laser beam. It has been observed that the generated magnetic field depends on the orbital angular momentum transfer and mass correction of a photon in the relativistic limit. The generated magnetic field depends on the Laguerre-Gaussian mode order, laser intensity, azimuthal angle and the relativistic factor. It is found that the generated magnetic field increases with the laser intensity. The strength of the magnetic field also depends on the polarization state of a laser field. It is shown that the excitation of the magnetic field for both linearly and circularly polarized laser beams depends on the azimuthal angle. The magnitude of generated magnetic field due to circularly polarized Laguerre-Gaussian beam of higher modes decreases with increasing azimuthal angle and is greater than that of the linearly polarized beam. It is further observed that the magnetic field generated due to the higher Laguerre-Gaussian modes is not quasistatic but changes with the spatial distribution of the plasma.

The analysis of short nonparaxial laser pulse in plasma channel has also been carried out. The electron energy gain in the wake of the laser pulse at different magnetic field strengths is determined. The effect of magnetic field on the wakefield structure, channel radius and accelerating length has been analyzed. The plasma channel profile has been considered to be parabolic. It has been found that the energy gain increases with increasing magnetic field. However, the result illustrates the variable pattern of the energy gain for different magnetic field

strengths. It is predicted that the autoresonance condition is achieved at $\omega_c/\omega_p = 2$, where the energy gain is maximum. The variation of the channel width as a function of magnetic field ratio ω_c/ω_p for different relativistic factors have shown that the channel width decreases with increasing ω_c/ω_p and increases with relativistic factor. This result shows that the laser gets self focused and hence there is a possibility of propagation of an intense short circularly polarized laser pulse over a significant extended distance. It is found that the excited wake has electrostatic as well as electromagnetic nature and thus excitation of the wake in the plasma is nonlocal. It is shown that the dephasing length increases linearly up to the ratio $\omega_c/\omega_p \leq 2.5$ and thereafter it becomes almost constant. The results indicate that the accelerating length can be varied by the external magnetic field and the relativistic factor. These results match with the relativistic two dimensional (2D) PIC simulation.

An attosecond pulse generation based on the deformation of the plasma mirror as a result of laser plasma mirror interaction is discussed. We have presented a simple analytical model for generation of an attosecond pulse from the relativistic oscillating plasma mirror with $\mathbf{E} \times \mathbf{B}$ effect that leads to the rotation in the oscillating plasma mirror. As the oscillating surface rotates it creates an additional phase shift and distortion in the field of the reflected harmonic beams. This phase distortion repeats itself with periodicity of the driving laser field leading to the more harmonics of the incident frequency. We have studied the effect of the rotation on the wavefront of the reflected laser field and the effect of the phase divergence on the generation of the attosecond pulse. The results of the harmonic generation and their dependence on the intensity of incident laser pulse have been presented. Also, the harmonic number of the reflected laser field increases with the intensity of the incident laser beam. Our numerical results show that the wave train of the attosecond pulses can be generated when the intensity of the laser beam exceeds 10^{18} W/cm^2. It is further found that the rotational effect of the relativistic oscillating plasma mirror changes the denting mechanism of the plasma mirror. The rotational effect of plasma mirror due to $\mathbf{E} \times \mathbf{B}$ changes the phase parameter of the harmonics.

The effect of magnetic field on the wakefield excitation for high intense ultra-short laser pulse in an underdense magnetized plasma has been analyzed. The relation between the generated electric field and the externally applied magnetic field has been obtained. It is observed that the generation of the wakefield in the plasma due to variation in the electron density depends on the external magnetic field. The magnitude of the wakefield increases with magnetic field strength. The analytical results are compared with the particle-in-cell (PIC) simulation results to give an insight into the wakefield evolution. The energy exchange is more effective at the higher values of the magnetic field.

Candidate's Declaration

I, hereby, certify that the work, which is being presented in the thesis, entitled '**Nonlinear interaction of an intense ultra-short pulse laser with magnetized plasma'** is in partial fulfilment of the requirement for the award of the Degree of Doctor of Philosophy, carried under the supervision of Professor/Dr **N. K. Jaiman** and submitted to the (University Department of Pure and Applied Physics), University of Kota, Kota represents my ideas in my own words and where others ideas or words have been included I have adequately cited and referenced the original sources. The work presented in this thesis has not been submitted elsewhere for the award of any other degree or diploma from any Institutions. I also declare that I have adhered to all principles of academic honesty and integrity and have not misrepresented or fabricated or falsified any idea/data/fact/source in my submission. I understand that any violation of the above will cause for disciplinary action by the University and can also evoke penal action from the sources which have thus not been properly cited or from whom proper permission has not been taken when needed.

Date:

(Ramesh Chand)

This is to certify that the above statement made by **Ramesh Chand** (Enrolment No. 2010/000132) is correct to the best of my knowledge.

Date:

(N. K. Jaiman)
Professor
Department of Pure and Applied Physics,
University of Kota, Kota-324005
Rajasthan (India)

Acknowledgement

I would like to express my sincere thanks to my supervisor Professor N. K. Jaiman for his excellent guidance, support and help. I am highly obliged to him for getting me introduced to the fascinating field of the laser plasma interaction.

I owe a lot to Dr. Bhawani Shankar Sharma, Joint Director, College Education, Rajasthan, Jaipur for his invaluable help, encouragement and continuous support. I am thankful to Professor K. P. Maheshwari, a guest faculty at Department of Pure and Applied Physics, University of Kota, Kota for his thought provoking discussion and suggestions. The research scholars of the Plasma Physics group namely, Mr. K. K. Soni and Ms. Shalu Jain have always extended their supporting hands in day to day matter.

I am highly thankful to my colleagues of Government College Kota, Kota and faculty members of the Department of Pure and Applied Physics, University of Kota, Kota for their kind support.

I would like to convey my hearty thanks to members of my family specially my son Maulik and daughter Charvi who not only supported me but also heightened my confidence. Thanks are also due to my wife Mrs. Pratibha for her unconditional support and care, without which it would have been impossible to complete the work. Her enduring patience and her love that helps me so much in completing this work. I am highly obliged to convey my heartiest regards to my parents whose blessings always kept me ahead in my pursuance to achieve my goal.

Finally, it is a great pleasure for me to acknowledge the cooperation and support of many people who generously guided, assisted me during my research work.

Thank you all.

Ramesh Chand

Contents

List of Figures

Chapter 1

Introduction

Laser plasma interaction has many applications, e.g., high-order harmonic generation, attosecond pulse generation, fast igniter fusion, laser ablation of material and radiation pressure driven acceleration, laser-plasma channeling and x-ray lasers [1-18].

After development of Chirped Pulse Amplification (CPA) technique in 1985, the laser pulse plasma interaction has considerable progress at laser intensities above 10^{19} W/cm^2, at these high intensities the laser field amplitude is so high that electrons will be driven almost equal to the velocity of light (i.e. v ≈ c) and the relativistic dynamics of electrons comes into play.

In relativistic regime many complex nonlinear phenomena such as instabilities in plasma, relativistic self-phase modulation, filamentation, Raman forward, Raman backward scattering, envelop self-modulation, relativistic self-focusing, super continuum generation, terahertz radiation generation and magnetic field generation occur.

The nonlinearity can be produced either by the relativistic effects [19, 20] or through the modification of plasma by the ponderomotive force (or light pressure) of ultra-intense laser pulses [2]. When high intense ultra-short laser pulses propagate through a plasma, electrostatic wakefields are generated due to the high energy electron oscillations in the plasma field [11].

Quasistatic magnetic field generation due to various phenomena [19-21] is one of the most significant nonlinear effects produced in high intense ultra-short laser pulse plasma interactions. S. C. Wilks *et al.* [2] found extremely high self generated magnetic fields (≈ 250MG) during numerical simulation. The physical explaination of the generation of these extremely high magnetic fields is an important subject of study.

1.1 Background and motivation

The interaction of laser pulse with plasma gives rise to a variety of phenomena. With the development of intense ultra-short laser pulse, there has been a lot of interest in nonlinear effects in laser plasma interaction. An electron in an intense short laser pulse acquires relativistic velocity and can be accelerated to high energies in the direction of laser pulse propagation by the ponderomotive force at the laser front [2] or by direct laser acceleration [22, 23] mechanism due to radiation pressure. There has been an increasing interest in the study of the propagation of laser pulses in plasma and the generation of electrostatic wakefields [6, 11, 24, 25]. The wakefield leads to high energy electron oscillations in the plasma field excited by the incident laser radiation. However, at ultra high intensities, two issues become important. First, strong self generated axial and/or azimuthal magnetic fields modify the electron dynamics and refractive index of the plasma. Second, electron motion is relativistic in the plasma in presence of high intense laser pulse. The propagation characteristic of the laser pulse changes due to increase in the relativistic mass (or decrease in the refractive index of the plasma). Many studies on the effect of magnetic field on relativistic electrons have been done by considering either self generated or externally applied magnetic fields. Wagner *et al.* [26] have observed the azimuthal magnetic fields of the order of 700 MG in overdense plasmas while in underdense plasmas, magnetic fields of the order of 100 MG [27]. Nazmudin *et al*. [28] have shown that a circularly polarized laser with intensity ~ 10^{19} W/cm^2 can generate axial magnetic field of the order of 7 MG in the direction of laser propagation. These self generated magnetic fields facilitate the electron acceleration by intense laser pulse plasma interaction [29-31] and observed beam collimation as well as electron acceleration up to ultra high energies with the value much greater than the ponderomotive energy. Qiao *et al*. [32] have developed an analytical model of magnetic field generation by a laser in plasma. The effects of magnetic field on the stimulated scattering and decay instabilities were studied [33, 34]. Liu *et al*. [35] have shown that the plasma electron acceleration depends on laser intensity and the ratio of cyclotron

frequency to laser frequency. Yu *et al.* [36] have observed the similar configuration using a linearly polarized laser. They reported electron acceleration to relativistic energies using weak magnetic field.

X. He *et al*. [37] have reported that the phase dependence of the relativistic electron dynamics is sensitive to the polarization of the laser field. For circularly polarized field only the axis of helical trajectories is changed with a change in the initial phase of the laser field whereas for linearly polarized field the effect is sensitive to the resonance parameter that is the ratio of cyclotron frequency to laser frequency. Liu and Tripathi [38] have examined the propagation of a linearly polarized intense Gaussian laser pulse in unmagnetized plasma and analyzed the nonlinear phase evolution and self distortion of the pulse. Sharma and Tripathi [39] have studied the interaction of circularly polarized intense laser pulse with plasma in the presence of axial magnetic field and found that the pulse suffers distortion due to nonlinearity induced by the relativistic mass in the refractive index of the plasma and they have examined electron acceleration by a circularly polarized Gaussian laser pulse in magnetized plasma and found that the ponderomotive force is significantly enhanced at the laser magnetic resonance also [12]. R. Singh and Tripathi [40] studied the filamentation instability of a circularly polarized relativistic short laser pulse under the combined effects of relativistic and ponderomotive nonlinearities in magnetized plasma.

Vortex beams carrying intrinsic angular momentum are widely analyzed and used [41-43].

High order harmonics are applied in the field of diagnostics, coherent radiation sources, lithography [44-46] and in the attosecond pulse generation.

Ivan P. Chriton *et al.* [47] theoretically studied high-order harmonic generation with excitation pulses shorter than 25 fs using three dimensional (3D) model. M. V. Frolov *et al.* [48] described analytic formulae related to harmonic generation by a weakly bound electron in the tunneling limit of a quantum mechanical analysis. F. Quéré *et al.* [49] theoretically and experimentally presented a mechanism of high-order harmonic generation by

reflection of laser from an overdense plasma. K. Eidmann *et al.* [50] investigated the emission efficiencies, polarization properties and the spectral shapes of the fundamental frequency and the second harmonic. H. Yang *et al.* [51] have experimentally shown that emission of electromagnetic radiation in ultraviolet region makes a major contribution to third-order harmonic. Guihua Zeng *et al.* [52] have shown that the relativistic harmonic excitation is more efficient in the short laser pulse regime than in the long laser pulse regime. L. Allen *et al.* [53] have studied the rate of electromagnetic energy flow per unit area, the Poynting vector, using local linear momentum density in Laguerre-Gaussian mode and experimentally shown the transfer of orbital angular momentum associated with Laguerre-Gaussian mode [54].

Simulation studies on the laser pulse plasma interaction have also a long history. Self consistent calculations have been initially used by Buneman [55] and Dawson [56] and they introduced the power of computational plasma physics. Birdsall and Langdon [57] and Hockney and Eastwood [58] described particle-in-cell (PIC) scheme in detail. Vahedi and Surendra [59] introduced differential cross section concept for laser plasma interaction simulation refining the results of particle-in-cell model. Object-oriented methods were applied to particle-in-cell codes to obtain realistic solutions of the problems [60]. Particle-in-cell simulation codes are not only used in the area of basic Physics but also in engineering devices. These codes have been used in various studies in order to have more reliable results in different conditions [61-64].

Some of the concepts/phenomena in the present thesis are briefly discussed as under.

1.2 High intense ultra-short laser pulses

After invention of Chirped Pulse Amplification (CPA) technique, firstly used by Strickland and Mourou [65] during 1985, high power lasers are used to investigate new features in laser plasma experiments. In Chirped Pulse Amplification technique, the laser pulse is stretched in time (i. e. chirped in frequency) then it is amplified and lastly compressed to achieve ultra-short laser pulses [66-68].

The advantage of chirped pulse amplification technique to achieve ultra-short pulses is that not only the duration of the pulse is shortened but also the power of the laser is greatly enhanced, due to which the power density or intensity of laser pulse goes much beyond 10^{19} W/cm^2. The invention of these high power laser pulses has opened up new areas in experimental Physics to discover more advanced phenomena [69].

In the present work the profiles of the laser pulse taken are Gaussian and Laguerre-Gaussian.

1.2.1 Gaussian mode

The wave equation in a three dimensional media is given as

$$\nabla^2 \mathrm{E} = \frac{1}{v^2}\frac{\partial^2 E}{\partial t^2}, \tag{1.1}$$

where

$$\nabla^2 = \frac{\partial^2}{\partial x^2} + \frac{\partial^2}{\partial y^2} + \frac{\partial^2}{\partial z^2}$$

is the Laplacian and υ is the phase velocity.

The solution of a wave propagated along z-axis may be given as

$$\mathrm{E}(x,y,z,t) = \mathrm{E}_0\ e^{-i(\omega t - kz)}, \tag{1.2}$$

where E_0, ω and k (= ω/υ) are the amplitude, frequency and propagation constant of the wave respectively.

Using the equation (1.2) in equation (1.1) gives

$$\frac{\partial^2 E_0}{\partial x^2} + \frac{\partial^2 E_0}{\partial y^2} + \frac{\partial^2 E_0}{\partial z^2} + 2ik\frac{\partial E_0}{\partial z} = 0. \tag{1.3}$$

Since E_0 slowly varies along the direction of propagation, that is along z, hence $\frac{\partial^2 E_0}{\partial z^2}$ can be neglected as compared to $ik\frac{\partial E_0}{\partial z}$. This kind of wave is known as paraxially propagating wave.

Under the paraxial approximation, the above equation has the form

$$\frac{\partial^2 E_0}{\partial x^2} + \frac{\partial^2 E_0}{\partial y^2} + 2ik\frac{\partial E_0}{\partial z} = 0. \quad (1.4)$$

Let the solution of the equation (1.4) under paraxial propagation is given as

$$E_0 = E_{00}\, e^{-\frac{ik\,r^2}{2a(z)}}\, e^{ib(z)}, \quad (1.5)$$

where E_{00} is a normalized constant, $r^2 = x^2 + y^2$, a(z) and b(z) are variables defined as under.

$$a(z) = z + i\, z_R, \quad (1.6)$$

here z_R is a constant known as Rayleigh range (distance from focal point to the point where beam area doubles, given by $z_R = kw_0^2/2 = \pi w_0^2/\lambda$, here w_0 is beam waist) which gives divergence of the beam, i.e., higher Rayleigh range indicate higher divergence and smaller Rayleigh range indicate smaller divergence of the beam .

Equation (1.6) can also be written as

$$\frac{1}{a(z)} = \frac{1}{z+\frac{z_R^2}{z}} - \frac{i}{z_R(1+\frac{z^2}{z_R^2})}. \quad (1.7)$$

Using this form of a(z) in equation (1.5) gives

$$E_0(x,y,z) = E_{00}\, e^{-\frac{ik\,r^2}{2R(z)}}\, e^{\frac{-r^2}{w(z)^2}} e^{ib(z)}, \quad (1.8)$$

where R(z) is called the radius of curvature at a point z and is given by

$$R(z) = z + \frac{z_R^2}{z}. \quad (1.9)$$

This shows a wavefront with varying radius of curvature.

If z = 0, R(z) = ∞ which shows it is a plane wavefront.

If $z >> z_R$, R(z) = z means it is a spherical wavefront,

and if $z = z_R$, R(z) = 2z is defined as the turning point.

w(z) in equation (1.8) shows z-dependence of the beam spot size at point z of the beam and is given by

$$w(z) = w_0\sqrt{1 + \frac{z^2}{z_R^2}}\ , \tag{1.10}$$

where

$$w_0 = \sqrt{\frac{\lambda}{\pi} z_R} \tag{1.11}$$

is the beam waist.

At z = 0, beam spot size w(z) = w_0, which is the minimum spot size (called as beam waist), hence, z = 0 is a special point in the propagation of the Gaussian beam.

For z > 0 and z < 0, the beam spot size w(z) increases.

At z = z_R, w(z) = $\sqrt{2}$ w_0 defines a turning point in the propagation of the beam where spot size does not remain constant but increases linearly.

For z >> z_R, w(z) = w_0 (z/z_R) ≈ z θ, where θ is called divergence angle of the beam and is given by

$$\theta = w_0/z_R \approx \sqrt{\frac{\lambda}{\pi z_R}} = \sqrt{\frac{\lambda}{\pi}\frac{\lambda}{\pi w_0^2}} = \frac{\lambda}{\pi w_0}, \tag{1.12}$$

which shows that larger is the beam waist, smaller shall be the divergence of the beam (Figure 1.1).

To obtain the solution of the equation (1.5), let $e^{ib(z)}$ has the form

$$e^{ib(z)} = \frac{w_0}{w(z)} e^{-i\phi(z)}, \tag{1.13}$$

where

$$\phi(z) = tan^{-1}\frac{z}{z_R} \tag{1.14}$$

is the Gouy phase, which shows the rapid phase change in the field when beam passes through the minimal diameter (focal point) of the beam. Gouy phase approaches the limit ± $\pi/2$ as $z \rightarrow \pm\infty$. It is an important factor in the situation where wavefront is very complex.

So, the solution of the equation (1.1) is obtained by using equations (1.2), (1.8) and (1.13) as

$$E(x,y,z,t) = E_{00}\frac{w_0}{w(z)}\, e^{\frac{-r^2}{w(z)^2}}\, e^{-i(\omega t - kz)}\, e^{-\frac{ikr^2}{2R(z)}}\, e^{i\phi(z)}, \qquad (1.15)$$

where first three terms give the amplitude of the beam and last three terms show phase of the beam.

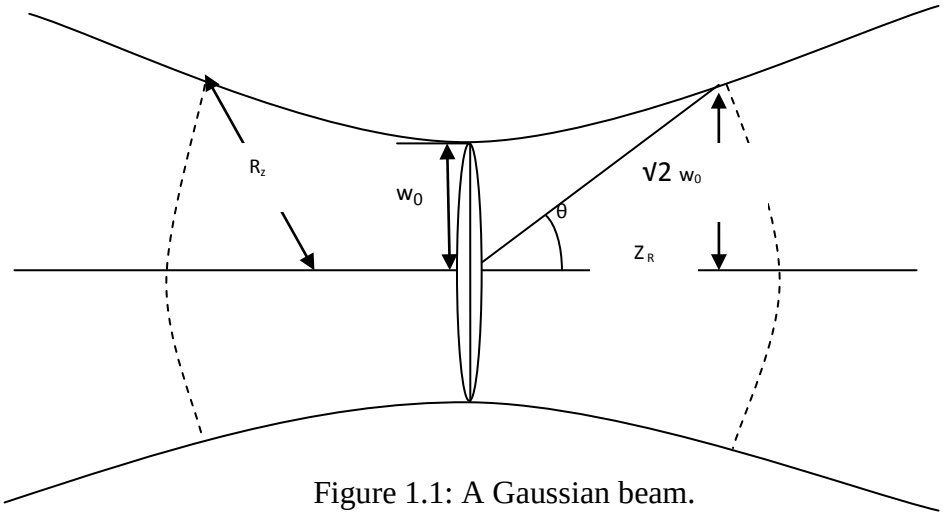

Figure 1.1: A Gaussian beam.

The value of the E_{00} in the equation (1.15) is determined by the normalization condition and is given by

$$E_{00} = \sqrt{(2/\pi)} \qquad (1.16)$$

The amplitude of a beam depends on a factor $w_0/w(z)$ which is nearly constant up to $z \leq z_R$ and for $z >> z_R$ it decreases as $1/z$.

1.2.2 Laguerre-Gaussian mode

The solution of the equation (1.4) in the above analysis is carried out under the assumption that x and y coordinates are dependent on each other.

Now, suppose the coordinates are independent and the solution given as

$$E(x,y,z) = E_0\, f(x,z)\, g(y,z)\; e^{-\frac{ik\,r^2}{2a(z)}} e^{ib(z)}, \qquad (1.17)$$

where E_0 is a constant part, f(x,z) and g(y,z) are variable parts of the amplitude and a(z), b(z) and k are as defined in the previous section.

After long and complex analytical calculations in the cylindrical coordinate system the more general solution is written as [70]

$$E_{p,|l|}(\rho,\theta,z,t) = A_{p,|l|}\; \frac{w_0}{w(z)}\; \left(\frac{\sqrt{2}\rho}{w(z)}\right)^{|l|} L_p^{|l|}\left(\frac{2\rho^2}{w(z)^2}\right) e^{-\left(\frac{\rho^2}{w(z)^2}\right)} e^{i(kz-\omega t)} \times$$

$$e^{\frac{ik\rho^2}{2R(z)}}\, e^{i|l|\theta}\, e^{i\Phi(z)}. \qquad (1.18)$$

Equation (1.18) contains the associated Laguerre function $L_p^{|l|}$ with (p+1) radial nods, where p and $|l|$ are the radial and azimuthal index of the Laguerre function. So, these modes are termed as Laguerre-Gaussian modes.

Since the solutions are dependent on radial distribution of the beam, hence the intensity profile has ring like structures. For $|l| \neq 0$, p = 0 beam has doughnut shaped structure with the radius of doughnut proportional to $|l|^{\frac{1}{2}}$. The phase of the Laguerre-Gaussian mode varies as $|l|\theta$ showing that the wavefront has helix like structure (i.e., Vortex) with pitch λ.

The Laguerre-Gaussian modes are cylindrically symmetric along the direction of propagation and carry orbital angular momentum equal to $|l|$ ħ per photon [71, 72]. Since the vortex beam possesses orbital angular momentum thus a torque is experienced by the refractive media placed along the direction of the propagation axis and thus a spiraling current is produced by the azimuthal gradient of the helical phase. That's

why the magnetic field so produced is very important to determine the plasma electron dynamics in the ultra-intense laser pulse.

1.3 Intense ultra-short laser pulse plasma interaction

1.3.1 Electron dynamics under ultra-short pulses

The equation of motion of electrons in ultra-short laser pulse is given by

$$\frac{d\boldsymbol{p}}{dt} = \frac{d}{dt}(\gamma m v) = -e\left(\boldsymbol{E} + \frac{1}{c}(\boldsymbol{v} \times \boldsymbol{B})\right), \tag{1.19}$$

where **p**, m, e, **v** and γ are relativistic linear momentum, effective mass, charge, velocity of the electrons and relativistic factor respectively.

Relativistic factor is given by

$$\gamma = \frac{1}{\sqrt{1-\frac{v^2}{c^2}}} = \sqrt{1+\frac{p^2}{m^2c^2}}\,. \tag{1.20}$$

The electric and magnetic fields are given as

$$\boldsymbol{E} = -\frac{1}{c}\frac{\partial \boldsymbol{A}}{\partial t}, \tag{1.21}$$

and $$\boldsymbol{B} = \nabla \times \boldsymbol{A}, \tag{1.22}$$

where **A** is the vector potential which is related by normalized vector potential α as

$$\boldsymbol{a} = \frac{e\boldsymbol{A}}{mc^2}. \tag{1.23}$$

1.3.2 Laser pulse propagation through plasma

When a laser pulse is propagated through plasma, it may go diffracted in the plasma, which can be prevented by relativistic self focusing.

The peak intensity of the laser pulse is related to the normalized vector potenatial as

$$I_0 = \frac{\pi c}{2}\left(\frac{mc^2 a_0}{e\lambda}\right)^2, \tag{1.24}$$

giving the laser parameter as

$$a_0^2 = \frac{2e^2\lambda^2 I_0}{\pi m^2 c^5} \cong 7.32 \times 10^{-19}\, \lambda^2[\mu m]\, I_0[W/cm^2], \quad (1.25)$$

where α_0 is the normalized vector potential of the laser pulse.

It is assumed that the electric field is linearly polarized.

The peak power is

$$P[GW] \cong 21.5\, (\frac{a_0 w_0}{\lambda})^2, \quad (1.26)$$

where w_0 is spot size at the focus, λ is wavelength, $\omega = c\, k$ is the frequency of the laser.

The peak laser electric field is given as

$$E_L[TV/m] \cong\ 3.21 \times \frac{a_0}{\lambda[\mu m]}. \quad (1.27)$$

However, the normalized quiver momentum of the laser field is physically related to normalized vector potential as

$$\boldsymbol{\alpha} = \mathbf{p}/mc. \quad (1.28)$$

If $\alpha_0 \geq 1$, the electron motion is highly relativistic and nonlinear phenomena are produced in the plasma.

When an intense laser pulse passes through a plasma, the relativistic factor due to quiver motion of a plasma electron is

$$\gamma \approx \sqrt{1 + \frac{a^2}{2}}. \quad (1.29)$$

When the laser intensity is peaked on the axis then relativistic quiver motion is along the axis and guiding of the laser pulse may be possible along the axis. This is the relativistic self-focusing [18].

Which can occur when $P > P_c$, i.e., laser power exceeds a critical power with

$$P_c\ = 2c\, \left(\frac{mc^2}{e}\right)^2 \left(\frac{\omega}{\omega_p}\right)^2 \quad (1.30)$$

or

$$P_c[GW] \approx 17.4 (\lambda_p/\lambda)^2, \quad (1.31)$$

where

$\lambda_p = 2\pi c/\omega_p$

is the plasma wavelength and ω_p is plasma frequency.

Hence, plasma electron acquired momentum and produced magnetic field in the plasma. In the presence of these fields, different nonlinear phenomena like enhancement of the ponderomotive force at the laser magnetic resonance [12], beam collimation, electron acceleration up to ultra high energies [29-31], pulse distortion due to nonlinearity induced by the relativistic mass in the refractive index of the plasma [39], relativistic and ponderomotive nonlinear effects on the stimulated scattering, decay instabilities [33, 34] and filamentation [40] take place.

1.4 High-order harmonic generation

The nonlinear interaction of intense short laser pulse with plasma produces coherent radiation at multiples of the incident laser frequency. This generated radiation with multiples of laser frequency is known as high-order harmonic of incident laser frequency and the phenomenon is called as High-order harmonic generation (HHG) [73]. The generated radiation has the frequency spectrum extended up to the extreme ultraviolet region.

When a high intense ultra-short laser pulse interacted with underdense and overdense plasmas then a large number of nonlinear phenomena occur in the plasma. The generation of high-order harmonics is the one of the important nonlinear phenomena that is observed in the laser plasma. If the intensity of the incident laser pulse is high enough to produce relativistic effects then the vacuum-plasma interface experiences a large ponderomotive force and thus produces a large amplitude oscillation by the laser pulse on the surface and provides a mechanism of harmonic generation (Figure 1.2) [74-83].

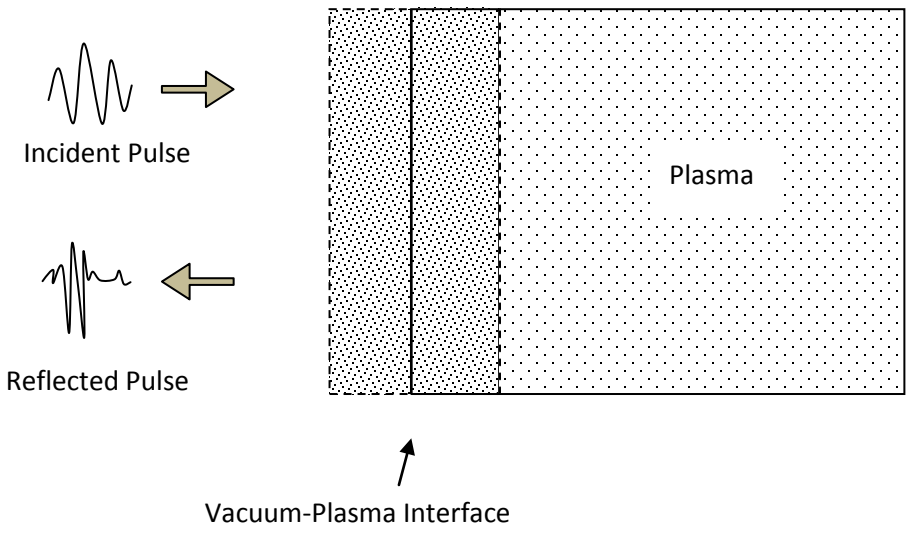

Figure 1.2: High-order harmonic generation mechanism.

High-order harmonic generation in underdense plasma is the result of parametric excitation produced by the interaction between intense electromagnetic and electrostatic plasma waves with different frequencies. When intense short laser pulse impinges on an overdense plasma, the harmonics of laser light are produced due to electron motion in the laser field at the vacuum-plasma interface [84] formed on the surface of the overdense plasma or solid target. When laser pulse is incident on the overdense plasma surface, it reflects back at the critical density of a graded density profile surface or at the vacuum-plasma interface of a sharp plasma boundary forming the oscillating layers of electron density. Even and odd harmonics in the reflected light are produced by these oscillations. The amplitude and polarization of the generated harmonics depend on the intensity, incident angle and polarization of the incident radiation.

R. Lichters *et al.* [85] and D. V. Linde *et al.* [74, 86] proposed the 'moving mirror model', according to which even and odd harmonics with monotonically decreasing intensities are generated when moving mirror

frequency and the incident laser frequency beat. Since high-order harmonic generation depends on the laser amplitude, the plasma density and the degree of inhomogeneity of plasma, the phenomenon can be explained by three different mechanisms [87], via, (i) oscillating mirror model [86-88], (ii) sliding mirror model [81, 89] and (iii) flying mirror model [90, 91].

1.4.1 Oscillating mirror model

Bulanov *et al.* [3, 92, 93] proposed the oscillating mirror model and gives a new idea that harmonics are generated from fast moving reflective surface. They explained the generation of harmonics as the result of periodic Doppler shift from oscillating reflective plasma surface (Figure 1.3).

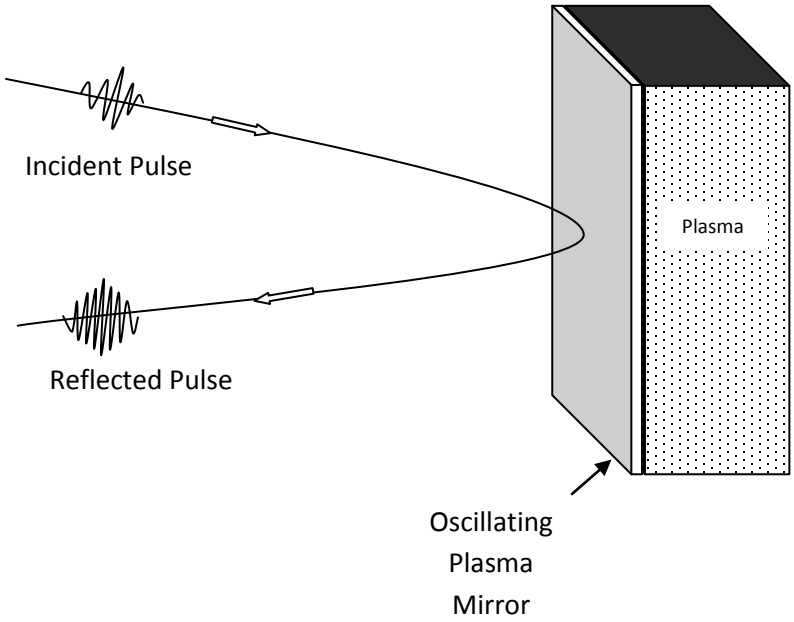

Figure 1.3: Oscillating plasma mirror scheme of high-order harmonic generation.

When a laser pulse is incident on a plasma surface, electrons are pushed back into the plasma because of the laser electric field due to the ponderomotive force acting upon the plasma electrons. But the ions are immobile on the time scale of ultra-short pulses, hence, the displaced electrons are pulled back because of restoring force due to the immobile ions and thus electrons oscillates with the frequency of the incident laser field. In the presence of high intensity pulses, the velocity of electrons approaches the speed of light leading to the relativistic effects. Thus, incident laser field experiences an extreme Doppler shift by the relativistically moving plasma surface [94] and produces frequency components much higher than the original one.

1.4.2 Sliding mirror model

When a laser pulse is incident upon a very thin layer of overdense plasma, the charge separation electric field suppresses the electrons motion in the direction perpendicular to the plasma surface because of the high plasma density [89, 92] and thus the reflecting electron layer is negligibly displaced in the direction perpendicular to the plasma surface. So the electron motion is along the plasma surface that forms the sliding mirror. This model is called sliding mirror model.

1.4.3 Flying mirror model

Bulanov *et al.* [93, 95] proposed the relativistic flying mirror model which is used in the interaction of intense laser pulse with sub-critical concentration plasma.

The electron density modulation excited during the interaction between an intense laser pulse with underdense plasma is responsible for flying mirror. Thin electron shells in a plasma are moving with the velocity equal to the velocity of light. These high density electron shells partially reflect the counter propagating laser pulse coherently. This results in the frequency multiplication, the shortening of the pulse in the longitudinal direction and intensification of electromagnetic wave.

1.5 Introduction to Attosecond Physics

There has been tremendous interest in the attosecond phenomena [96] over the last two decades. Important among which are the measurement of the electric field of a laser pulse [97], the observation of the electron transport near the surface of a metal [98] and the time resolution of the electron tunneling process [99].

Attosecond pulses were generated by the process of high-order harmonic generation in atomic media [100, 101] in which the harmonics emission take place by the electrons which tunnel away from the nucleus and then interacted with the nucleus while oscillating in the laser field and have high emission efficiency for shorter laser pulses of high intensity. Fourier analysis technique gives an idea of ultra-short pulse generation [102].

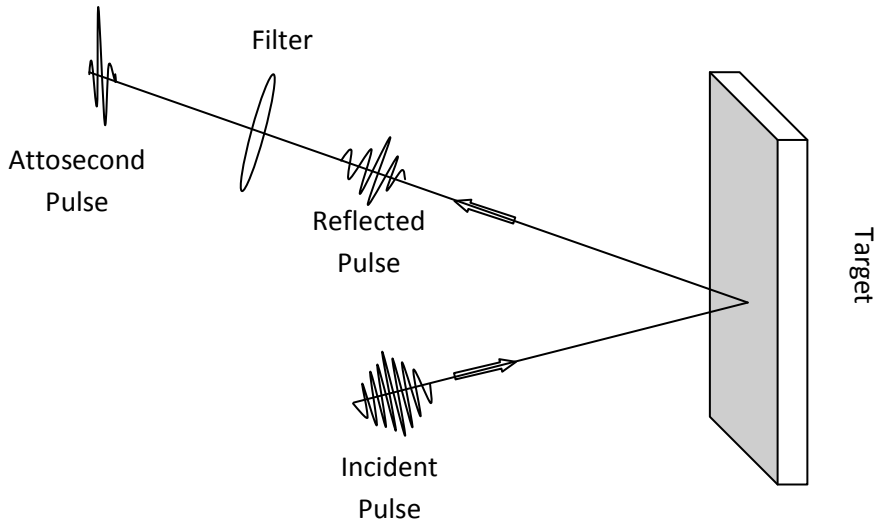

Figure 1.4: Attosecond pulse generation technique.

Attosecond pulse generation through the high-order harmonic generation is possible only if the harmonics are phase synchronized. Corkum [101] proposed the three step model of the generation of gas harmonics. These gas harmonics were first used to generate the attosecond pulses during which incoming light was transformed into a broad spectrum with odd harmonics. The method of generation of attosecond pulses by high harmonics is explained in the Figure 1.4. A focused high intense laser pulse on a plasma is created on the solid target surface generating high order harmonics of incident laser frequency and an attosecond pulse may be separated by an appropriate filter.

Many experimental and theoretical studies of attosecond pulse generation were illustrated in the literature [4, 85, 86, 103-105].

1.6 Outline of the proposed work

This thesis presents a study of the nonlinear interaction of high intense ultra-short laser pulse with a magnetized plasma. At high intensities about 10^{19} W/cm^2 and above, the laser field is high enough to produce many nonlinear relativistic phenomena, e.g., wakefield exctatation, magnetic field generation, high-order harmonic generation and attosecond pulse generation.

In chapter 2, we present a study of the nonlinear interaction of the linearly and circularly polarized Laguerre-Gaussian laser beams with an inhomogeneous parabolic plasma channel, especially, the transfer of the orbital angular momentum (OAM) from the photon to the plasma electrons which results in the excitation of the axial magnetic field (B_z) and the transverse azimuthal magnetic field (B_φ). Laguerre-Gaussian beams provide the basis for discussing the new and increasingly important concept of the orbital angular momentum of a photon. We have used the Proca equation and calculated the effective mass of photons in plasma and worked out the coupling of angular momentum to plasma for the different Laguerre-Gaussian beams and their effect on magnetic field generation. A theory of interaction of the Laguerre-Gaussian laser beam with plasma is outlined and the governing equations for the transfer of orbital angular momentum and the effective mass of photons in plasma are derived. The analysis

of the generation of magnetic fields B_z and B_φ for different azimuthal angles and beam intensities is carried out. The results obtained are in good agreement with that of the PIC simulation. It has been shown that the generated magnetic field is not quasistatic. The magnitude of the generated magnetic field depends on the order of laser beam mode, beam intensity, plasma density and laser frequency.

In chapter 3, the analysis of short nonparaxial laser pulse in a magnetized plasma channel has been carried out. The electron energy gain in the wake of the laser pulse at different magnetic field strengths is determined. The effects of magnetic field on the wakefield structure, channel radius and accelerating length have been analyzed. It has been found that the energy gain increases with increasing magnetic field. It has been observed that the excited wake has electrostatic as well as electromagnetic nature and thus excitation of the wake in the plasma is nonlocal.

In chapter 4, we have presented a simple analytical model for generation of an attosecond pulse from the relativistic oscillating plasma mirror with $\mathbf{E} \times \mathbf{B}$ effect that leads to the rotation in the oscillating plasma mirror. This results in the spatial variation of intensity on the target giving rise to the deformation in the surface of the plasma mirror. Deformation in the relativistic plasma mirror surface in the form of an elliptical curvature is considered which can affect the spatial and spectral properties of the reflected beam. This in turn rotates the plasma mirror which could bring a change in spatio-temporal coupling mechanism and the Doppler shift of the reflected laser field. The effect of the rotation on the wavefront of the reflected laser field and the phase divergence on the generation of the attosecond pulse has been analyzed. The results of the harmonic generation and their dependence on the intensity of incident laser pulse are presented.

In chapter 5, the effect of magnetic field on the wakefield excitation for high intense ultra-short laser pulse in underdense magnetized plasma has been analyzed. The relation between the generated electric field and the externally applied magnetic field has been obtained. The analytical results are compared

with the particle-in-cell (PIC) simulation results to give an insight into the wakefield evolution.

Conclusions and discussions are presented **in chapter 6**. The future work is also outlined in this chapter in view of the continuity of our present work.

Bibliography

[1] N. Kumar and V.K. Tripathi, Phys. Plasmas 14, 103108 (2007).

[2] S.C. Wilks, W.L. Kruer, M. Tabak and A.B. Langdon, Phys. Rev. Lett. 69, 1383 (1992).

[3] S.V. Bulanov, N.M. Naumova and F. Pagoraro, Phys. Plasmas 1, 745 (1994).

[4] T. Baeva, S. Gordienko and A. Pukhov, Phys Rev. E 74, 046404 (2006).

[5] S.L. Anisimov and B.S. Lukyanchuk, Phys. Usp. 45, 293 (2002).

[6] T. Tajima and J.M. Dawson, Phys Rev. Lett. 43, 267 (1979).

[7] X. Wang *et al*., Phys Rev. Lett. 84(23), 5324-5327 (2000).

[8] M.E. Dieckmann, B. Aliasson and P.K. Shukla, Phys Rev. E 70, 036401 (2004).

[9] Sandeep kumar and Hitendra K. Malik, J. Plasma Phys., 72(6), 983-987(2006)

[10] K. Schmid *et al.*, Phys Rev. Lett. 102,124801 (2009).

[11] V.B. Krasovitskii, V.G. Dorofeenko, V.I. Sotnikov and B. S. Bauer, Phys. Plasmas 11(2), 724-742(2004).

[12] A. Sharma and V.K. Tripathi, Phys. Plasmas 16, 043103 (2009).

[13] M. Kumar and V. K. Tripathi, Phys Plasmas 17, 053103 (2010).

[14] P. Polynkin, M. Kolesik, J.V .Moloney, G.A. Siviloglou, D.N. Christodoulides, science 324,229-232 (2009).

[15] A. Proulx, A. Talebpour, S. Petit, S.L. Chin, Opt. Commun. 174, 305(2000).

[16] C. D'Amico *et al*., Phys. Rev. Lett. 98, 235002 (2007).

[17] J. Kasparian *et al*., Opt.Express, 16, 5757 (2008).

[18] E. Esarey, P. Sprangle and J. Krall, IEEE J. Quant. Elect. 33(11), 1879-1914 (1997).

[19] A. Modena, Z. Najmudin, A. E. Dangor, C. E. Clayton, K. A. Marsh, C. Joshi, V. Malka, C.B. Darrow and C. Danson, IEEE Trans.Plasma Sci., 24,289 (1996).

[20] C.E. Max, J. Arons and A.B. Langdon, Phys. Rev. Lett., 33, 209 (1974).

[21] M.S. Wei *et al*., Phys Rev. Lett. 93, 155003 (2004).

[22] A. Pukhov *et al.*, Phys. Plasmas 6, 2847 (1999).

[23] G.D. Tsakiris, C. Gahn and V.K. Tripathi, Phys. Plasmas 7, 3017 (2000).

[24] P.K. Shukla, Phys. Scr. 52, 73 (1994).

[25] G. Berdin and J. Lundberg, Phys. Rev. E 57, 7041 (1998).

[26] U. Wagner *et al*., Phys Rev. E 70, 026401 (2004).

[27] A. Pukhov and J. Meyer-terVehn, Phys Rev. Lett. 76, 3975 (1996).

[28] Z. Najmudin *et al*., Phys Rev. Lett. 87, 215004 (2001).

[29] B. Qiao, X.T. He, S. Zhu, C.Y. Zheng, Phys. Plasmas 12,083102 (2005).

[30] H.Y. Niu, X.T. He, B. Qiao and C.T. Zhou, Laser Part. Beam 26, 51 (2008).

[31] C.Y. Zheng, X.T. He and S.P. Zhu, Phys. Plasmas 12,044505 (2005).

[32] B. Qiao, S. Zhu, C.Y. Zheng and X.T. He, Phys. Plasmas 12, 053104 (2005).

[33] C. Grebogi and C.S. Liu, Phys. Fluids 23, 1330 (1980).

[34] H.C. Barr *et al*., Phys. Fluids 27, 2730 (1984).

[35] H. Liu, X.T. He and S.G. Chen, Phys. Rev. E 69, 066409 (2004).

[36] W. Yu *et al*., Phys. Rev. E 66, 036406 (2003).

[37] X. He *et al*., Phys. Rev. E 68, 056501(2003).

[38] C.S. Liu and V.K. Tripathi, Phys. Plasmas 12, 043103 (2005).

[39] A. Sharma and V.K. Tripathi, Phys. Plasmas 12, 093109 (2005).

[40] R. Singh and V.K. Tripathi, Phys. Plasmas 16, 052108 (2009).

[41] L. Allen, M.J. Padgett and M. Babiker, Prog. Opt.34, 291 (1999).

[42] S. Franke-Arnold, L. Allen and M.J. Padgett, Laser and Photon. Rev. 2, 299 (2008).

[43] J.P. Torres and L. Torner, Eds., *Twisted Photons* (Willey-VCH, 2011).

[44] J. Zhou, J. Peatross, M.M. Murnane, H.C. Kapteny and Christov, Phys. Rev. Lett. 76, 752 (1996).

[45] G. Mourou, Z. Chang, Maksimhuk, J. Nees, S.V. Bulanov, V. Y. Bychenkov, T.Z. Esirkepov, N.M. Naumova, F. Pegorero and H. Ruhl, Plasma Phys. Rep. 28, 12 (2002).

[46] S.V. Bulanov, T.Z. Esirkepov, N.M. Naumova and I.V. Sokolov, Phys. Rev. E. 67, 016405 (2003)

[47] I.P. Christov, M.M. Murnane and H.C. Kapteyn, Phys. Rev. Lett. 78, 1251-1254 (1997).

[48] M.V. Frolov, N.L. Manakov, T.S. Sarantseva and A.F. Starace, J. Phys. B: At. Mol. Opt. Phys. 42, 035601 (2009).

[49] F. Quéré, C. Thaury, P. Monot, S. Dobosz and P. Martin, Phys. Rev. Lett. 96, 125004 (2006).

[50] K. Eidmann, T. Kawachi, A. Marcinkevicius, R. Bartlome, G.D. Tsakiris and K. Witte, Phys. Rev. E 72, 036413 (2005).

[51] H. Yang, J. Zhang, J. Zhang, L.Z. Zhao, Y.J. Li, H. Teng, Y.T. Li, Z.H. Wang, Z.L. Chen, Z.Y. Wei, J.X. Ma, W. Yu and Z.M. Sheng, Phys. Rev. E 67, 015401 (2003).

[52] G. Zeng, B. Shen, W. Yu and Z. Xu, Phys Plasmas 3(11), 4220-4224 (1996).

[53] L. Allen and M.J. Padgett, Optics Communications 184, 67-71 (2000).

[54] L. Allen, M.W. Beijersbergen, R.J.C. Spreeuw and J.P. Woerdman, Phys. Rev. A 45(11), 8185-8189 (1992).

[55] O. Buneman, Phys. Rev. 115, 503-17 (1959).

[56] J.M. Dawson, Phys. Fluids 5, 445-59 (1962).

[57] C.K. Birdsall and A.B. Langdon, Plasma Physics via Computer Simulation, Mc-Graw Hill, Newyork (1985).

[58] R.W. Hockney and J.W. Eastwood, Computer Simulation Using Particles, Mc-Graw Hill, Newyork (1981).

[59] V. Vehadi and M. Surendra, Comput. Phys. Commun. 87, 179-98 (1995).

[60] J.P. Verboncoeur, A.B. Langdon and N.T. Gladd, Comput. Phys. Commun. 87, 199-211 (1995).

[61] J. Yoo *et al*., Comp. Phys. Commun. 177, 93-94 (2007).

[62] Y. Chen and S.E.Parker, Phys. Plasmas 16, 052305 (2009).

[63] S. Morsed, T. M. Antonsen and J. P. Palastro, Phys. Plasmas 17, 063106 (2010).

[64] N. Nasari, S. G. Bochkarev and W. Rozemus, Phys. Plasmas 17, 033107 (2010).

[65] D. Strickland and G. Mourou, Opt. Commun. 56, 219 (1985).

[66] M.D. Perry and G. Mourou, Science 264, 917 (1994).

[67] P. Gibbon and E. Forster, Plasma Phys. Control Fusion 38, 769 (1996).

[68] S. Backus, C.G. Durfee III, M.M. Murname and H.C. Kapteyn, Rev. Sci. Instrum. 69, 1207 (1998).

[69] Shalom Eliezer, The Interaction of High Power Lasers with Plasmas, Institute of Physics Publishing, Bristol (2002).

[70] Enrique J. Galvez, Gaussian Beams, Colgate University (2009), (http://www.colgate.edu/portaldata/imagegallerywww/98c178dc-7e5b-4a04-b0a1-a73abf7f13d5/imagegallery/gaussian-beams.pdf).

[71] A. T. O'Neil, I. MacVicar, L. Allen, M. J. Padgett, Phys. Rev. Lett. **88**, 053601 (2002).

[72] N. B. Simpson, K. Dholakia, L. Allen, M.J. Padgett, Opt. Lett. **22**, 52-54 (1997).

[73] C. Winterfeldt and G. Gerber, Rev. Mod. Phys.80, 117 (2008).

[74] D.V. Linde, Applied Phys. B 68, 315-319 (1999).

[75] S. Nuzzo, M. Zarcone, G. Ferrante and S. Basile, Laser and Particle beams 18, 483-487 (2000).

[76] P. Villoresi, P. Barbiero, L. Poletto, M. Nisoli, G. Cerullo, E. Priori, S. Stagira, C. De, R. Bruzzese and C. Altucci, Laser and Particle beams 19, 41-45 (2001).

[77] A. Pukhov, Rep. Prog. Phys. 65, R1-R55 (2002).

[78] M. Nisoli, G. Sansone, S. Stagira, S.D. Silverstri, C. Vozzi, M. Pascolini, L. Poletto, P. Villoresi and G. Tondello, Phys. Rev. Lett 91, 2139051-54 (2003).

[79] I.B. Foldes, G. Kocsis, E. Racz, S. Szatmari and G. Veres, Laser and Particle beams 21, 517-521 (2003).

[80] T. Baeva, S. Gordienko and A. Pukhov, Phys. Rev. E 74, 046404(1-11) (2006).

[81] A.S. Pirozkov, S.V. Bulanov, T.Z. Esirkepov, A.S. Mori and H. Daido, Phys. Plasmas 13, 013107(1-12) (2006).

[82] R.A. Ganeev, Physics –Uspekhi. 52, 55-77 (2009).

[83] U. Teubner and P. Gibbon, Rev. Mod. Phys. 81, 445-479 (2009).

[84] B. Dromey, M. Zepf, A. Gopal, K.Lancaster, M.S. Wei, K. Krushelnick, M. Tatarakis, N. Vakakis, S. Moustaizis, R. Kodama, M. Tampo, C. Stoeckl, R. Clarke, H. Habara, D. Neely, S. Karsch and P. Norreys, Nature Phys. 2, 456 (2006).

[85] R. Lichters, J. Meyer-ter-vehn and A. Pukhov, Phys. Plasmas 3, 3425-3437 (1996).

[86] D. Von der Linde and K. Rzazewski, Applied Phys. B 63, 499 (1996).

[87] Vinita Jain, An analytical and numerical investigation of generation of high order optical Harmonics as a result of the interaction of intense laser pulses with solid surfaces/gaseous medium (Doctoral Thesis), University of Kota, Kota, India (2014).

[88] G.D. Tsakiris, K. Eidmann, J. Meyer-ter-vehn and F. Krausz, New J. Phys. 8, 19 (2006).

[89] A.S. Pirozhkov, S.V. Bulanov, T.Z. Esirkepov, M. Mori, A. Sagisaka and H. Daido, Phys. Rev. Lett. A 349, 256-263 (2006).

[90] T.Z. Esirkepov, S.V. Bulanov, M. Kando, A.S. Pirozhkhov and A.G. Zhidkov, Proc. of Spie vol. 7359, 735909-1-735909-11 (2009).

[91] S.V. Bulanov, T.Z. Esirkepov, M. Kando, J.K. Koga, A.S. Pirozhkov, N.N. Rosanov and A.G. Zhidkov, AIP Conf. 1032, 221 (2011).

[92] V.A. Vshivkov, N.M. Naumova, F. Pegarero and S.V. Bulanov, Phys. Plasmas 5, 2727-2741 (1998).

[93] S.V. Bulanov, T.Z. Esirkepov and T. Tajima, Phys. Rev. Lett. 91, 085001 (2003).

[94] S. Gordienko, A. Pukhov, O. Shorokhov and T. Baeva, Phys. Rev. Lett. 93, 115002 (2004).

[95] S.V. Bulanov, I.N. Inovenkov, V.I. Kirsanov, N.M. Naumova and A.S. Sakharov, Phys. Fluids B 4, 1935-1942 (1992).

[96] A.D. Bandrauk, F. Krausz and A.F. Starace, New J. Phys. 10, 025004 (2008).

[97] E. Goulielmakis, M. Uiberackar, R. Kienberger, A. Baltuska, V. Yakovlev, A. Scrinzi, T. Westerwalbesloh, U. Kleineberg, U. Heinzmann, M. Drescher and F. Krausz, Science 305, 1267 (2004).

[98] A.L. Cavalieri, N. Müllar, T. Uphues, V.S. Yakovlev, A. Baltuska, B. Horvath, B. Schmidt, L. Blumel, R. Hozwarth, S. Hendel, M. Drescher, U. Kleineberg, P.M. Echenique, R. Kienberger, F. Krausz and U. Heizmann, Nature 449, 1029 (2007).

[99] M. Uiberacker, T. Uphues, M. Schultze, A.J. Verhoef, V. Yakovlov, M.F. Kling, J. Rauschenberger, N.M. Kabachnik, H. Schröder, M. Lezius, K.L. Kompa, H.G. Mullar, M.J.J. Vrakking, S. Hendel, U. Kleineberg, U. Heinzmann, M. Drescher and F. Krausz, Nature 446, 627 (2007).

[100] M. Lewenstein, P. Balcou, M. Y. Ivanov, A. L'Huillier and P.B. Corkum, Phys. Rev. A 49, 2117 (1994).

[101] P.B. Corkum, Phys. Rev. Lett. 71, 1994 (1993).

[102] T.W. Hansch, Opt. Commun. 80, 71 (1990).

[103] S. Kohlweyer, G.D. Tsakiris, C.G. Wahlstrom, C. Tillman and L. Mercer, Opt. Commun. 117, 431 (1995).

[104] P.A. Norreys, M. Zepf, S. Moustaizis, A.P. Fews, J. Zhang, P. Lee, M. Bakarezos, C.N. Danson, A. Dyson, P. Gibbon, P. Loukakos, D. Neely, F.N. Walsh, J.S. Wark and D.A.E., Phys. Rev. Lett. 76, 1832 (1996).

[105] M. Zepf, G.D. Tsakiris, G. Pretzler, I. Watts, D.M. Chambers, P.A. Norreys, U. Andiel, A.E. Dangor, K. Eidmann, C. Gahn, A. Machacek, J.S. Wark and K. Witte, Phys. Rev. E 58, R5253 (1998).

Chapter 2

Nonlinear interaction of Laguerre-Gaussian laser pulses with an inhomogeneous plasma

2.1 Introduction

In this chapter, we analyze the nonlinear interaction of Laguerre-Gaussian laser pulse with an inhomogeneous parabolic plasma channel. The nonlinearity depends upon the beam and plasma parameters. The Chirped Pulse Amplification (CPA) technology has made it possible to have the ultra-intense ($\approx 10^{23}$ W/cm^2) and ultra-short (subpicosecond duration) laser pulses, the nonlinear interaction of such pulses with plasma gives rise to several new phenomena [28, 106-114] which have not encountered so far in classical physics. In fact, it has led to a new field of physics, known as high intensity particle physics. Apart from several others, the generation of quasistatic magnetic fields [115-121] has drawn tremendous interest as the field could have a strong influence on the overall plasma dynamics. The generation of axial magnetic field due to the various phenomena has already been reported by many [122, 123].

The numerical simulations carried by S.C. Wilks *et al*. [2] predict extremely high self generated magnetic fields (≈ 250 MG). These immense fields of such high strength cannot be properly explained by the existing theories. Sudan [124] suggested that the spatial gradient and the non-stationary character of the ponderomotive force may lie in the origin of such strong magnetic fields. Tripathi and Liu [125] have reported a non-relativistic two dimensional treatment of self-generated magnetic field in an underdense inhomogeneous plasma. Sheng and Meyer-ter-Vehn [126] derived an expression for the magnetic field of the order of magnitude ~100 MG in an overdense plasma. Gorbunov and Ramazashvili [127] investigated the magnetic field generated in a homogeneous plasma due to interaction of a circularly polarized short laser pulse. Haines [128] has reported the magnetic field of tens of MG due to an ultra-intense ultra-short

circularly polarized laser pulse. The phenomenon becomes more important, particularly when it is very relevant to hybrid-inertial confinement fusion [129].

In general, the laser beams are circularly polarized or rotational symmetric about the beam axis. The wave vectors and the angular momentum are directed along the axis. However, any distortion in the rotational symmetry may produce helical wavefronts and gain an extrinsic orbital angular momentum in addition to the spin angular momentum. Thus, the photon beam possesses both the spin and orbital angular momentum due to their polarization and angular phase structure respectively.

The helical wavefronts can be represented in a basis set of orthogonal Laguerre-Gaussian mode ($LG_p^{|l|}$), where |l| and p refer to the azimuthal and radial modes of the beam respectively. A well defined state of an orbital angular momentum (OAM) is associated with each of the Laguerre-Gaussian (LG) mode [54]. In the LG laser beam, the equation for the radial electric field is proportional to the product of the Gaussian function and associated Laguerre polynomial ($L_p^{|l|}$). When |l| = p = 0, the beam is Gaussian. When |l| is greater than zero, the electric field has an azimuthal phase change of 2π |l|. The beam not only exerts longitudinal force when it impinges on any dielectric medium but also exerts a transverse force in the radial and azimuthal directions. The azimuthal force causes a torque on the dielectric (plasma) with a corresponding transfer of the angular momentum from beam to the dielectric (plasma electrons). The paraxial photon beam can appropriately be described by a linear superposition of LG functions providing a natural orthonormal basis for the beam representation.

When a laser pulse impinges on the plasma, it produces an electron current and thus generates the magnetic field [130, 131]. Laser photon carries momentum in the direction of propagation regardless of their polarization. It is believed that finite contribution of the orbital angular momentum in laser plasma interaction leads to strong rotational motion to the electrons. The rotational motion of the electrons constitutes a nonlinear current in axial and azimuthal directions and results in the excitation of magnetic fields in the respective directions. The linearly polarized LG beam can also generate the

vorticity in plasma same as the circularly polarized laser beam leads to the generation of magnetic fields.

Nonlinear interaction of higher order Gaussian beams and their consequences in terms of transfer of the orbital angular momentum to plasma and excitation of axial magnetic field (B_z) and transverse azimuthal magnetic field (B_φ) have been analyzed in this chapter. Laguerre-Gaussian beams provide the basis for discussing the new and increasingly important concept of the transfer of orbital angular momentum of photon. We have used the Proca equation [132] and calculated the effective mass of photons in plasma. The coupling of angular momentum to plasma for the different Laguerre-Gaussian beams and their effect on the magnetic field generation is analyzed. The electric and magnetic fields components are computed in terms of different LG potential mode. It is shown that the generated magnetic field is not quasistatic and its magnitude depends on the order of laser beam mode, beam intensity, plasma density and laser frequency. In the present treatment, both the longitudinal and the transverse plasmon mode have been considered for the transfer of orbital angular momentum whereas in the earlier models [133] only the longitudinal mode was taken into account.

This chapter is organized as follows. In section 2.2, an analytical treatment of interaction of the circularly polarized Laguerre-Gaussian laser beam with plasma is outlined. In section 2.3, the governing equations for the transfer of orbital angular momentum and effective mass of photons in plasma are derived. We also present the essential formalism for the generation of magnetic fields B_z and B_φ for different azimuthal angles (φ) and beam intensities (I). In section 2.4, the results are analyzed numerically and compared with the results of 2D particle-in-cell (PIC) simulation of the Laguerre-Gaussian mode of laser beam. It is concluded that the excitations of B_z and B_φ are possible with both the linearly polarized and the circularly polarized laser beam. Summary of results are given in section 2.5.

2.2 Field structure of a Laguerre-Gaussian pulse in an inhomogeneous plasma

The magnetic vector potential [207] for a circularly polarized Laguerre-Gaussian laser pulse is written as

$$\boldsymbol{A}(r,\varphi,z,t) = \frac{\hat{e}_r \pm \iota\, \hat{e}_\varphi}{\sqrt{2}}\; A_{p|l|}(r,\varphi,z)\; e^{-i\left(\omega t - \int_0^z k dz\right)}, \tag{2.1}$$

where $A_{p|l|}(r, \varphi, z)$ is a potential function for LG mode, $\hat{e}_r$ and $\hat{e}_\varphi$ are the unit vectors in radial and azimuthal directions, ± refers to left circularly polarized (LCP) and right circularly polarized (RCP) laser beams respectively.

The wave vector k(z) [108] of the laser pulse is

$$k(z) = \sqrt{\left(\frac{\omega^2}{c^2}\right)\left(1 - \left(\frac{\omega_{p0}^2}{\omega^2}\right)\left(1 + \frac{\delta n(r,\varphi,z)}{n_0} \times \frac{r^2}{r_0^2}\right)\right)},$$

where ω is the frequency of the laser beam, $\omega_{po} = \sqrt{4\pi n_0 e^2/\gamma m}$ is the unperturbed plasma frequency, δn(r,φ,z) is perturbation in the plasma density, $\gamma = \sqrt{(1+\alpha^2)}$ is the relativistic factor, $\alpha = eA/mc^2$ is the normalized vector potential.

In terms of vector potential **A**, the magnetic and electric fields are given by

$$\boldsymbol{B} = (\nabla \times \boldsymbol{A}), \tag{2.2}$$

$$\boldsymbol{E} = -\frac{i\omega}{c}\left[\boldsymbol{A} + \left(\frac{1}{k^2}\right)\nabla(\nabla \cdot \boldsymbol{A})\right]. \tag{2.3}$$

The normalized potential function a has the appropriate form as

$$a = a_{p|l|}(r,\varphi)\; \frac{w_0}{w(z)}\; e^{-\frac{r^2}{w(z)^2}}\; e^{-i\left(\frac{k(z)r^2}{2R(z)}\right)}. \tag{2.4}$$

In equation (2.4), $a_{p|l|}(r,\varphi)$ is the transverse laser profile normalized to peak field α_0 and is given as

$$a_{p|l|}(r,\varphi) = a_{0,p|l|}\,(-1)^{|l|}\; \left(\frac{r\sqrt{2}}{w(z)}\right)^{|l|}\; L_p^{|l|}\left(\frac{2r^2}{w(z)^2}\right)\; e^{i\{(2p+|l|+1)\psi + |l|\varphi\}}, \tag{2.5}$$

where $a_{0,p|l|}$ is the amplitude coefficient, R(z) is the radius of curvature of the wavefront, w(z) is the radius at which the Gaussian term falls 1/e of its axis value, $(2p+|l|+1)\psi$ is Gouy phase, p and |l| are the radial and azimuthal index of the LG mode respectively, r is the radius of beam, φ is the azimuthal angle and $L_p^{|l|}(2r^2/w^2(z))$ is the generalized Laguerre polynomial.

The approximate description of $a_{p|l|}(r,\varphi,z)$ given in equation (2.4) is valid in the paraxial approximation $r^2 << z^2$. Also, $a_{p|l|}(r,\varphi,z)$ is assumed to vary slowly with z in comparison with the phase factor $\exp(-i(\omega t-\int kdz))$, that is $|\partial/\partial z\ \alpha_{p|l|}(r,\varphi,z)| << |k\alpha_{p|l|}(r,\varphi,z)|$.

Normalizing the amplitude $\alpha_{p|l|}$

$$\int_o^\infty \int_o^{2\pi} \left|a_{p|l|}(r,\varphi)\right|^2 dr\, d\varphi \ = \ 1. \tag{2.6}$$

Using the normalization condition, the value of the amplitude coefficient is obtained as [134]

$$a_{0,p|l|} = \frac{a_0}{\sqrt{1+\delta_{0|l|}}}\sqrt{\left\{\frac{(p+|l|)!}{4\pi\ p!}\right\}}, \tag{2.7}$$

where $\delta_{0|l|}$ is Kronecker delta function such that $\delta_{0|l|} = 1$ for $|l| = 0$ and $\delta_{0|l|} = 0$ for $|l| \neq 0$.

Here, $\alpha_{p|l|}(r,\varphi) = \alpha$ satisfies the following equation in plasma channel of the form $n(r) = n_0\left(1 + \frac{\Delta n(r,\varphi,z)}{n_0} \times \frac{r^2}{r_0^2}\right)$,

$$\left(\nabla_\perp^2 - 2\imath k(z)\frac{\partial}{\partial z} - \frac{\omega_p^2}{c^2}\right)a = 0\ , \tag{2.8}$$

where we assume that $\partial^2\alpha/\partial z^2 << 2\imath k(z)\,\partial\alpha/\partial z$ and $2\imath\partial^2 k/\partial z^2$ and $\alpha_{p|l|}(r,\varphi,z) = \alpha$, and $\omega_p^2 = \omega_{p0}^2(1+\delta(r,\varphi,z)r^2/r_0^2)$, here $\delta(r,\varphi,z) = \Delta n(r,\varphi,z)/n_0$ is the perturbation in the plasma at a distance r from the laser beam axis, r_0 is the channel radius and n_0 is the unperturbed density of the plasma.

The dispersion relation for the laser beam is

$$c^2k^2(z) = \omega^2 - \omega_{p0}^2\left(1 + \frac{\delta(r,\varphi,z)r^2}{r_0^2}\right). \quad (2.9)$$

The magnetic and electric fields can be derived with the help of equations (2.1-2.5) and are given as

$$\boldsymbol{B} = \left(-\frac{\iota\omega mca_0\sqrt{2}}{e}\right)\left(\frac{w_0}{w(z)}\right) e^{-\iota\left(\frac{r^2}{w(z)^2}+\frac{kr^2}{2R(z)}\right)}\left(\frac{r}{w(z)}\right)^{\frac{|l|}{2}} \left[\left\{\frac{-4r}{kw(z)^2} L_{|l|+p}^{|l|-1}(\rho^2) + \frac{|l|}{kr} L_p^{|l|}(\rho^2) - \left(\frac{2r}{kw(z)^2} - \frac{r}{R(z)} L_p^{|l|}(\rho^2)\right) - \frac{\cos\varphi}{rk}|l| L_p^{|l|}(\rho^2)\right\} sin\,\varphi\, \hat{e}_z + \left(\hat{e}_r \pm \iota\hat{e}_\varphi\right)\frac{r}{R(z)} sin\,\varphi\right] e^{\iota|l|\varphi}\, 2^{|l|}(-1)^{|l|}\, e^{-\iota\left(\omega t - \int_0^z kdz\right)}, \quad (2.10)$$

$$\boldsymbol{E} = \left(-\frac{\iota\omega mc\, a_0\sqrt{2}}{e}\right)\left(\frac{w_0}{w(z)}\right) e^{-\iota\left(\frac{r^2}{w^2(z)}+\frac{kr^2}{2R(z)}\right)}\left(\frac{r}{w(z)}\right)^{\frac{|l|}{2}} \left[\left(\frac{-4r}{kw(z)^2} L_{|l|+p}^{|l|-1}(\rho^2) + \frac{|l|}{kr} L_p^{|l|}(\rho^2) - \left(\frac{2r}{kw(z)^2} - \frac{r}{R(z)} L_p^{|l|}(\rho^2)\right) - \frac{sin\,\varphi}{rk}|l| L_p^{|l|}(\rho^2)\right) cos\,\varphi\, \hat{e}_z + \left(\hat{e}_r \pm \iota\hat{e}_\varphi\right)\frac{r}{R(z)} sin\,\varphi\right] e^{\iota|l|\varphi}\, 2^{|l|}\,(-1)^{|l|}\, e^{-\iota\left(\omega t - \int_0^z kdz\right)}, \quad (2.11)$$

where $\rho^2 = 2r^2/w(z)^2$.

Equations (2.10) and (2.11) show that the electric field and the magnetic field of LG modes have longitudinal components (E_z, B_z) along with the transverse components (E_r, B_r) and (E_φ, B_φ). These relations imply that when a photon travels through plasma, it acquires an additional component of angular momentum on account of acquiring mass by the photon in plasma. This can be understood in a semi-classical way that acquiring mass along with rotation of photon in LG mode is equivalent to acquiring additional angular momentum. This component may have significant role in various stimulated scattering processes and magnetic field generation.

2.2 Orbital angular momentum transfer and magnetic field generation

Laguerre-Gaussian beams carry orbital angular momentum. This is different from the spin angular momentum. The amplitude of LG mode has an

azimuthal angular dependence of exp (±ι |l| φ)), where |l| is the azimuthal mode indices.

Analogy between the paraxial optics and quantum mechanics suggest that such modes are the eigenmodes of the angular momentum operator and carry an angular momentum of |l| ħ. Since this momentum has an azimuthal component, there is a finite longitudinal angular momentum of the beam along the direction of propagation and is proportional to ± |l|. The factor exp ±(ι|l|φ) can be considered responsible for the plasma vorticity imparting helicoidal motion to the photons.

The interaction of a photon with a spatially structured plasma, e.g., vortex, can be interpreted by an additional mass (effective mass) like term that appears in Proca-Maxwell equations. Following Anderson [135] and using the Proca equation

$$((\Box - c^2\,\mu_\gamma^2/\hbar^2)\,(\mathbf{E} + \nabla\Phi) = -4\pi en(r)/c^2\,\partial\mathbf{v}/\partial t$$

and equation (2.8), we get the following relation for the effective mass of the photon in an inhomogeneous plasma for LG beam.

$$\frac{c^2\mu_\gamma^2}{\hbar^2}\left(1+\frac{\hat{\boldsymbol{v}}.\boldsymbol{\nabla\Phi}}{|E|}\right)+\frac{4\pi en\,(r)\delta\dot{v}}{c^2|E|}-\;4\pi\;\frac{\hat{\boldsymbol{v}}.\Box(\boldsymbol{\nabla\Phi})}{|E|}\;\;=\frac{\omega_p^2}{c^2}\;(1+cos\;(|l|\varphi+\;kz)),\quad(2.12)$$

where μ_γ is the effective mass acquired by a photon in an inhomogeneous plasma, $\Phi(r) = \Phi_0\;\alpha_{p|l|}(r,\varphi,z)\;e^{(\,\pm\,i\,|\,l\,|\,\varphi)}\;e^{-\iota(\omega t-kz)}$ is the scalar potential and $\hat{\mathbf{v}} = \mathbf{v}/v$ is unit velocity vector in an arbitrary direction and $\delta\dot{v}$ is variation in the time derivative of the velocity.

The effective mass of a photon may be written as

$$\mu_\gamma^2\;=\;\frac{E}{E+\hat{\boldsymbol{v}}\cdot\boldsymbol{\nabla\varphi}}\left[\frac{\hbar^2\omega_{p0}^2}{c^4}\left(1+\delta(r,\varphi,z)\frac{r^2}{r_0^2}\right)\left(1+cos(|l|\varphi+\;kz)\right)\right]\;-\frac{1}{E+\hat{\boldsymbol{v}}\cdot\boldsymbol{\nabla\varphi}}$$

$$\times\left[\frac{4\pi\hbar^2e\delta\dot{v}n_0}{c^4}\left(1\;+\frac{n(r)}{n_0}\;cos(|l|\varphi+\;kz)\right)\right].\qquad(2.13)$$

Equation (2.13) is simplified to obtain

$$\mu_\gamma^2 = \frac{a}{a+\frac{\omega_p^2}{\omega^2}}\left[\frac{\hbar^2\omega_{p0}^2}{c^4}\left(1+\delta(r,\varphi,z)\frac{r^2}{r_0^2}\right)\left(1+cos(|l|\varphi+kz)\right)\right] - \frac{\delta a}{a+\frac{\omega_p^2}{\omega^2}}$$

$$\times\left[\frac{\hbar^2\omega_p^2}{c^4}\left(1+\frac{n(r)}{n_0}cos(|l|\varphi+kz)\right)\right]. \quad (2.14)$$

Obviously, the mass acquired by a photon in a plasma depends on the degree of spatial homogeneity and hence, on the plasma frequency ω_p. It is further observed that the effective mass is less than what has been ascribed by the Proca equation. The term $|l|\varphi$ ensures here that the orbital angular momentum changes the characteristic properties of a photon in a plasma and, hence, the interaction mechanism.

Since $a \gg \delta a$, neglecting the second term in equation (2.14), we obtain

$$\mu_\gamma^2 = \frac{a}{a+\frac{\omega_p^2}{\omega^2}}\left[\frac{\hbar^2\omega_{p0}^2}{c^4}\left(1+\delta(r,\varphi,z)\frac{r^2}{r_0^2}\right)\left(1+cos(|l|\varphi+kz)\right)\right]. \quad (2.15)$$

A photon has spin 1 ħ and in a circularly polarized light these spins are aligned, so the beam of a finite radius has a spin angular momentum. Following Beth [136], axial and azimuthal components of the spin angular momentum density for the circularly polarized light can be given as

$$J_z = \pm\frac{r}{\omega c}\frac{\partial I(r,\varphi)}{\partial r} \quad (2.16a)$$

and $J_\varphi = \pm\frac{r\sin\varphi}{\omega c}\frac{\partial I(r,\varphi)}{r\partial\varphi}$. (2.16b)

In addition to the spin angular momentum, the photon also acquires orbital angular momentum (OAM). The axial and azimuthal components of the orbital angular momentum density in terms of the effective mass of photon are written as

$$L_z = \pm\left(|l|\frac{I(r,\varphi)}{\omega c} \mp \mu_\gamma\, rc\cos\varphi\right) \quad (2.17a)$$

and $L_\varphi = \pm\sin\varphi\left(|l|\frac{I(r,\varphi)}{\omega c} \mp \mu_\gamma\, rc\right)$, (2.17b)

where the quantity μ_γ rc cos φ is the axial component of the angular momentum density of a photon due to its effective mass in the plasma which couples with

plasmon electrostatic mode to impart orbital angular momentum. The component of total angular momentum density **M** = **L** + **J** of a plasmon at relativistic intensities of light can be written as

$$M_z = \pm \left(\frac{r}{\omega c} \frac{\partial I(r,\varphi)}{\partial r} + |l| \frac{I}{\omega c} \mp \mu_\gamma rc \cos\varphi \right) \quad (2.18a)$$

and $M_\varphi = \pm \sin\varphi \left(\frac{1}{\omega c} \frac{\partial I(r,\varphi)}{\partial \varphi} + |l| \frac{I}{\omega c} \mp \mu_\gamma rc \right)$. (2.18b)

In order to derive expressions for B_z and B_φ, we have assumed that the response time of the background ions in the plasma is much more than the plasma electrons. On such a time scale the ion motion may be reasonably neglected in comparison to the electron motion. It is also assumed that the collision frequency is much less than ω_p.

Using the conservation of angular momentum, the average rate of change of plasmon angular momentum in presence of the photon angular momentum can be written as

$$-e\, rE_z - \frac{1}{n} \frac{dM_\varphi}{dt} = 0 \quad (2.19a)$$

and $-e\, rE_\varphi - \frac{1}{n} \frac{dM_z}{dt} = 0$, (2.19b)

where M_z and M_φ are axial and azimuthal components of total angular momentum density.

Following Haines [129], equations (2.19a) and (2.19b) can be written as

$$rE_z = -\frac{r\omega}{en L_z} M_\varphi \quad (2.20a)$$

and $rE_\varphi = -\frac{\omega}{en} M_z$ respectively, (2.20b)

where L_z is the interaction length.

Using Faraday's law, the axial and the azimuthal components of the electric field and magnetic field can be expressed as

$$\frac{1}{r}\frac{\partial}{\partial r}\left(rE_{\varphi}\right) = -\frac{1}{c}\frac{\partial B_z}{\partial t} \tag{2.21a}$$

and $\frac{\partial E_z}{\partial r} = \frac{1}{c}\frac{\partial B_{\varphi}}{\partial t}$. (2.21b)

Substituting equation (2.20b) in equation (2.21a), equation (2.20a) in equation (2.21b) and using equation (2.18), we obtain

$$\frac{\partial B_z}{\partial t} = \pm\frac{1}{en}\frac{1}{r}\frac{\partial}{\partial r}\left(r\frac{\partial I}{\partial r} + |l|I \mp \mu_{\gamma} r\omega c^2 cos\,\varphi\right), \tag{2.22}$$

$$\frac{\partial B_{\varphi}}{\partial t} = \mp\frac{\sin\varphi}{en L_z}\frac{\partial}{\partial r}\left(\frac{\partial I}{\partial \varphi} + |l|I \mp \mu_{\gamma} r\omega c^2\right). \tag{2.23}$$

After integration of the equations (2.22) and (2.23), we have

$$B_z = \pm\frac{1}{e\omega n}\frac{1}{r}\frac{\partial}{\partial r}\left(r\frac{\partial I}{\partial r} + |l|I \mp \mu_{\gamma} r\omega c^2 cos\,\varphi\right), \tag{2.24}$$

$$B_{\varphi} = \mp\frac{\sin\varphi}{e\omega n\, L_z}\frac{\partial}{\partial r}\left(\frac{\partial I}{\partial \varphi} + |l|I \mp \mu_{\gamma} r\omega c^2\right). \tag{2.25}$$

To estimate B_z and B_{φ}, we assume $\partial/\partial r = 1/r$ and $r = w_0$. Equation (2.24) can be written as

$$B_z = \left(\frac{1}{e\omega n\, w_0^2}\right)\left[(|l| \pm 1)I \mp \mu_{\gamma} w_0 \omega c^2 cos\,\varphi\right]. \tag{2.26}$$

Similarly, we have the following form of the azimuthal magnetic field

$$B_{\varphi} = -2\pi\,\sin\varphi\,\left(\frac{1}{e\omega n\, L_z w_0}\right)\,\left[(|l| \pm 1)I \mp \mu_{\gamma} w_0 \omega c^2\right]. \tag{2.27}$$

The LG normalized potential function α(r,φ) in the focal plane (z = 0) of the beam can be obtained from equation (2.1) and equation (2.4) and is written as

$$a(r,\varphi) = \frac{a_0}{\sqrt{1+\delta_{0|l|}}}\sqrt{\frac{(p+|l|)!}{4\pi p!}}\,(-1)^l\,\left[\frac{\sqrt{2}r}{w_0}\right]^{|l|} L_p^{|l|}\left(\frac{2r^2}{w_0^2}\right) e^{-\frac{r^2}{w_0^2}} cos\,(|l|\varphi). \tag{2.28}$$

The laser intensity profile in the focal plane (z = 0) can be expressed as

$$I(r,\varphi) = I_0\,(-1)^{2|l|}\left(\frac{(p+|l|)!}{4\pi p!}\right)\rho^{2|l|}\,L_p^{|l|}(\rho^2)\,e^{-\rho^2}\,cos^2(|l|\varphi), \tag{2.29}$$

where $I_0 = a_0^2 \frac{1}{(1+\delta_{0|l|})}$ is the maximum intensity of laser pulse, $\rho^2 = 2r^2/w_0^2$ and $\alpha_0 = eA_0/mc^2$ is the maximum amplitude of the laser pulse.

2.4 2D PIC simulation results

The magnetic field generation due to the exchange of angular momentum between photons of the laser pulse and the plasma electrons depends on the radial and azimuthal modes. For circularly polarized Gaussian laser pulse $|l| = 0$ and $p = 0$.

Using Equation (2.29), the intensity profile of Gaussian laser beam ($|l| = 0$, $p = 0$) can be written as

$$I(r,\varphi) = I_0 \exp(-\rho^2), \tag{2.30}$$

where we have used $L_0^0(\rho^2) = 1$. This yields the following relations for B_z and B_φ

$$B_z = \left(\frac{1}{e\omega n\, w_0^2}\right)\left[I_0 e^{-\rho^2} \mp \mu_\gamma w_0 \omega c^2 \cos\varphi\right] \text{ and} \tag{2.31}$$

$$B_\varphi = -2\pi \sin\varphi \left(\frac{1}{e\omega n\, L_z w_0}\right)\left[I_0 e^{-\rho^2} \mp \mu_\gamma w_0 \omega c^2\right]. \tag{2.32}$$

These results match the relativistic two dimensional (2D) PIC simulation [114] for the normalized vector potential α (= eA/mc^2) which varies from $\alpha = 1.0$ to 4.0, where A, c, e and m are vector potential, speed of light, charge and mass of the electron respectively. We have taken a typical set of parameters for a laser pulse, e. g., intensity ranging from 1.0×10^{18} -1.3×10^{19} W/cm^2, central wavelength $\lambda = 1$ μm, spot size $w_0 = 50$ μm and pulse duration 33 fs. We have considered the profile of the plasma density as $n = n_0\left(1 + \frac{\Delta n}{n_0}\frac{r^2}{r_0^2}\right)$, where the unperturbed plasma density is $n_0 \approx 10^{19}$ cm^{-3}, r is radial distance and r_0 is the channel radius. The dimensions of the simulation box are 400 × 200 μm^2. The simulation box moves and scans 8000 × 400 cells with five particles per cell.

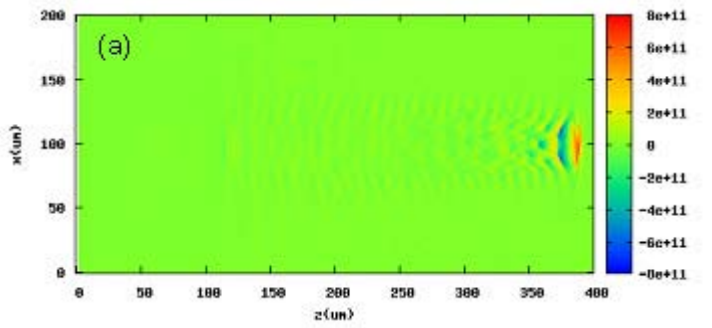
(a)
x(um)
z(um)
8e+11
6e+11
4e+11
2e+11
0
-2e+11
-4e+11
-6e+11
-8e+11

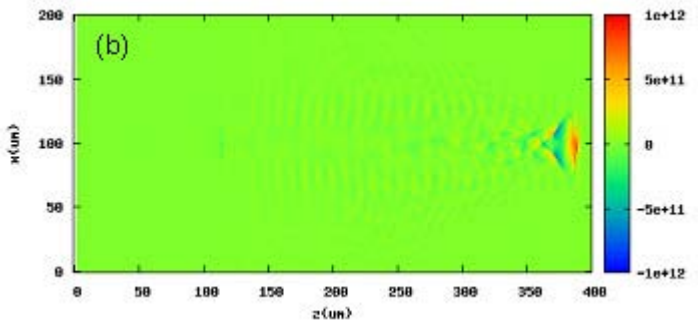
(b)
x(um)
z(um)
1e+12
5e+11
0
-5e+11
-1e+12

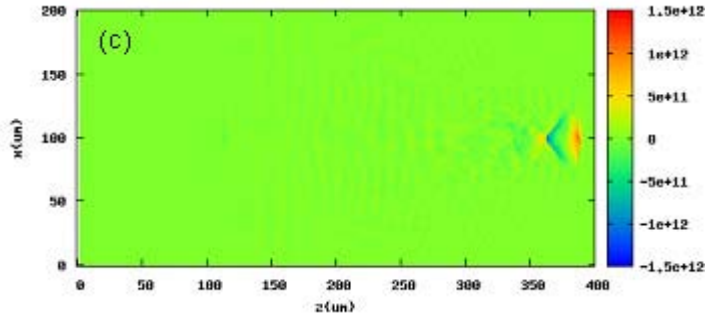
(c)
x(um)
z(um)
1.5e+12
1e+12
5e+11
0
-5e+11
-1e+12
-1.5e+12

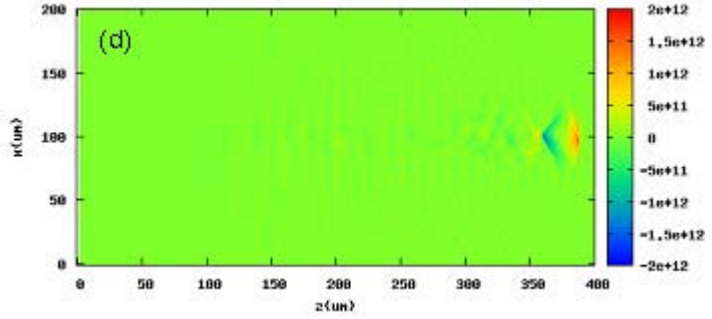
(d)
x(um)
z(um)
2e+12
1.5e+12
1e+12
5e+11
0
-5e+11
-1e+12
-1.5e+12
-2e+12

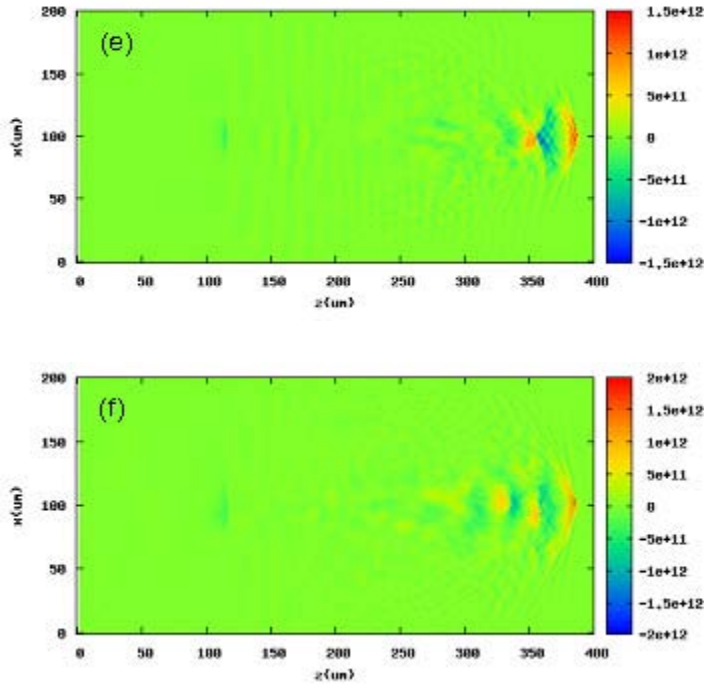

Figure 2.1: The laser pulse evolution in the parabolic channel for |ℓ| = 0, p = 0 (a) a =1.0 (b) a = 1.5 (c) a = 2.0 and for |ℓ| = 1, p = 0 (d) a = 1.0 (e) a = 2.0 and (f) a = 3.0 for plasma density n = 1.2×10^{24} m^{-3}.

The results are shown in Figures 2.1 -2.12. It is found that the magnitudes of the generated magnetic fields B_φ and B_z depend on the laser mode, plasma density, laser frequency and the vector potential α. The strength of the magnetic fields depends on the type of the polarization of laser field. It is observed that dynamics of coupling of OAM with plasma fluid depends on the effective mass of photons leading to the change in magnitude of generated magnetic field.

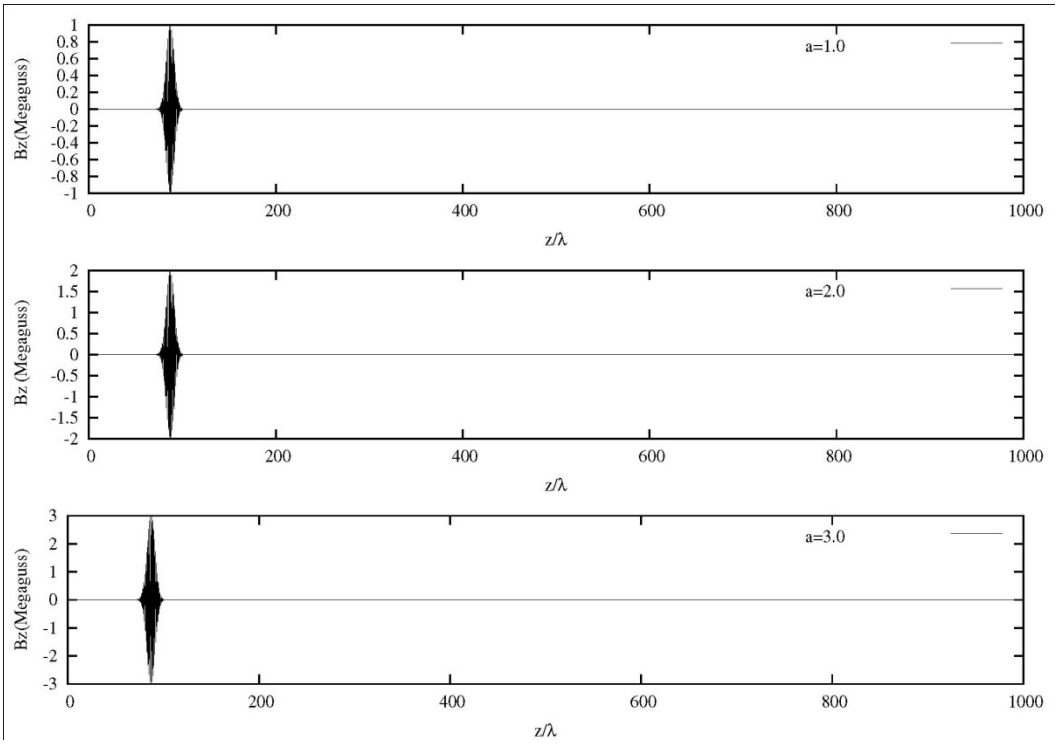

Figure 2.2: Axial magnetic field generation due to left circularly polarized laser beam (|l| = p = 0) for (a) a = 1.0 (b) a = 2.0 (c) a = 3.0 and plasma density $n=1.2\times10^{24}$ m^{-3}.

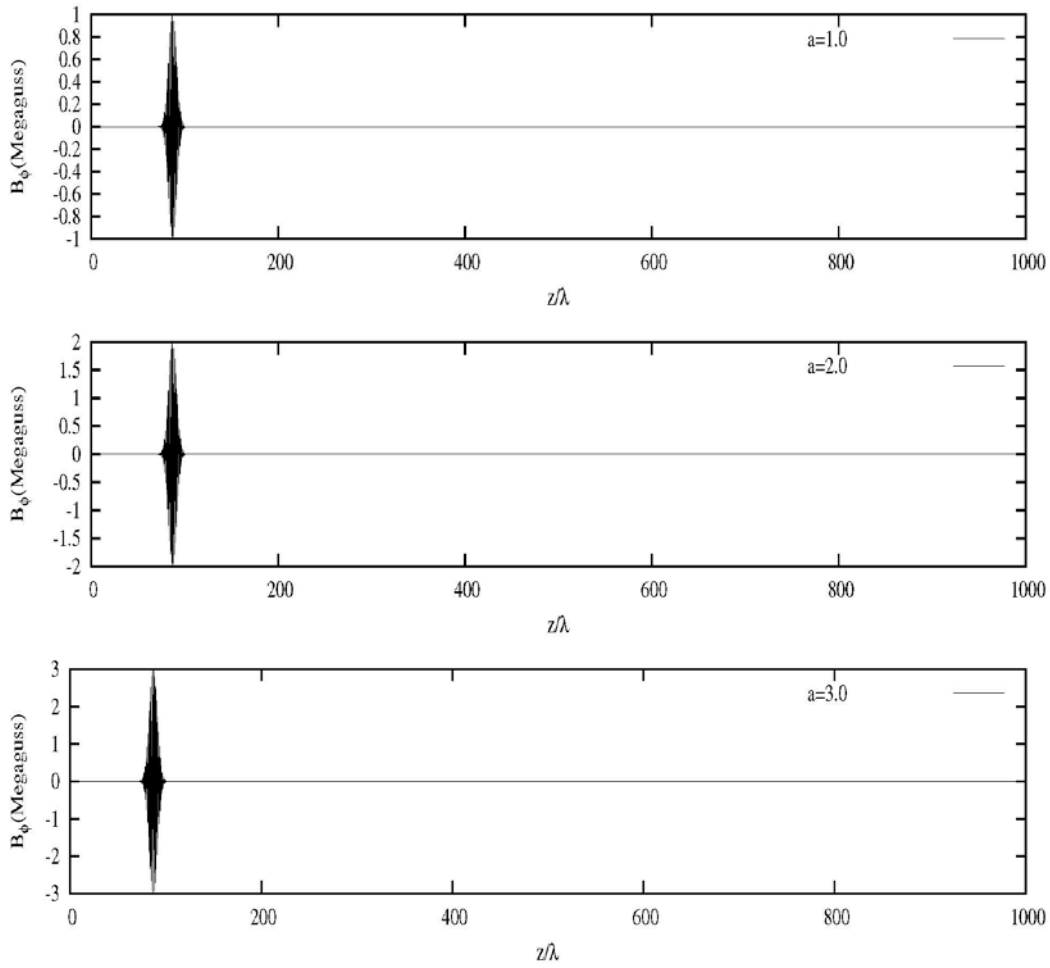

Figure 2.3: Azimuthal magnetic field generation due to left circularly polarized laser beam (|l| = p = 0) for (a) a = 1.0 (b) a = 2.0 (c) a = 3.0 and plasma density $n=1.2\times10^{24}$ m^{-3}.

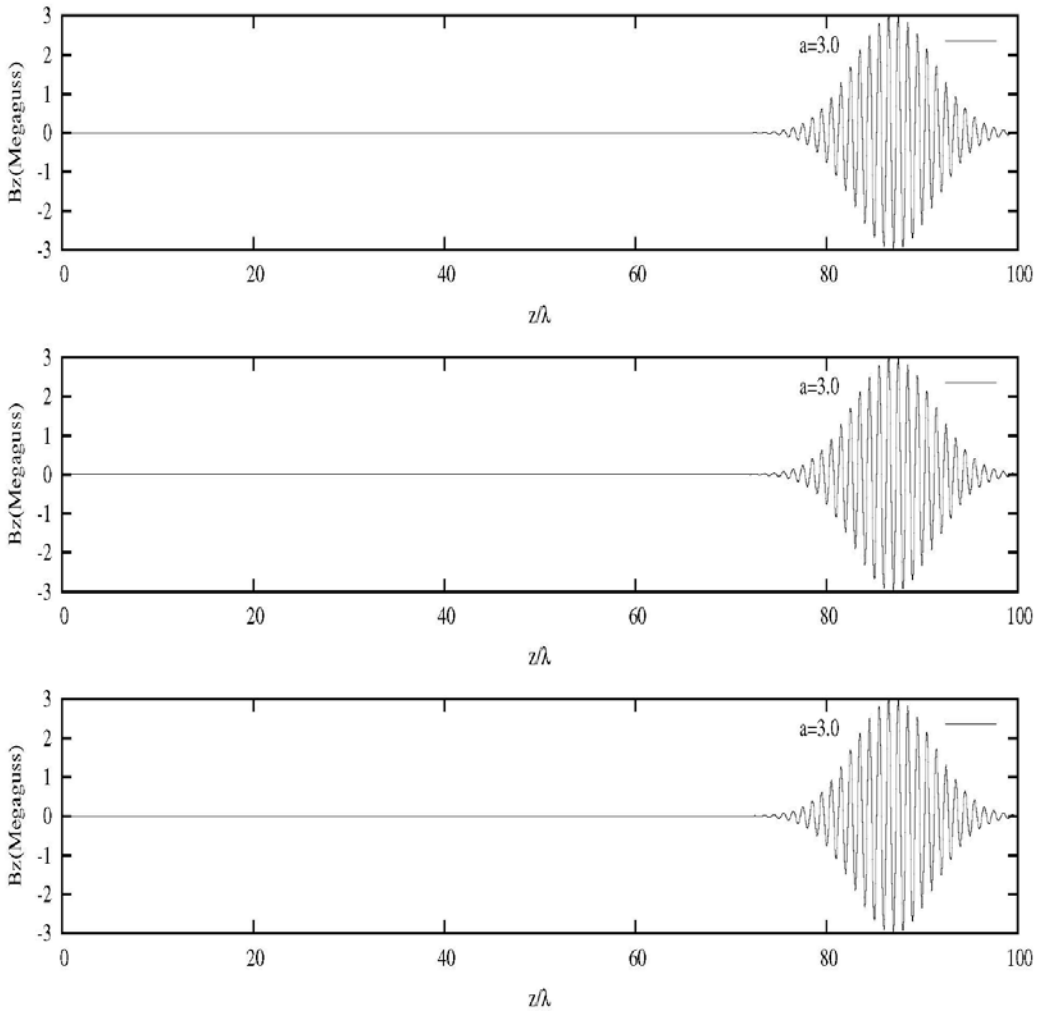

Figure 2.4: Axial magnetic field generation due to left circularly polarized laser beam ($|l| = p = 0$) for a = 3 and plasma densities (a) $n=1.2\times10^{24}$ m^{-3} (b) $n=2.24\times10^{23}$ m^{-3} and (c) $n=2.22\times10^{21}$ m^{-3}.

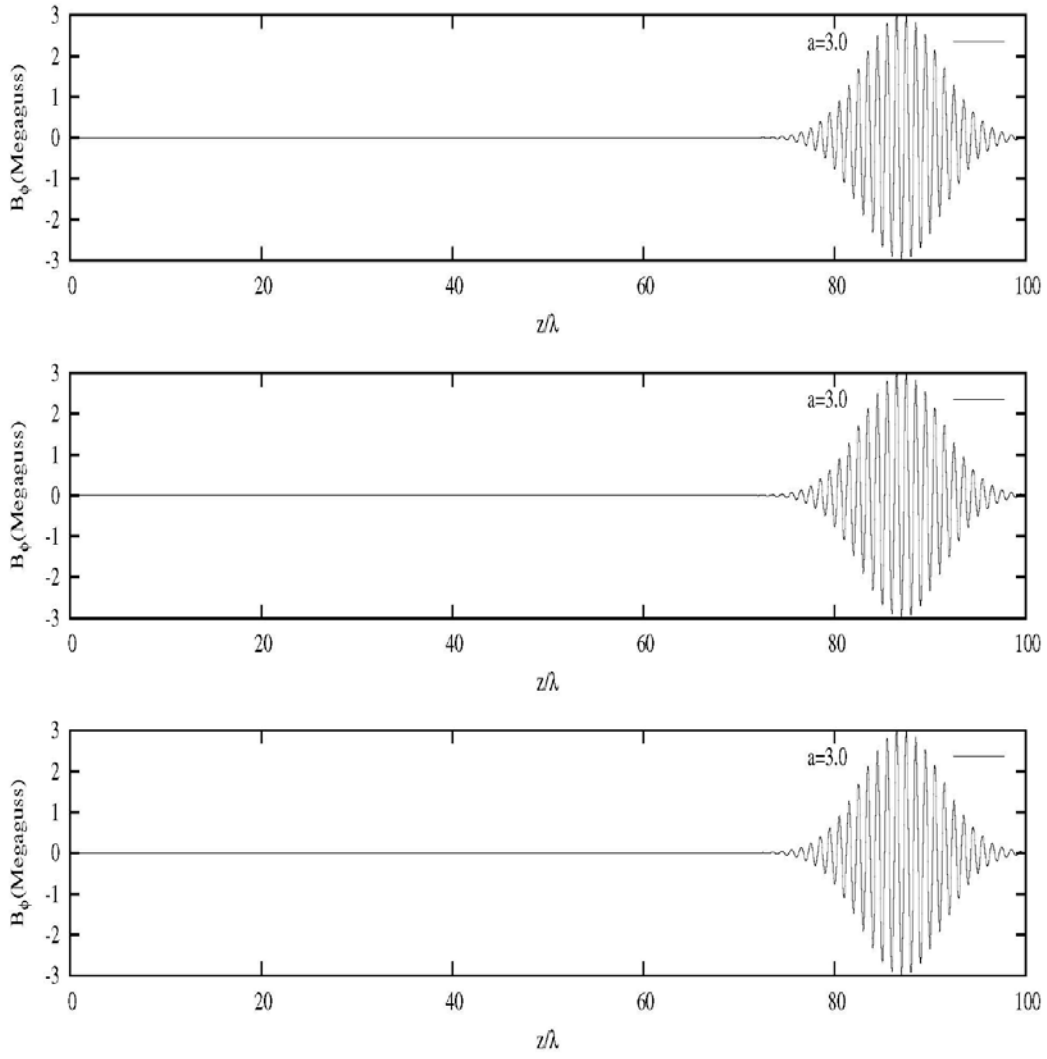

Figure 2.5: Azimuthal magnetic field generation due to left circularly polarized laser beam (|l| = p = 0) for a = 3 and plasma densities (a) $n = 1.2 \times 10^{24}$ m^{-3} (b) $n = 2.24 \times 10^{23}$ m^{-3} and (c) $n = 2.22 \times 10^{21}$ m^{-3}.

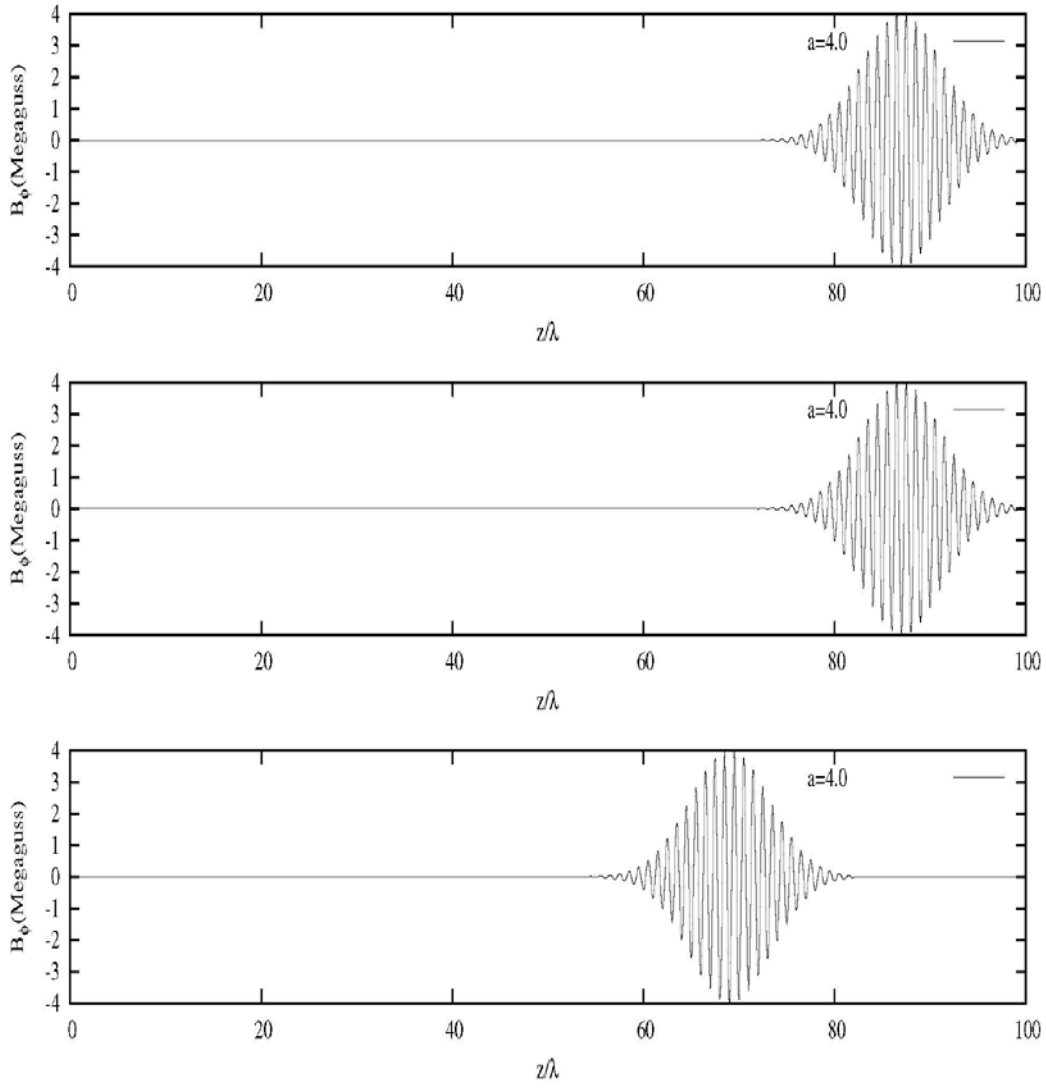

Figure 2.6: Azimuthal magnetic field generation due to left circularly polarized laser beam ($|l| = p = 0$) for $a = 4$ and plasma densities (a) $n = 1.2 \times 10^{24}$ m^{-3} (b) $n = 2.24 \times 10^{23}$ m^{-3} and (c) $n = 2.22 \times 10^{21}$ m^{-3}.

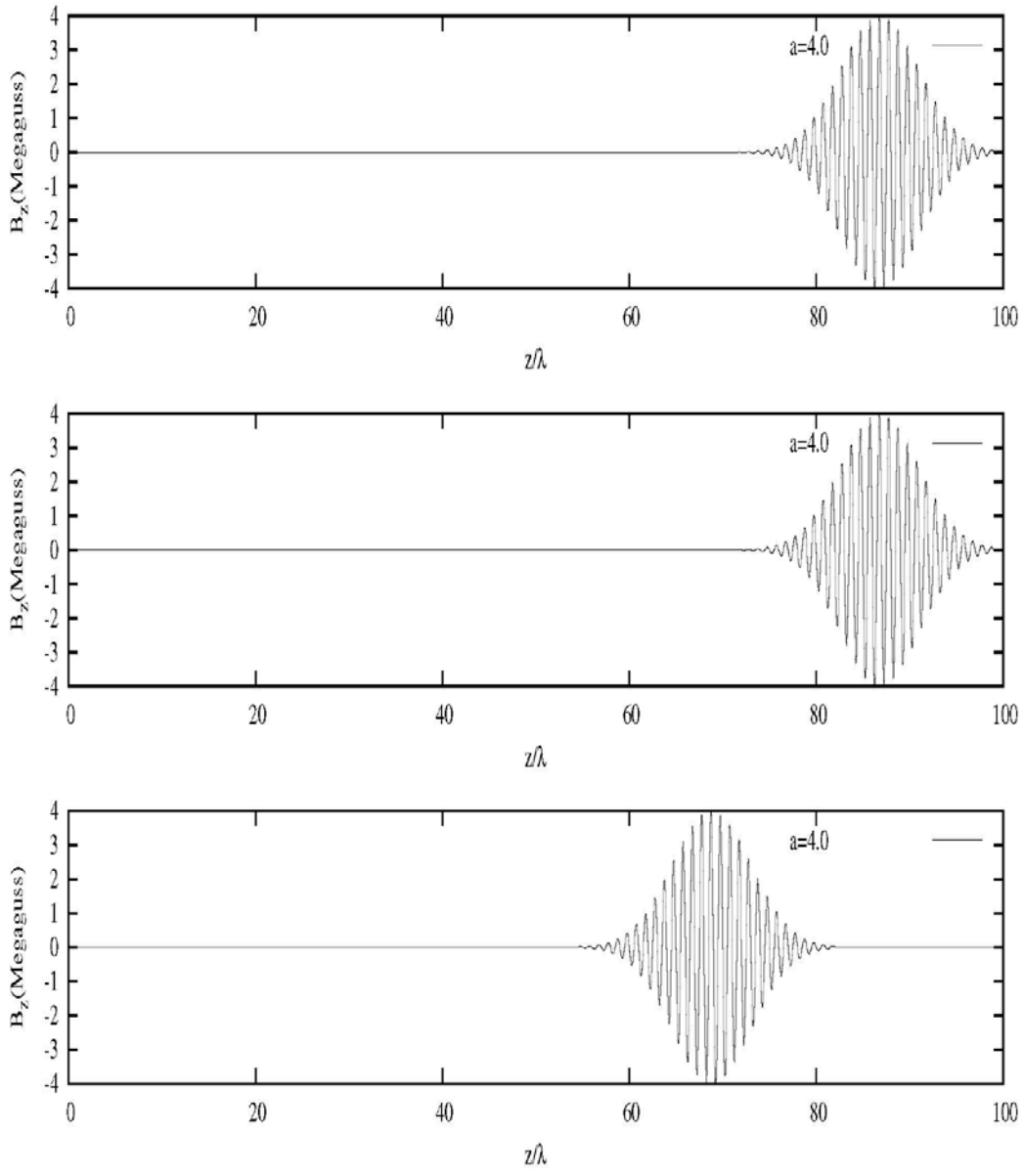

Figure 2.7: Axial magnetic field generation due to left circularly polarized laser beam ($|l| = p = 0$) for a = 4 and plasma densities (a) $n = 1.2 \times 10^{24}$ m^{-3} (b) $n = 2.24 \times 10^{23}$ m^{-3} and (c) $n = 2.22 \times 10^{21}$ m^{-3}.

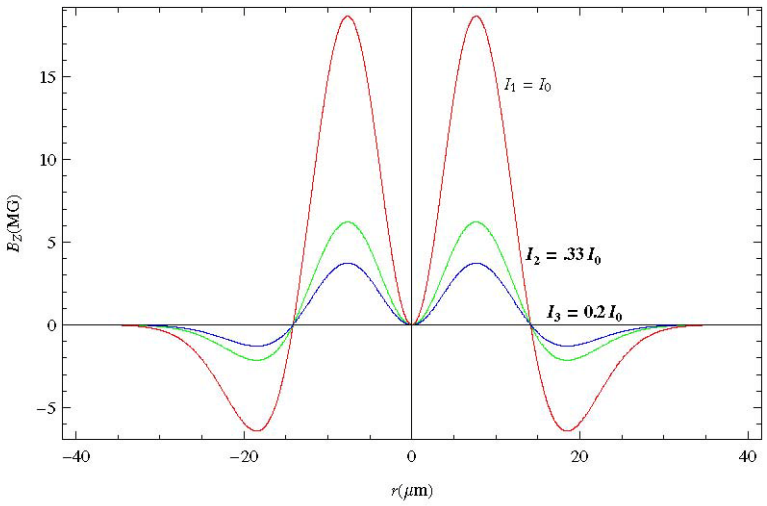

Figure 2.8: Axial magnetic field B_z due to left circularly polarized laser beam ($|l| = 1$, $p = 0$) of intensities (a) $I_1 = I_0$ (b) $I_2 = 0.33\ I_0$ and (c) $I_3 = 0.2\ I_0$.

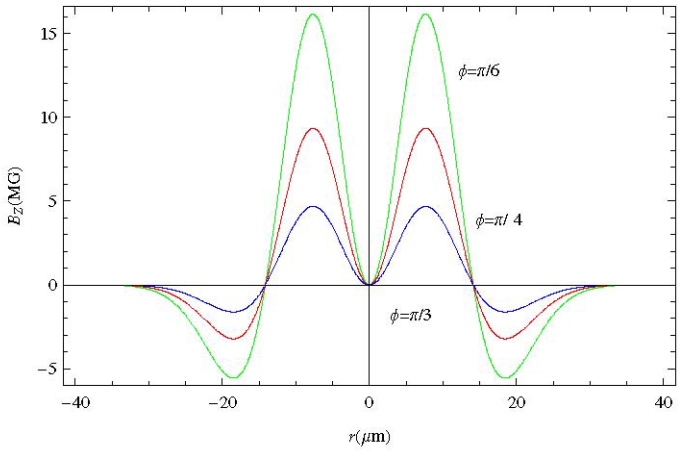

Figure 2.9: Axial magnetic field B_z due to left circularly polarized laser beam ($|l| = 1$, $p = 0$) of intensity I_0 and azimuthal angles (a) $\varphi = \pi/6$ (b) $\varphi = \pi/4$ and (c) $\varphi = \pi/3$.

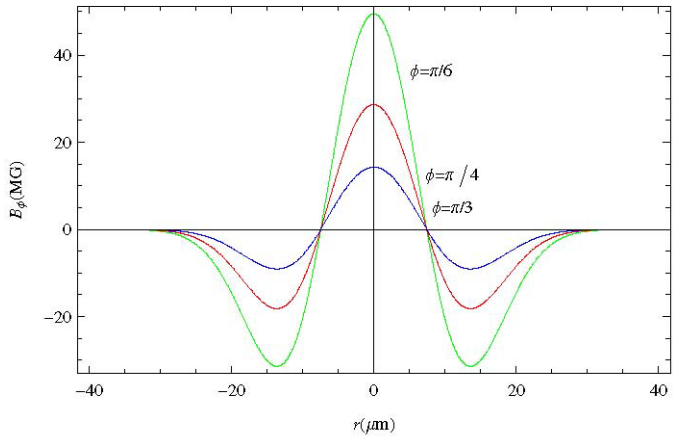

Figure 2.10: Azimuthal magnetic field B_φ due to left circularly polarized laser beam ($|l| = 1$, $p = 0$) of intensity I_0 at azimuthal angles (a) $\varphi = \pi/6$ (b) $\varphi = \pi/4$ and (c) $\varphi = \pi/3$.

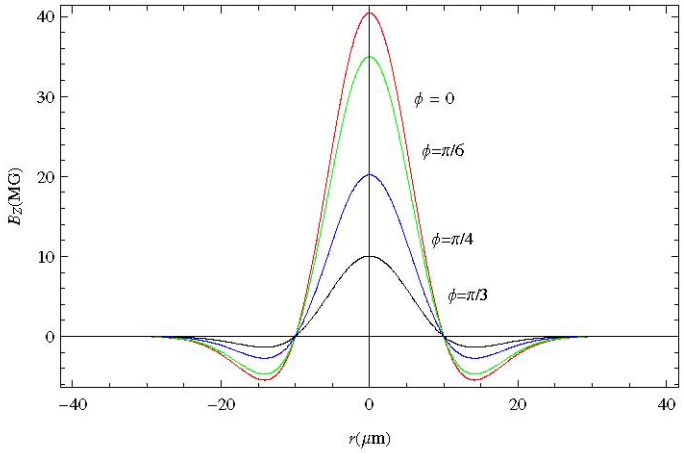

Figure 2.11: Axial magnetic field B_z of linearly polarized laser beam ($|l| = 1$, $p = 0$) of intensity $I_0 = 1.2 \times 10^{19}$ W/m^{-2} at azimuthal angles (a) $\varphi = 0$ (b) $\varphi = \pi/6$ (c) $\varphi = \pi/4$ and (d) $\varphi = \pi/3$.

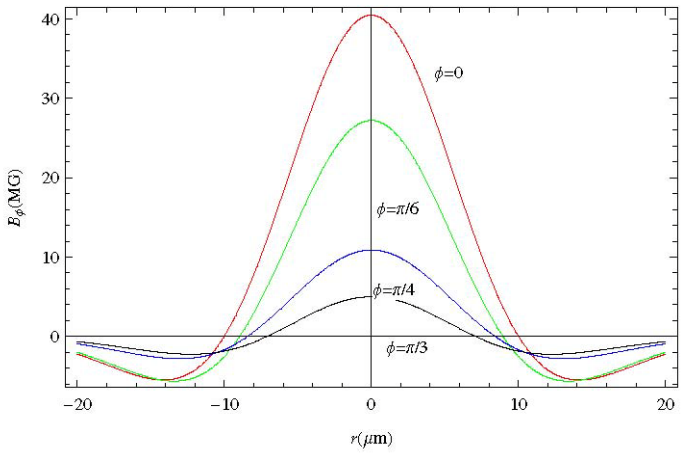

Figure 2.12: Azimuthal magnetic field B_φ due to linearly polarized laser beam (|l| = 1, p = 0) of intensity $I_0 = 1.2 \times 10^{19}$ W/m^{-2} at azimuthal angles (a) φ = 0 (b) φ = π/6 (c) φ = π/4 and (d) φ = π/3.

For |l| = 1 and p = 0, the intensity profile of LG beam can be given as

$$I(r,\varphi) = I_0\, \rho^2 \exp(-\rho^2) \cos^2\varphi. \tag{2.33}$$

Using equations (2.26), (2.27) and (2.33) relations for B_z and B_φ can be given as

$$B_z = \left(\frac{1}{e\omega n\, w_0^2}\right)\left[2I_0\, \rho^2\, e^{-\rho^2} \cos^2\varphi \mp \mu_\gamma w_0 \omega c^2 cos\, \varphi\ \right], \tag{2.34}$$

$$B_\varphi = -2\pi\ \sin\varphi\ \left(\frac{1}{e\omega n\, L_z w_0}\right)\ \left[2I_0\, \rho^2\, e^{-\rho^2} \cos^2\varphi \mp \mu_\gamma w_0 \omega c^2\right]. \tag{2.35}$$

Figures 2.8-2.12 demonstrate the variation of B_z and B_φ as a function of r for different beam intensity profiles with mode index |l| = 1 and p = 0. It is found that the generated magnetic field increases with the laser intensity. We conclude that the magnitude of the generated axial and azimuthal magnetic fields change with the mode order of $LG_p^{|l|}$ and the azimuthal symmetry.

For a linearly polarized photon beam, equation (2.34) can be rewritten as

$$B_z = \left(\frac{1}{e\omega n\, w_0^2}\right)\left[I_0\, \rho^2\, e^{-\rho^2} \cos^2\varphi \mp \mu_\gamma w_0 \omega c^2 cos\, \varphi\ \right]. \tag{2.36}$$

Figure 2.11 shows the variation of B_z as a function of r for a linearly polarized laser beam with polynomial $LG_0^{|1|}$ at different phase angles (a) φ = 0 (b) φ = π/6 (c) φ = π/4 and (d) φ = π/3. It is observed that B_z decreases on increasing φ when beam intensity is constant. The generated magnetic fields are strong for the circularly polarized laser beam than the linearly polarized beam. We further conclude that the inverse Faraday effect can also be observed in linearly polarized beams.

B_φ of a linearly polarized laser beam can be given as

$$B_\varphi = -2\pi \sin\varphi \left(\frac{1}{e\omega n L_z w_0}\right) \left[I_0 \rho^2 e^{-\rho^2} \cos^2\varphi \mp \mu_\gamma w_0 \omega c^2\right]. \quad (2.37)$$

Figure 2.12 shows the variation of B_φ as a function of r for a linearly polarized laser beam of polynomial $LG_0^{|1|}$ at different values of φ. It is seen that B_φ is not quasistatic and it decreases as φ increases for a given intensity.

2.5 Summary

A detailed analysis of angular momentum transfer and magnetic fields generation for both the linearly and circularly polarized LG beams are presented at relativistic limit. It is observed that generated magnetic fields depend on the OAM transfer and mass correction of photon in the relativistic limit. The effective mass of photons becomes more significant at higher Gaussian beam modes and plasma densities. The generated magnetic field depends on the LG beam mode, laser intensity, azimuthal angle and the relativistic gamma factor. Further, it is observed that excitation of magnetic fields is possible for both linearly and circularly polarized laser beams for different azimuthal angles. The magnitude of generated magnetic field due to circularly polarized Laguerre-Gaussian beam of higher modes decreases with increasing azimuthal angle and is greater than that of the linearly polarized beam. It is further observed that the magnetic fields generated due to higher Gaussian modes is not quasistatic but changes over some spatial distribution of plasma.

Bibliography

[2] S.C. Wilks, W.L. Kruer, M. Tabak and A.B. Langdon, Phys. Rev. Lett. 69, 1383 (1992).

[28] Z. Najmudin *et al*., Phys Rev. Lett. 87, 215004 (2001).

[106] P. Sprangle, E. Esarey and A. Ting, Phys. Rev. A 41, 4463 (1990).

[107] Philip Sprangle and Eric Esarey, 67, 2021 (1991).

[108] E. Esarey, P. Sprangle, J. Krall and A. Ting, IEEE Trans. Plasma Sci. 24, pp.252-288 (1996).

[109] P. Yadav, D.N. Gupta and K. Avinash, Discharges and Electrical Insulation in Vacuum (ISDEIV), International Symposium, pp. 657-659 (2014).

[110] H. Hamster, A. Sullivan, S. Gordon, W. White and R.W. Falcone, Phys. Rev. Lett. 71, 2725 (1993).

[111] K.P. Singh, D.N. Gupta, V.K. Tripathi and V.L. Gupta, Phys. Rev. E 69, 046406 (2004).

[112] Palavi Jha, Akanksha Saroch, Rohit Kumar Mishra and Ajay Kumar Upadhyay, Phys. Rev. ST Accel. Beams 15, 081301 (2012).

[113] M. Moshkelgosha and R. Sadighi-Bonabi, IEEE Trans. Plasma Sci. 41, pp. 1570-1574 (2013).

[114] B.S. Sharma, Archna Jain, N.K. Jaiman, D.N. Gupta, D.G. Jang, H. Suk and V.V. Kulagin, Phys. Plasmas 21, 023108 (2014).

[115] D.A. Tidman and L.L. Burton, Phys. Rev. Lett. 37, 1397 (1976).

[116] Partrick Mora and Rene Pellat, Phys. Fluids 24, 2219 (1981).

[117] R.J. Kingham and A.R. Bell, Phys. Rev. Lett. 88, 045004 (2002).

[118] Bin Qiao, X.T. He and Shao-ping Zhu, Phys. Plasmas 13, 053106 (2006).

[119] N. Naseri, V. Yu. Bychenkov and W. Rozmus, Phys. Plasmas 17, 083109 (2010).

[120] Bhuvana Srinivasan and Xian-Zhu Tang, Phys. Plasmas 19, 082703 (2012).

[121] Hong-bo Cai, Wei Yu, Shao-ping Zhu and Cang-tao Zhou, Phys. Rev. E. 76, 036403 (2007).

[122] J. Briand, V. Adrian, M. E. Tamer, A. Gomes, Y. Quemener, J.P. Dinguirard and J.C. Kieffer, Phys. Rev. Lett.54, 38 (1985).

[123] P. Auvray, J. Larour, S.D. Moustaizis, 2009 IET European Pulsed Power Conference, pp. 1-8 (2009).

[124] R.N. Sudan, Phys. Rev. Lett. 70, 3075 (1993).

[125] V.K. Tripathi and C.S. Liu, Phys. Plasmas 1, 990 (1994).

[126] Z.M. Sheng and J. Meyer-ter-Vehn, Phys. Rev. E 54, 1833 (1996).

[127] L.M. Gorbunov and R.R. Ramazashvili, J. Exp. Theor. Phys. 87, 461 (1998).

[128] M.G. Haines, Phys. Rev. Lett. 87, 135005 (2001).

[129] E. Kolka, S. Eliezer and Y. Pais, Phys. Lett. A 180, 132 (1993).

[130] M. Borghesi, A.J. MacKinnon, A.R. Bell, R. Gaillard and O. Willi, Phys Rev. Lett. 81, 112 (1998).

[131] L.M. Gorbunov, P. Mora and T.M. Antonsen, Phys. Plasmas 4, 4358 (1997).

[132] F. Tamburini, A. Sponselli, B. Thide and J. T. Mendonca, EPL 90, 45001 (2010).

[133] S. Ali, J.R. Davies and J.T. Mendonca, 37th EPS conference on Plasma Physics P5.211, 1952 (2010).

[134] Enrique J. Galvez, Am. J. Phys. 74, 355 (2006).

[135] P.W. Anderson, Phys. Rev. 130, 439 (1963).

[136] R.A.Beth, Phys. Rev. 50, 115 (1936).

[207] B. S. Sharma and Arachna Jain, Phys. Scr. 87, 025501(2013).

Chapter 3

Analytical and numerical analysis of nonlinear interaction of a laser pulse with an inhomogeneous magnetized plasma

3.1 Introduction

When a tightly focused short laser pulse propagates through a plasma various fundamentally important issues arise in the field of laser-plasma interactions [7, 12, 137-143]. Tajima and Dawson [6] have proposed a scheme of charged particle acceleration by plasma waves so that stable propagation of an intense laser pulse over long distances has been possible. The production of tightly focused high power laser pulses with nanosecond time duration is possible with the development of the chirped pulse amplification (CPA) technology. X-ray lasers, high-order harmonic generation, laser-plasma channeling and fast ignition for laser fusion are some of the applications in which these high intense laser pulses can be used [18, 144-150]. The laser driven particle accelerators are based on the single intense laser pulse propagation in a plasma. Relativistic modification in the refractive index gives rise to self-guiding of the laser pulses in the self-modulated regime [151] but these modulated pulses were highly unstable. In the self-guided laser wakefield acceleration (LWFA) regime [152, 153], self guiding of the laser pulse occurred as the laser pulse has the power above the critical value for self-focusing, but the self guided laser pulse propagation is highly unstable. The simplicity in the use of the self-guided laser wakefield acceleration regime [154-156] is more attractive than the use of plasma guiding structures. The acceleration process in the self-guided laser wakefield acceleration regime is significantly affected by the laser pulse evolution and the propagation instabilities. For example, a stable wakefield structure cannot occur if the laser pulse breaks into filaments [157, 158] and the characteristics of the electron beam such as beam spatial profile, temporal profile and energy spread are degraded as compared to the stable propagation of a laser beam.

The optical guiding method in a plasma channel has been found to extend acceleration length up to a distance of many Rayleigh lengths ($z_R = \pi r_0^2/\lambda$, where r_0 is the spot size at focus (z = 0), $\lambda = 2\pi c/\omega$ is laser wavelength and ω is laser frequency) for laser-based schemes for propagation of an intense laser pulse. Several methods for plasma channel formation are currently being proposed for this purpose. Some of which [159-161] include (i) production of a line focus in a gas by passing a long laser pulse through a lexicon resulting in a radially expanding hydrodynamic shock, (ii) a capillary discharge used to control the plasma profile and (iii) the ponderomotive force of a relativistically intense self-guided laser pulse in a plasma are used to creates a channel in preformed plasma. Using these methods, high intense short laser pulses have been guided over the distances of the order of 20 z_R to 100 z_R. These experiments have shown the dependence of the guiding mechanism to laser intensity and plasma channel can be used in plasma based acceleration, fast ignition as well as the production of monochromatic x-ray laser.

Many of the research works are carried out on the problem of propagation of the low power and low intensity ($P < P_c$) laser pulses, where $P_c[GW] \approx 17.4\,(\lambda_p/\lambda)^2$ is the critical power, $\lambda = 2\pi c/\omega$ is the laser wavelength with frequency ω and $\lambda_p = 2\pi c/\omega_p$ is plasma wavelength with $\omega_p = (4\pi n_0 e^2/m)^{1/2}$ the plasma frequency, propagated through a plasma channel with plasma density $n = n_0 + \Delta n r^2/r_0^2$ with the matched condition $r_0 = R_{ch}$, under this condition $\Delta n = \Delta n_c$, where n_0 is unperturbed plasma density, Δn is density perturbation, R_{ch} is the channel radius and $\Delta n_c = 1/\pi r_e r_0^2 \approx 1.13\times10^{20}/r_0^2[mm]$ is the critical channel depth and $r_e = e^2/m_e c^2$ is the classical electron radius. Higher electron energies produced in preformed plasma channel have been studied [162-165].

Another type of the low frequency mode having electrostatic and electromagnetic characteristics is produced in an inhomogeneous plasma channels. Excitation of plasma waves in a channel with a parabolic transverse density profile with the matched condition for Gaussian beam propagation had been investigated [166]. Generation of the wakefields in a plasma channel by an intense short laser pulse (especially hollow channels with a sharp vacuum-plasma

boundary) has been studied [167]. Numerical simulation carried out on the stable propagation of short pulses in an un-tapered channel over many Rayleigh lengths has shown that higher laser power and increasing laser spot size is required to increase z_R but this requirement is still limited to distances of a few hundred micrometers. Many experiments have shown that the self-guided and energetic electrons generated when the laser power exceeds the critical power [168-171]. Excitation of a damped quasi-mode is an attractive feature of the wakefield generation in sharp edged plasma channels.

It is demonstrated that a continuous frequency spectrum can be generated during the response of a plasma channel with a smooth density profile unlike a hollow channel with an infinitely sharp interface which only supports a single surface mode at certain frequency and a bulk plasma mode at $\omega_p(z)$. Collisionless damping is possible in the discrete channel mode in the continuum of modes.

Paraxial approximation is used as a conventional approach for intense finite radius laser pulses which propagated through plasmas [18]. However, the paraxial approximation approach is unable to describe many nonlinear phenomena such as group velocity dispersion, finite pulse length effect and axial transport of energy within the pulse [172-176]. In addition, the transverse variation of the laser pulse during the propagation through plasma cannot be neglected. Thus, a new approach derived from the paraxial theory is strongly required.

In this chapter, the nonparaxial theory for short laser pulse propagation in a single mode nonuniform plasma channel including the effect of finite pulse length and some related nonlinear phenomena is discussed. The electron energy gain in the wake of the laser pulse at different magnetic field strengths is determined. The effects of magnetic field on the wakefield structure, channel radius and accelerating length [114, 177] have been analyzed.

This chapter is organized as follows. The laser pulse and plasma wave evolution equations in an inhomogeneous magnetic plasma channel with

parabolic density profile have been derived in section 3.2. In the next section, the dynamics of the laser wakefield acceleration has been analyzed. In section 3.4, we have examined the effects of external magnetic field on dephasing length of an accelerated particle in the wake and the energy gain by the electrons. The effect of the external magnetic field on the wakefield excitation has been studied and the same has been compared with the results of the two dimensional particle-in-cell simulation in section 3.5. The conclusions are presented in section 3.6.

3.2. Evolution of a laser pulse and a plasma wave

The nonlinear propagation of a circularly polarized Gaussian laser pulse with the intensity I ≈ 1.3×10^{19} Wcm^{-2}, central wavelength ≈ 1.0 μm and pulse duration ≈ 33 fs is considered. The laser pulse propagates through a preformed inhomogeneous plasma channel generated by an ultra-relativistic laser pulse ($\alpha_0 \approx 3$). The length of the propagated laser pulse is comparable to the plasma wavelength λ_p. A plasma channel with a positive gradient in plasma density that has inhomogeneous underdense plasma with density of $n_0 \approx 10^{19}$ cm^{-3} on the axis is analyzed. The externally applied magnetic field B_0 is taken along the pulse propagation direction, i. e., along z-axis.

The electric component along the transverse direction of a circularly polarized tightly focused laser pulse in an inhomogeneous plasma channel is assumed as [114]

$$\boldsymbol{E}_{\perp}(r,t) = \frac{1}{\sqrt{2\eta(r,z)}}\left(\hat{e}_x \pm i\hat{e}_y\right)E_0\left(r, z - v_g(z)t\right)\left(\frac{r_0}{r_s}\right)e^{\left(\frac{t-\int\frac{dz}{v_g(z)}}{\tau_L}\right)^2} \times$$

$$e^{-\frac{r^2}{R_{ch}^2}}\ e^{-i\left(\omega t - \int k_0(z)dz\right)}, \qquad (3.1)$$

where $\hat{e}_x$ and $\hat{e}_y$ are the orthogonal unit vectors along the x-axis and y-axis respectively, η(r,z) is the refractive index, $k_0(z)$ is spatially varying wave number and R_{ch} is the channel radius. The spot size r_s of the laser pulse at z for the proposed conditions is taken as $r_s = r_0\,(1+z^2/z_R^2)$. For short laser pulse propagated through plasma channel ($L_p < \lambda_p$), $dr_s/dz = 0$ and $r_s = r_0+\delta r$ at z = 0 with $\delta r_0^2/r_0^2$

<< 1 is used [178]. For convenience, choose independent variables z and τ in place of z and t considering the relation $\tau = t - \int dz'/v_g(z')$. Using $v_g(z)$ $(t - \int dz'/v_g(z')) = \xi$ and pulse length $L_p = c\tau_L$, where τ_L is pulse duration, the transverse electric field in terms of independent variables turns out to be

$$\boldsymbol{E}_{\perp}(r,t) = \frac{1}{\sqrt{2\eta(r,z)}} \left(\hat{e}_x \pm i\hat{e}_y\right) E_0(r,\xi) \frac{r_0(\xi=0)}{r_s(\xi)} e^{\frac{-\xi^2}{L_p^2}} e^{-\frac{r^2}{R_{ch}^2}} e^{-i\left(\omega t - \int k_0(z)dz\right)}. \tag{3.2}$$

The radial component of the normalized laser vector field of the circularly polarized laser pulse has the form

$$a = a_0(r,\xi) \frac{r_0}{r_s} e^{\frac{-\xi^2}{L_p^2}} e^{-\frac{r^2}{R_{ch}^2}} e^{-i\left(\omega t - \int k_0(z)dz\right)},$$

where α is the transverse normalized laser vector field has the form of $\alpha_{\perp}(eA_{\perp}/mc^2)$. The dispersion relation, which relates the frequency and the wave vector k_0 for a left-hand circularly polarized electromagnetic wave propagating along z-direction, is given as [24]

$$\omega^2 = k_0^2(z)c^2 + \frac{\omega_p^2(z)\omega}{\gamma(z)\omega - \omega_c}, \tag{3.3}$$

here relativistic factor $\gamma(z) = (1 + \alpha_0^2/\eta(z))^{1/2}$, cyclotron frequency $\omega_c = eB_0/mc$ and propagation constant $k_0(z) = \eta(z)\omega/c$.

The dispersion relation for a very high frequency electromagnetic wave can be written as

$$\omega_p^2(z) = \left(\frac{\omega^3}{2\omega_c}\right)(1 - \eta^2(z))\left(1 + \frac{a_0^2}{\eta(z)}\right). \tag{3.4}$$

Since the radial shear of the plasma density does not much contribute in the excitation of the plasma modes than for the propagation of the left circularly polarized electric field in a wide plasma channel $\eta(z) \approx \eta(r,z)$ is considered. The complex field amplitude $\alpha_0(r,\xi)$ can be taken equal to the radial amplitude $\alpha_0(r)$ or the longitudinal normalized field amplitude $\alpha_0(z)$ for a very short laser pulse.

Considering the normalized field strength α_0 (=$eE_0/mc\omega$), the refractive index [18] is obtained as

$$\eta(r,z) \approx 1 - \frac{\omega_p^2}{\omega(\gamma(z)\omega - \omega_c)}\left(1 + \frac{\Delta n(r,z)}{n_0} + \frac{\delta n(r,z)}{n_0} - \frac{a_0^2}{2} - \frac{4c^2}{r_s^2\omega^2}\right), \tag{3.5}$$

where ω_p is the plasma frequency at z = 0, $\gamma(z) = (1 + a_0^2/\eta(z))^{1/2}$, $\Delta n(r,z)$ is the density variation due to pre-existing structure of the plasma and $\delta n(r, z)$ is the change in plasma density due to wake response.

Hence, the wave equation for the normalized vector potential $\alpha(r, z, t)$ of the laser field is [18]

$$(\nabla_\perp^2 - k_0^2(z) + \frac{\omega_0^2}{c^2} + i\frac{\partial k_0}{\partial z} + 2ik_0(z)\frac{\partial}{\partial z} + 2i\frac{\omega}{c^2}\frac{\partial}{\partial t} + \frac{\partial^2}{\partial z^2} - \frac{1}{c^2}\frac{\partial^2}{\partial t^2})\,\boldsymbol{a}(r,\tau,z) = \frac{\omega_p^2\omega_c^2}{\omega(\gamma(z)\omega-\omega_c)c^2}\,(1 + \frac{r^2}{R_{ch}^2} - \frac{r^2}{r_s^2} + \frac{\delta n(z)}{n_0} - \frac{|a|^2}{4})\,\boldsymbol{a}(r,\tau,z). \tag{3.6}$$

The density profile for a nonuniform plasma is

$$\frac{n(r,z)}{\omega^2} = \frac{n(z)}{\omega^2}\,(1 + \frac{r^2}{R_{ch}^2} - \frac{r^2}{r_s^2}). \tag{3.7}$$

It is convenient to change the independent variables from z, t to z, τ in equation (3.6) by considering $\tau = t - \int \frac{dz'}{v_g(z')}$.

Using new variables, $\frac{\partial}{\partial z} \to \frac{\partial}{\partial z} - \frac{1}{v_g(z)}\frac{\partial}{\partial \tau}$ and $\frac{\partial}{\partial t} \to \frac{\partial}{\partial \tau}$, equation (3.6) becomes

$$[\nabla_\perp^2 - \frac{\omega_p^2(z)\omega_c^2}{\omega\, c^2\,(\gamma(z)\omega-\omega_c)} + \frac{4}{r_s^2} + \left(\frac{\omega^2}{c^2} - k_0^2(z) - \frac{4}{r_s^2}\right) + 2ik_0(z)\left(1 + \frac{i}{k_0(z)v_g(z)}\frac{\partial}{\partial\tau}\right)\frac{\partial}{\partial z} + 2i\left(\frac{\omega}{c} - k_0(z)\right)\frac{1}{v_g(z)}\frac{\partial}{\partial\tau} + i\frac{\partial k_0}{\partial z}\left(1 - \frac{i}{k_0(z)v_g(z)}\frac{\partial}{\partial\tau}\right) + \frac{(1-\beta_g^2)}{v_g^2(z)}\frac{\partial^2}{\partial\tau^2} + \frac{\partial^2}{\partial z^2} - \frac{\omega_p^2\omega_c^2}{\omega c^2(\gamma(z)\omega-\omega_c)}\,(\frac{\delta n(z)}{n_0} - \frac{a^2}{4})]\boldsymbol{a}(r,\tau,z) = 0. \tag{3.8}$$

In order to find solutions, an algebraic transformation from the laboratory frame variables (z, t) to the variables (ξ, τ), where $\xi = z - \int \frac{dt'}{v_g^{-1}(t')}$ and τ = t is

performed using transformation rules $\frac{\partial}{\partial z} \rightarrow \frac{\partial}{\partial \xi}$ and $\frac{\partial}{\partial t} \rightarrow \frac{\partial}{\partial \tau} - \left(\frac{1}{v_g^{-1}(z)}\right)\frac{\partial}{\partial \xi}$ in the equation (3.8), the equation becomes

$$\left[\nabla_{\perp}^{2} + \frac{4}{r_s^2} + \left(\frac{\omega^2}{c^2} - k_0^2(z) - \frac{\omega_p^2(z)\omega_c^2}{\omega\, c^2(\gamma(z)\omega - \omega_c)} - \frac{4}{r_s^2}\right) + 2ik_0(z)\left(1 + \frac{i}{k_0(z)}\frac{\partial}{\partial \xi}\right)\frac{\partial}{\partial z} \;+\right.$$
$$2i\left(\frac{\omega}{c} - k_0(z)\right)\frac{\partial}{\partial \xi} \;+\; i\frac{\partial k_0}{\partial z}\left(1 - \frac{i}{k_0(z)}\frac{\partial}{\partial \xi}\right) + \gamma_g^2\frac{\partial^2}{\partial \xi^2} \;+$$
$$\left.\frac{\partial^2}{\partial z^2} - \frac{\omega_p^2\omega_c^2}{\omega c^2(\gamma(z)\omega - \omega_c)}\left(\frac{\delta n(z)}{n_0} - \frac{a^2}{4}\right)\right]\boldsymbol{a}(r,\xi,z) = 0\,, \qquad (3.9)$$

where $\gamma_g(z) = \left(1 - \beta_g^2(z)\right)^{\frac{1}{2}}$ and $\beta_g(z) = v_g(z)/c$. In absence of the Raman backscattering, i.e., in the limit of $1/k_p << r_0 << R_{ch}$, the wave number $k_0(z)$ is given by

$$k_0(z) = \frac{1}{c}\left(\omega^2 - \frac{\omega_p^2(z)\omega}{\gamma(z)\omega - \omega_c} - \frac{4c^2}{r_s^2}\right)^{\frac{1}{2}}. \qquad (3.10)$$

and the group velocity is given as

$$v_g(z) \;=\; c\int k_0(z)dz \;=\; \int\left(\omega^2 - \frac{\omega_p^2(z)\omega}{\gamma(z)\omega - \omega_c} - \frac{4c^2}{r_s^2}\right)^{\frac{1}{2}} dz. \qquad (3.11)$$

The operator $\nabla_\perp$ in equation (3.8) for a short laser pulse propagation in a parabolic plasma channel can be represented as $\nabla_\perp \approx 1/r_s(r)$, where $r_s(r) = r_0 + \partial r$ in the mismatched condition and ∂r is the transverse variation due to the spot oscillation in transverse direction in the relativistic limit. These oscillations are responsible for modification in the channel width at the given spatial coordinates. Hence, the surface waves and the wakefield generated in the plasma will be different. Assumed $\partial/\partial\xi \approx 1/L_p$, $\partial/\partial z \approx 1/z_R$ and neglect the terms of $\partial^2\alpha/\partial z^2$, $\partial^2\alpha/\partial\xi\partial z$ and $c\tau/\lambda$, equation (3.9) becomes

$$\left[\nabla_{\perp}^{2} + \frac{4}{r_s^2} - \frac{\omega_p^2(z)\omega}{c^2(\gamma(z)\omega - \omega_c)}\left(\frac{r^2}{R_{ch}^2} - \frac{r^2}{r_s^2} - \frac{a^2}{4}\right) + \gamma_g^2(z)\,\frac{1}{L_p^2} \;+\frac{1}{z_R^2} \;+\; 2ik_0(z)\,\frac{\partial}{\partial \xi} \;+\right.$$
$$\left.\frac{r_0}{r_s(\xi)}\,i\frac{\partial k_0(z)}{\partial \xi}\right]a(r,\xi,z) \;= 0. \qquad (3.12)$$

The channel radius for a unscratched laser pulse with a Gaussian radial profile $\alpha(r,\xi,\tau) = A(\xi,\tau)\exp(-r^2/r_s^2)$, is estimated as

$$R_{ch}(\xi) \approx \frac{\omega_p \omega r_0}{c\left(\omega(\gamma(z)\omega-\omega_c)\right)^{\frac{1}{2}}} \frac{r_0 L_p}{\left(r_0^2+4L_p^2\right)^{\frac{1}{2}}} \left(1+\frac{1}{2}\left(1+\frac{r_0^2}{r_s^2(\xi)}\right)\left(\frac{4L_p^2+r_0^2}{L_p^2 r_0^2}\right) \frac{\omega c^2(\gamma(z)\omega-\omega_c)}{\omega_p^2 \omega_c^2}\right), \quad (3.13)$$

where the values of z_R, $\gamma(z)$ and $\eta(z)$ are used for an initial constant spot size in ξ.

The laser intensity distribution in the transverse plane at any given location along laser pulse for quasi-matched conditions can be represented by a Gaussian envelope with a flat phase fronts, $\alpha_{qm}(r,\xi) = \alpha_{qm}^{*} = A(\xi,\tau)\ r_0/r_s(\xi)\ \exp(-r^2/r_s^2(\xi))$, where α_{qm} refers to the amplitude of laser pulse in quasi-matched conditions. In terms of the independent variables, the envelope equation for $\alpha_{qm}(r,\xi)$ is described by

$$\left[2k_0 \frac{\partial}{\partial \xi} + \frac{r_0}{r_s(\xi)} \frac{\partial k_0(z)}{\partial \xi}\right] A(\xi,\tau) = 0. \quad (3.14)$$

If the nonlinearity effect is almost insignificant, the oscillations along the longitudinal direction are small and the laser spot size r_s can be determined. Thus the laser spot size at any value of z for the oscillatory motion of the laser spot around its focal point can be obtained by the equation [178] $\partial^2 r_s/\partial z^2 = -4\Delta n r_s/\ \Delta n_c k^2(r_\perp, z=0) r_0^4$, where $r_s \approx 2R_{ch}(z)/r_0 k_0(z)$. In nonparaxial approximation $(\Delta n/\Delta n_c)^{1/2} \approx R_{ch}(z)/r_0$. The result indicates that the plasma channel can support higher modes at $R_{ch}(z)$ and if the relativistic laser pulse propagates through the channel, the pulse distorts the plasma channel.

The variation of channel width (R_{ch} [μm]) as a function of ω_c/ω_p for different relativistic factors $\gamma(z)$ is presented in Figure 3.1 showing that the channel width decreases with increasing ω_c/ω_p and increases with $\gamma(z)$. The result refers to the possibility of propagation of an intense short circularly polarized laser pulse over a significant extended distance. Furthermore, the laser pulse can have a much greater stability during propagation in the inhomogeneous magnetized plasma channel compared with the homogeneous plasma channel.

3.3 Dynamics of laser wakefield

The wakefield excitation by a laser pulse in an inhomogeneous magnetized plasma channel is analyzed in this section by considering the on-axis accelerating wakefield within the pulse and behind the pulse. The dynamics of the plasma wave excited by the ponderomotive force in a plasma is governed by the following set of equations.

The first one is the continuity equation,

$$\frac{\partial n}{\partial t} + n_0 \boldsymbol{\nabla}.\boldsymbol{v}_\perp + n_0 \frac{\partial v_z}{\partial z} = 0, \tag{3.15}$$

where n is the particle number density perturbation, n_0 is the unperturbed particle number density, $v_\perp$ and v_z are the components of the electron fluid velocity along perpendicular and z direction respectively.

The equation of motion for plasma electrons in the laser field and the external magnetic field B_0 applied along the z-direction, is given by

$$m\gamma(z)\frac{d\boldsymbol{v}}{dt} = -e\boldsymbol{E} - eB_0(\boldsymbol{v} \times \hat{\mathrm{z}})$$

where d/dt = ∂/∂t + c ∂/∂z and laser magnetic field is neglected under the assumption that it is weak enough as compared with the applied magnetic field.

The temporal variation of $v_\perp$, the perpendicular component of electron velocity, is given by

$$m\gamma(z)\frac{\partial v_\perp}{\partial t} = -mc\,\frac{\partial v_\perp}{\partial z} - eE_\perp - e\,v_\perp\,B_0, \tag{3.16}$$

where the perpendicular component of laser electric field $E_\perp = \nabla_\perp(\phi + \phi_p)$ for high frequency, ϕ is the ambipolar potential and ϕ_p is the ponderomotive potential. The relation between perpendicular velocity and the potentials is given as

$$\left(\gamma^2(z)\frac{\partial^2}{\partial t^2} + \omega_c^2\right)v_\perp = \frac{e\gamma(z)}{m}\frac{\partial}{\partial t}\nabla_\perp\left(\phi + \phi_p\right) - \frac{e\gamma(z)\omega_c}{m}\,\frac{\partial\left(\phi+\phi_p\right)}{\partial z}. \tag{3.17}$$

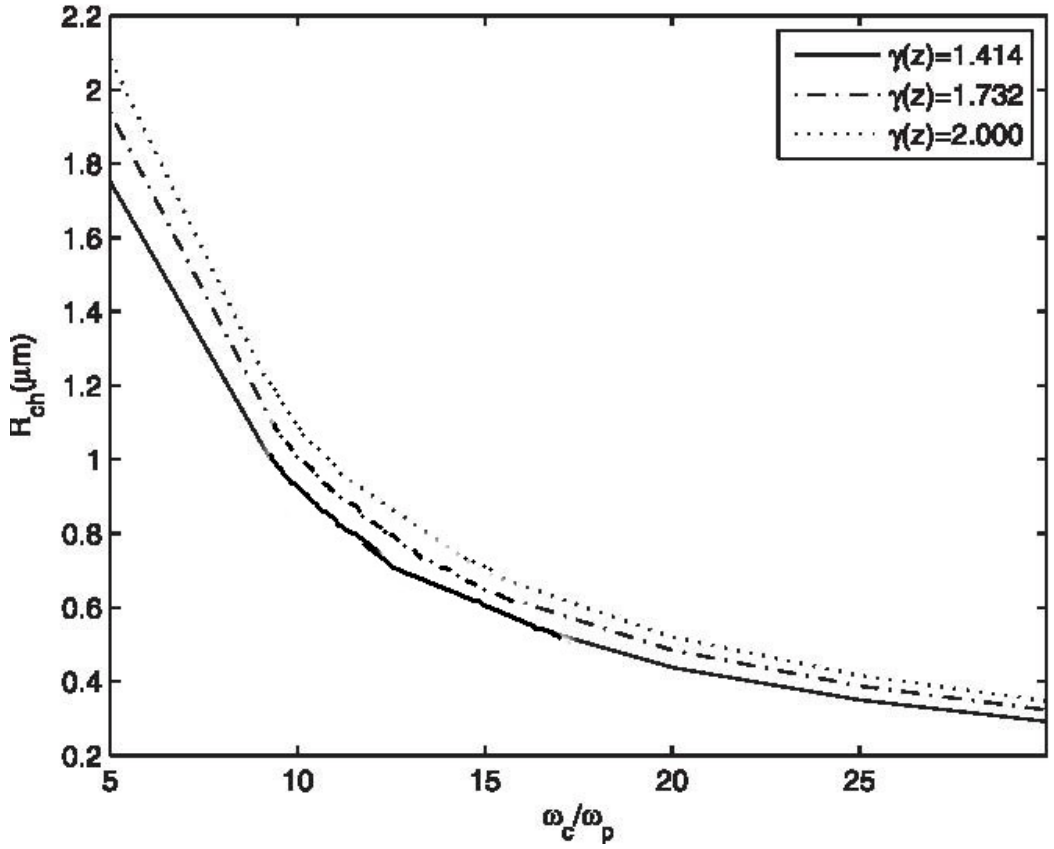

Figure 3.1: Variation of the channel radius at different values of relativistic factors.

Also,

$$\frac{\partial v_z}{\partial t} = -\frac{F_z}{m} + \frac{e\gamma(z)}{m}\frac{\partial \phi}{\partial z}, \tag{3.18}$$

and Poisson's equation is

$$\nabla^2\phi = 4\pi en, \tag{3.19}$$

where F_z is the ponderomotive force.

Component of ponderomotive force parallel to B_0 is given by [179]

$$F_z = \left[\frac{\partial}{\partial z} - \frac{k_0(z)\omega_c}{\omega(\gamma(z)\omega-\omega_c)}\frac{\partial}{\partial t}\right]\left[\frac{e^2E^2}{\gamma(z)m\omega(\gamma(z)\omega-\omega_c)}\right], \tag{3.20}$$

and component perpendicular to B_0 of the ponderomotive potential is given by [179]

$$\phi_p \;=\; -\frac{eE^2}{m(\gamma(z)\omega-\omega_c)^2}. \tag{3.21}$$

The equation for a plasma wave in the magnetized plasma channel can be obtained by solving equations (3.15) to (3.21).

The equation turns out to be

$$\left[\left(\gamma^2(z)\frac{\partial^2}{\partial t^2} \;+\; \omega_c^2\right)\nabla^2 + \left(\frac{\partial^2}{\partial t^2}+\omega_p^2(z)\right)\frac{\partial^2}{\partial z^2}+\frac{\partial^2}{\partial t^2}\;\nabla_\perp^2\right]\phi \;=\; \left[\left(\frac{\partial^2}{\partial t^2} \;+\; \omega_c^2\right)\frac{\partial}{\partial z}\left(\frac{\partial}{\partial z}-\frac{k_0(z)\omega_c}{\omega(\gamma(z)\omega-\omega_c)}\frac{\partial}{\partial t}\right)+\;\gamma(z)\frac{\omega}{\gamma(z)\omega-\omega_c}\frac{\partial^2}{\partial t^2}\;\nabla_\perp^2\right]\frac{eE^2\gamma^3(z)}{m\omega\,(\gamma(z)\omega-\omega_c)}. \tag{3.22}$$

Equation (3.22) for the plasma waves propagating along the z-direction, i.e., along magnetic field B_0 reduces to

$$\left(\frac{\partial^2}{\partial t^2} \;+\; \omega_p^2\right)\frac{\partial\phi}{\partial z} \;=\; \left[\left(\frac{\partial}{\partial z}-\frac{k_0(z)\omega_c}{\omega(\gamma(z)\omega-\omega_c)}\frac{\partial}{\partial t}\right]\frac{eE^2\omega_p^2\gamma^3(z)}{m\omega\,(\gamma(z)\omega-\omega_c)}. \tag{3.23}$$

Further, equation (3.23) can be written in terms of independent variables as

$$\left(\frac{\partial^2}{\partial\tau^2} \;+\; \omega_p^2(z)\right)\phi \;=\; \left[1+\frac{k_0(z)v_g\omega_c}{\omega(\gamma(z)\omega-\omega_c)}\right]\frac{eE^2\omega_p^2\gamma^3(z)}{m\omega\,(\gamma(z)\omega-\omega_c)}\;, \tag{3.24}$$

where $v_g\, k_0(z) \approx \omega_p(z)$.

The electric field inside the laser pulse along the z direction satisfies the equation given below

$$\left(\frac{\partial^2}{\partial\tau^2} \;+\; \omega_p^2(z)\right)E_p(z) \;=\; \left[1+\frac{k_0(z)v_g\omega_c}{\omega(\gamma(z)\omega-\omega_c)}\right]\frac{mc^2\omega\nabla|a_{qm}|^2\omega_p^2(z)\gamma^3(z)}{e(\gamma(z)\omega-\omega_c)}\;. \tag{3.25}$$

By using the value of a_{qm}, equation (3.25) becomes

$$E_p(z) \;=\; -\left(\frac{k_0(z)R_{ch}(z)}{\omega_p^2}\right)\times\left(1+\frac{k_0(z)v_g\omega_c}{\omega(\gamma(z)\omega-\omega_c)}\right)\times\left(\frac{mc^2\omega\omega_p^2(z)\gamma^3(z)}{e(\gamma(z)\omega-\omega_c)}\right)\times \int\frac{\partial a_0^2(\tau')}{\partial\tau'}\frac{1}{r_s(\tau')}\;sin\,[\omega_p(z)(\tau-\tau')]\,d\tau'. \tag{3.26}$$

The envelope equation (3.26) can be used to obtain the axial electric field behind the pulse for which the appropriate boundary conditions are given as

$\alpha_0(\tau) = \alpha_0 \sin(\pi\tau/\tau_0) \quad 0 \le \tau \le \tau_0,$ (3.27)

and

$\alpha_0(\tau) = 0 \qquad \tau > \tau_0,$ (3.28)

where it is assumed that the front of the pulse is at $\tau = 0$ and the back of the pulse is at $\tau = \tau_0$ in the above equations.

Since $\partial\alpha_0^2(\tau)/\partial\tau = \alpha_0^2/2\ (2\pi/\tau_0) \sin(2\pi\tau/\tau_0)$ and $r_s(\tau')$ at τ_0 is $r_s(\tau_0)$, using these values in equation (3.26), the axial component for the wakefield within the pulse is given as

$$E_p(z) = -\frac{a_0^2}{2}\frac{k_0(z)R_{ch}(z)}{\omega_p^2}\frac{1}{r_s(\tau_0)}\left(1+\frac{k_0(z)v_g\omega_c}{\omega(\gamma(z)\omega-\omega_c)}\right)\left(\frac{mc^2\omega\omega_p^2(z)\gamma^3(z)}{e(\gamma(z)\omega-\omega_c)}\right)\times$$

$$\frac{\left(\frac{2\pi}{\tau_0}\right)^2}{\omega_p^2-\left(\frac{2\pi}{\tau_0}\right)^2}\left[sin\,(\omega_p\tau) - \left(\frac{\omega_p(z)\tau_0}{2\pi}\right) sin\,\left(\frac{2\pi\tau}{\tau_0}\right)\right]. \quad (3.29)$$

Above equation can be written as

$$E_p(z) = -E_0(z)\left[sin\,(\omega_p\tau) - \left(\frac{\omega_p(z)\tau_0}{2\pi}\right) sin\,\left(\frac{2\pi\tau}{\tau_0}\right)\right], \quad (3.30)$$

where $E_0(z)$ is the peak value of wakefield and has the form as

$$E_0(z) = \frac{a_0^2}{2}\frac{k_0(z)R_{ch}(z)}{\omega_p^2}\frac{1}{r_s(\tau_0)}\left(1+\frac{k_0(z)v_g\omega_c}{\omega(\gamma(z)\omega-\omega_c)}\right)\left(\frac{mc^2\omega\omega_p^2(z)\gamma^3(z)}{e(\gamma(z)\omega-\omega_c)}\right)\frac{\left(\frac{2\pi}{\tau_0}\right)^2}{\omega_p^2-\left(\frac{2\pi}{\tau_0}\right)^2}. \quad (3.31)$$

$\psi(z,\tau) = \frac{\omega_c\omega_p(z)}{\gamma(z)(\gamma(z)\omega-\omega_c)}\Delta\tau$ is the phase of the axial component of the wakefield behind the laser pulse, where $\Delta\tau$ refers to the temporal change in the front of the laser pulse with respect to its back. The phase velocity of the plasma wave is $v_{ph} = \Omega(z,\tau)/K(z,\tau) = c \int K(z',\tau)\, dz'/[1- (v_g(\tau-\tau_0)/\omega_p)\, \partial\omega_p(z)/\partial z]$ and the wavelength associated with the wakefield is $\lambda_w(z,\tau) = 2\pi/K(z,\tau)$, where the frequency and wave number associated with the phase of the accelerating wave in the laboratory frame are $\Omega(z,\tau)$ and $K(z,\tau)$ respectively. The above result can be used to obtain the form of density tapering for optimal acceleration. The analysis further gives the result that the phase velocity of the wakefield increases

(decreases) with distance from the laser pulse with increasing (decreasing) plasma density. When the group velocity of the laser pulse is nearly equal to the phase velocity of the plasma wave, the temporal location behind the laser pulse at any point z is given by

$$\tau_c(z) = \left(\frac{\omega_p^2\omega_c^2}{\gamma^2(z)\omega^2\left(\gamma^2(z)\omega^2-\omega_c^2\right)} + \frac{2c^2}{\omega_0^2 r_s^2}\right)\left(\frac{\omega_c c}{\omega(\gamma(z)\omega-\omega_c)}\frac{\partial\left(ln\ \omega_p(z)\right)}{\partial z}\right)^{-1} + \frac{\tau_0}{2}. \quad (3.32)$$

The location behind the pulse for which v_{ph} = c also moves with the propagating laser pulse. The plasma density tapering for the point, a point which remains stationary with respect to the axial wakefield and known as luminous point [180], must satisfy the following relation for N plasma wavelength, where N is a natural number.

$$\frac{\partial\omega_p(z)}{\partial z} = \left[\frac{\omega_p^2\omega}{\gamma^2(z)\left(\gamma^2(z)\omega^2-\omega_c^2\right)r_s}\right]\left[\frac{1}{2\pi N}\right]\left[1+\left(\frac{\pi R_{ch}(z)}{\lambda}\right)^2\frac{\omega_p^2(z)}{\gamma^2(z)\left(\gamma^2(z)\omega^2-\omega_c^2\right)}\right]. \quad (3.33)$$

The electron energy gain in the wake of the laser pulse ($\tau > \tau_0$) can be determined by solving the following coupled equations for the relativistic factor $\gamma(z)$ and the phase $\psi(z, \tau)$ of wake at the position of particles

$$\frac{\partial\gamma(z)}{\partial z} = 2\frac{e}{mc^2}E_0\ sin\left(\frac{\omega_p(z)\tau_0}{2}\right)cos\,\psi(z,\tau), \quad (3.34)$$

$$\psi(z,\tau) = \left[\psi(z=0)+\frac{\omega_p(z)\omega_c}{c(\gamma(z)\omega-\omega_c)}\right]\int\left[\left(1-\gamma^2(z)\right)^{-1}-\beta_g^{-1}\right]dz, \quad (3.35)$$

with the initial position of the particle is z_0.

Figure 3.2 shows the variation of phase $\psi(z, \tau)$ of the axial component of the wakefield as a function of ω_c/ω_p for different values of $\gamma(z)$ at different time intervals $\Delta\tau$. It is observed that the phase of the axial component of the wakefield increases linearly with ω_c/ω_p and decreases with $\gamma(z)$. Thus, the phase shift of electrons with respect to the wakefield could be effectively controlled by an appropriate value of ω_c/ω_p .

3.4 Effect of external magnetic field on dephasing length and energy gain by electrons

When the laser pulse propagates through the plasma, it will deplete its energy to the wake over a distance. The distance L_p over which the deposited energy on the wake equals the pulse energy evaluated from equation (3.30) by expressing the fields in terms of the normalized vector potential $a_0(\tau)$ at time τ turns out to be

$$L_p = \frac{E_{laser}^2 \; c\tau_L}{E_{wake}^2} = \frac{\left(\frac{\omega mc \; a_0(\tau)}{e}\right)^2 c\tau_L}{\left(\frac{\omega_p(z) mc}{e}\right)^2 \frac{a_0^2(\tau)}{4}} = \frac{4\lambda_p^2(z)}{\lambda}, \tag{3.36}$$

where $\lambda_p(z)$ is the plasma wavelength at point z.

Since the wake propagates with the group velocity of the laser, the accelerated electrons will eventually outrun the wake and therefore they will slip into the decelerating phase over a distance called the dephasing length. The dephasing or slippage distance is obtained by relation

$$\frac{\Delta v_{ew} L_d}{c} = \frac{\lambda_p(z)}{2} = \frac{\pi c}{\omega_p(z)}, \tag{3.37}$$

where $\Delta v_{ew} = (c - v_g)$ is the relative velocity between the electrons and the wave. The equation (3.37) predicts that the slippage changes as $\omega_p^{-1}(z)$. Since the $\omega_p^{-1}(z)$ depends on the applied external magnetic field, the beam slippage can be effectively controlled by the external magnetic field.

Using the value of v_g from equation (3.11) into the equation (3.37), we get

$$\frac{\lambda_p(z)}{2} \approx c\left[1 - \omega\left(1 - \frac{1}{2}\left(\frac{\omega_p^2(z)}{\omega(\gamma(z)\omega - \omega_c)} - \frac{4c^2}{r_s^2\omega^2}\right)\right)\tau_L\right]\frac{L_d}{c}. \tag{3.38}$$

The solution of the above equation gives the dephasing length as

$$L_d \approx \frac{\lambda_p(z)}{\frac{\omega_p^2(z)}{\omega(\gamma(z)\omega - \omega_c)} + \frac{4c^2}{r_s^2\omega^2}}. \tag{3.39}$$

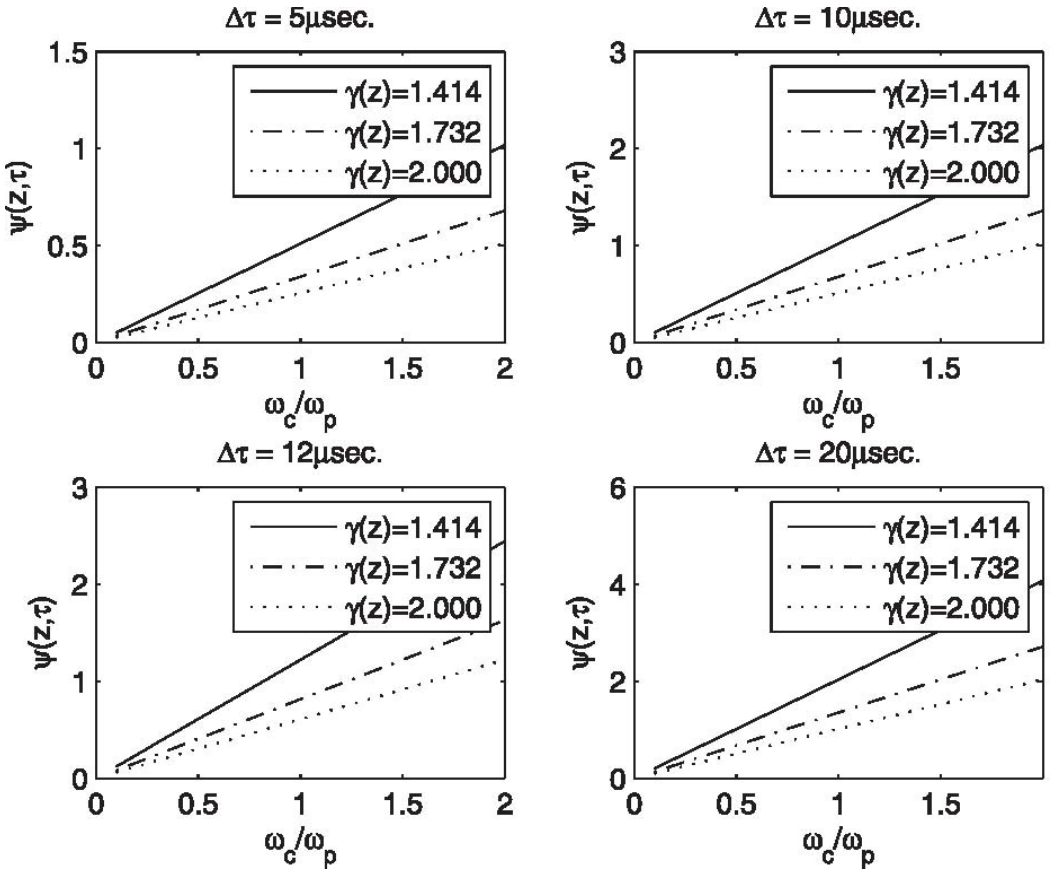

Figure 3.2: Variation of the phase of the axial component of wakefield as a function of ω_c/ω_p.

The maximum energy gained by the electrons from the wakefield can be given as [181, 182]

$$E_{dephase}[eV] = E_{pmax} = eE_0(z)\frac{\lambda_p^3(z)}{\lambda^2}, \tag{3.40}$$

where E_{pmax} is the maximum achievable energy by the wake and $E_0(z)$ is defined by equation (3.31). To obtain the maximum energy, low densities are better than the higher densities. Since the dephasing length increases with decreasing density, hence, the low plasma densities are required for longer acceleration lengths. But, if the acceleration length is limited to the diffraction range, the maximum energy is comparable to the product of the wakefield amplitude and the Rayleigh length, which is typically much lower than the dephasing energy.

Figure 3.3 illustrates the variation of L_d with ω_c/ω_p as a function of $\gamma(z)$ which suggests that the dephasing length increases linearly up to the magnetic field ratio $\omega_c/\omega_p \leq 2.5$ and thereafter it becomes almost constant whereas the accelerating length increases with $\gamma(z)$ due to which enhancement takes place in the combined focusing effects of the relativistic, channel coupling nonlinearities and wakefield. The results indicates that the decelerating length or the accelerating length can be increased by the external magnetic field and the relativistic factor $\gamma(z)$. Thus, the dephasing length can be enhanced over the conventional decelerating length by strong magnetic field.

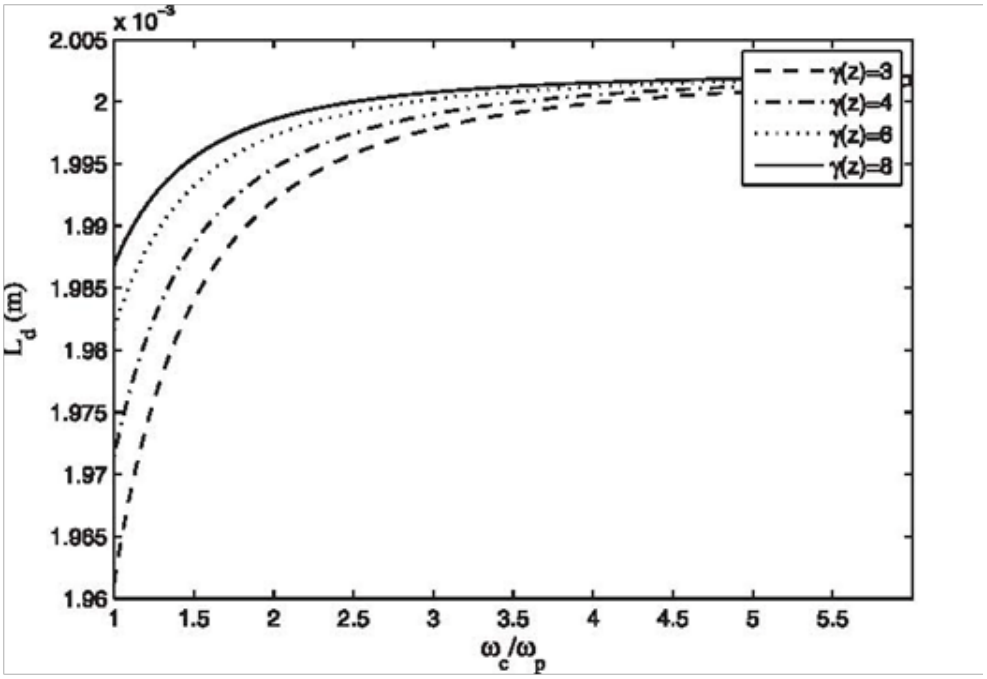

Figure 3.3: Variation of the dephasing length as a function of ω_c/ω_p.

3.5 2D PIC simulation for wakefield generation

Our results match the relativistic 2D PIC simulation for the laser pulse propagation in the inhomogeneous plasma channel for different values of the magnetic field ranging from $B_0 = 10^3$ T ($\omega_c = 17.8\times10^{13}$ rad/s) to 7×10^3 T ($\omega_c = 12.5\times10^{14}$ rad/s). The dimensions etc of simulation box are same as earlier.

Although, magnetic field of such high strength cannot be generated in the laboratory easily, the possibility of generation of such kind of magnetic field by the laser has been explored [2]. The magnetic field effect is examined in terms of ratio ω_c/ω_p.

Figure 3.4 illustrates the spatio-temporal evolution of the profile of the laser pulse in the given plasma channel.

Figure 3.5 shows the spatial evolution of the laser wakefield for different magnetic field ratios ω_c/ω_p and Figure 3.6 describes the spatial evolution of the total accelerated electron energy for different values of ω_c/ω_p.

It has been found that the energy gain increases with increasing magnetic field. However, the simulation illustrates the variable growth rate pattern of the energy gain for different magnetic field ratios. Figure 3.6 shows that the energy gain is maximum at $\omega_c/\omega_p = 2$, which could be an autoresonance condition.

The transverse wakefield spectrum for different magnetic field ratios ω_c/ω_p is shown in Figures 3.7 and 3.8. The transverse wakefield spectrum for different strengths of magnetic field predicted that the wake has maximum amplitude at $z \approx 270\lambda$, where z and λ are the axial location and the laser wavelength respectively. It has also been shown that the transverse profile of the channel remains stable under variation of applied magnetic field.

Spatial evolution of longitudinal wakefield (E_z) for different magnetic field ratios ω_c/ω_p is presented in Figure 3.9 which shows that the wakefield has a maximum amplitude at $z \approx 270\lambda$.

The spatial evolution of the plasma density for different magnetic field ratios ω_c/ω_p is considered in Figure 3.10. It is explained by the figure that the density perturbation increases with the external magnetic field. Some undesired singularities and the instabilities can be suppressed by the modulation in the plasma density that changes the response of the relativistic nonlinear regime. Thus, the nonlocal perturbation in plasma density makes an

inhomogeneous plasma channel more significant as compared with a homogeneous plasma channel [160, 183].

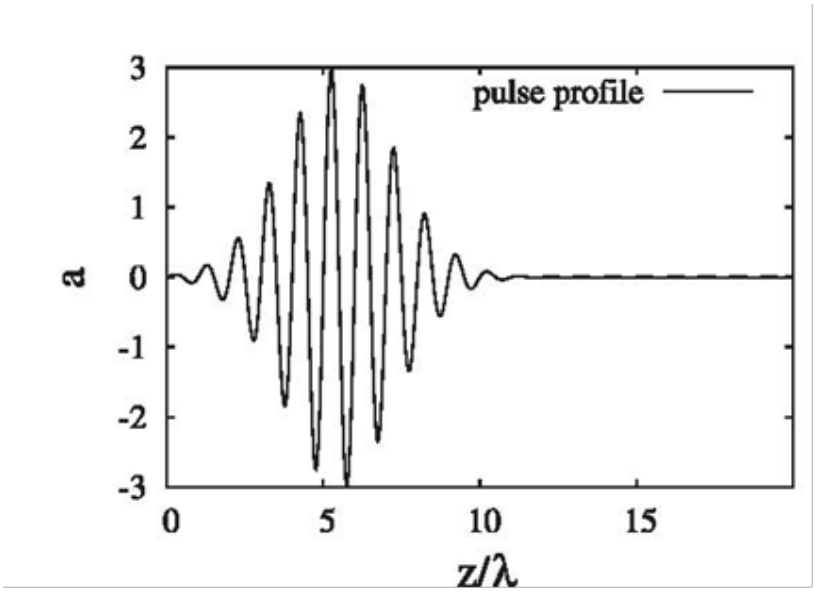

Figure 3.4: Spatio-temporal evolution of the profile of the laser pulse.

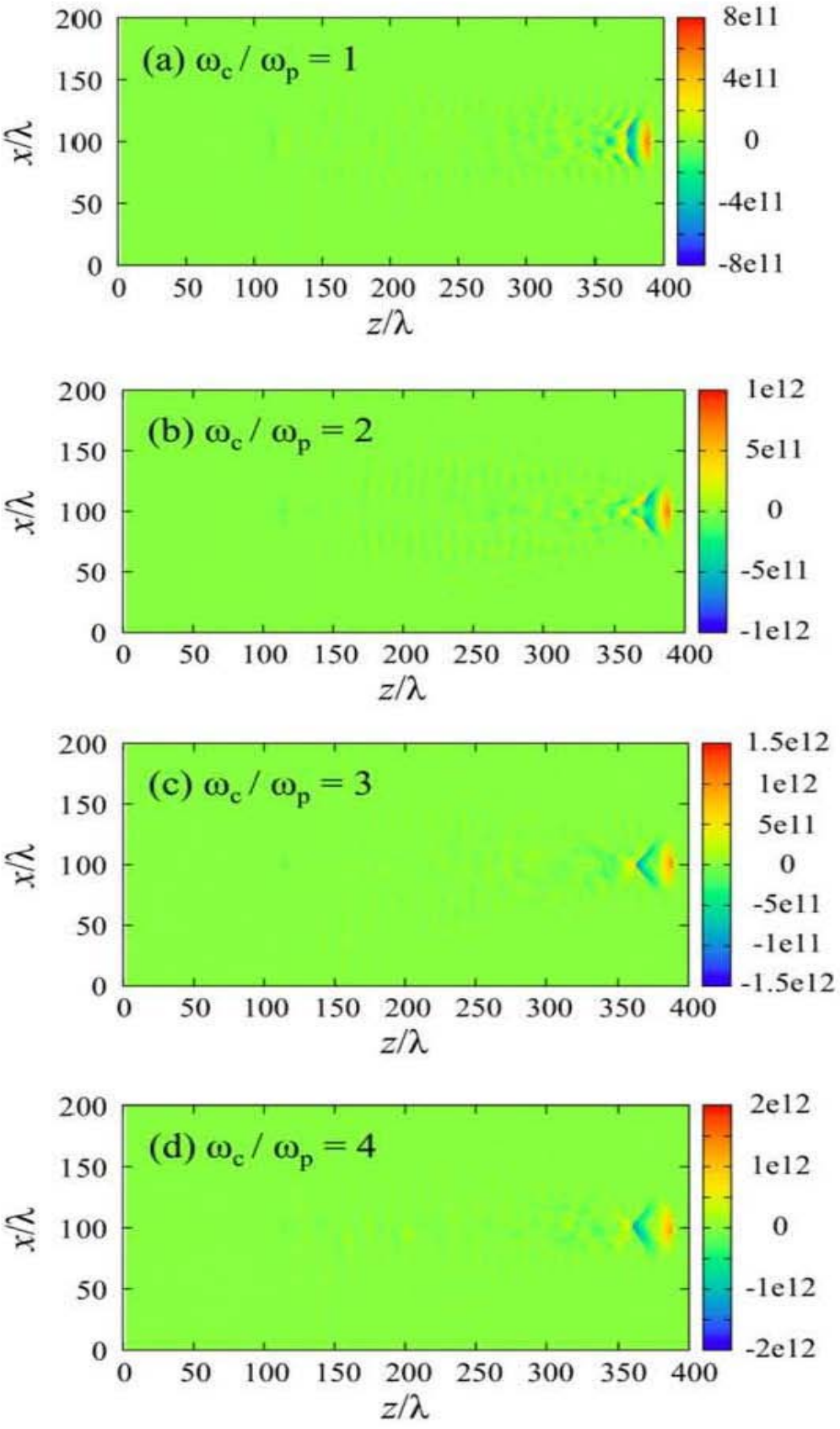
(a) $\omega_c / \omega_p = 1$
8e11
4e11
0
-4e11
-8e11
(b) $\omega_c / \omega_p = 2$
1e12
5e11
0
-5e11
-1e12
(c) $\omega_c / \omega_p = 3$
1.5e12
1e12
5e11
0
-5e11
-1e11
-1.5e12
(d) $\omega_c / \omega_p = 4$
2e12
1e12
0
-1e12
-2e12
x/λ
z/λ
0
50
100
150
200
250
300
350
400

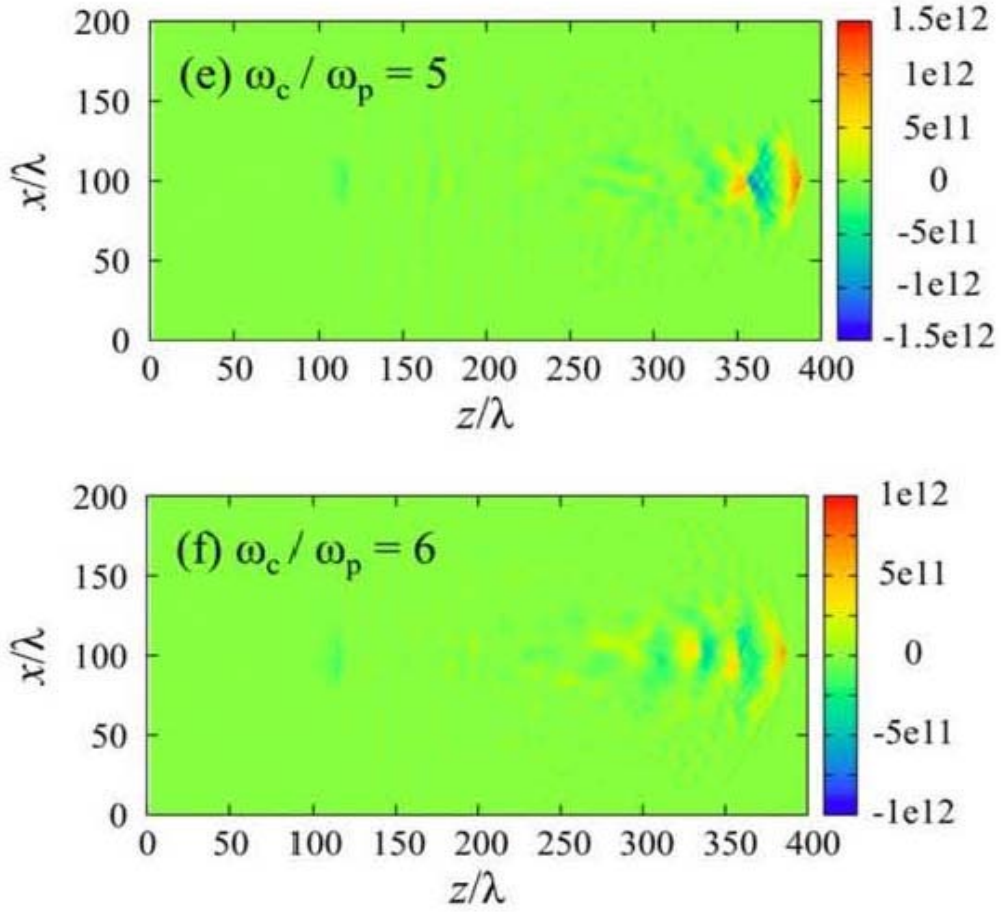

Figure 3.5: Spatial evolution of the laser wakefield for different magnetic field ratios ω_c/ω_p (a) 1.00, (b) 2.00 (c) 3.00, (d) 4.00, (e) 5.00 and (f) 6.00. The wakefield amplitude is shown on the right side.

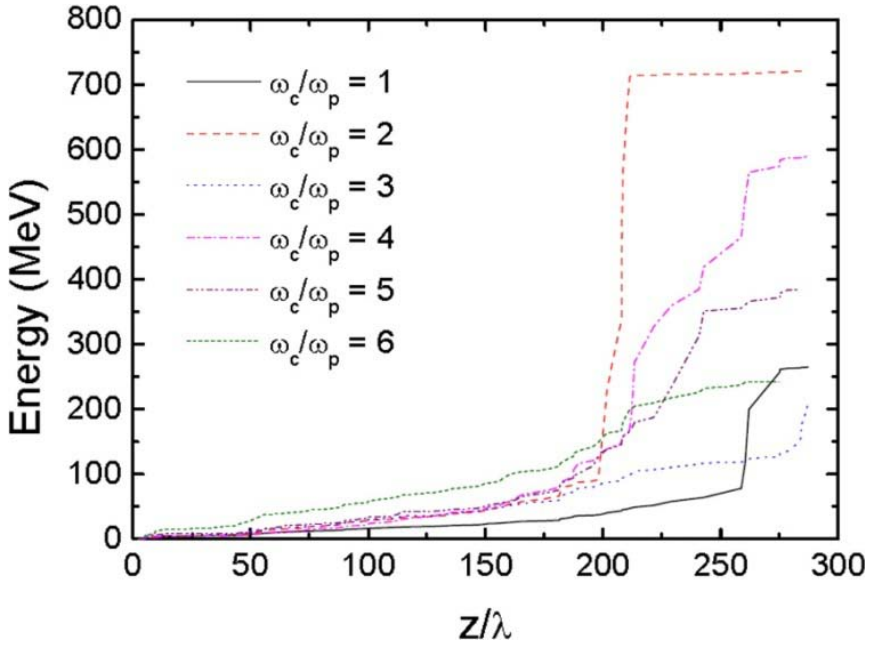

Figure 3.6: Spatial evolution of the total accelerated electron energy for different magnetic field ratios ω_c/ω_p (a) 1.00, (b) 2.00 (c) 3.00, (d) 4.00, (e) 5.00 and (f) 6.00.

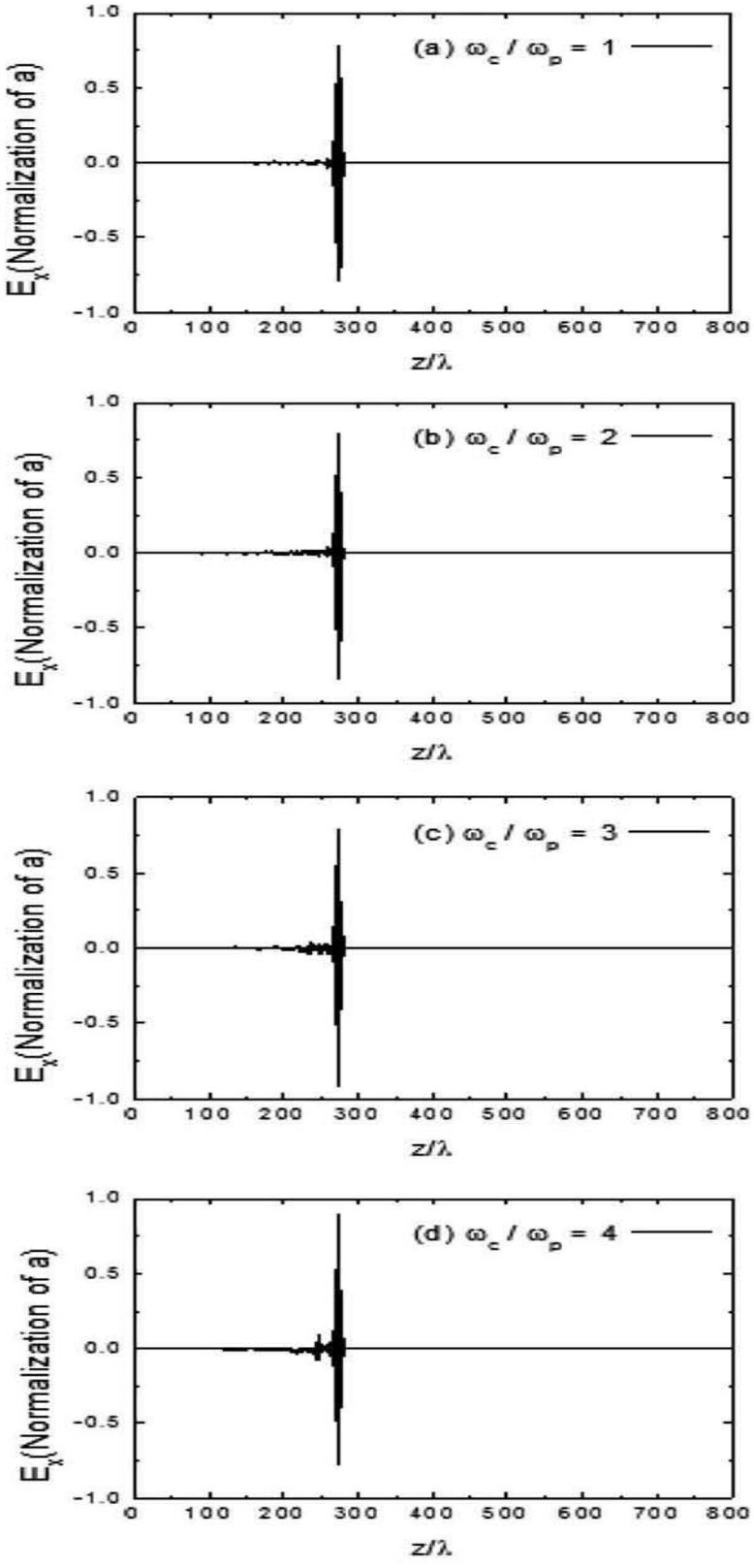
(a) ω_c / ω_p = 1
(b) ω_c / ω_p = 2
(c) ω_c / ω_p = 3
(d) ω_c / ω_p = 4
E_x(Normalization of a)
z/λ
1.0
0.5
0.0
-0.5
-1.0
0
100
200
300
400
500
600
700
800

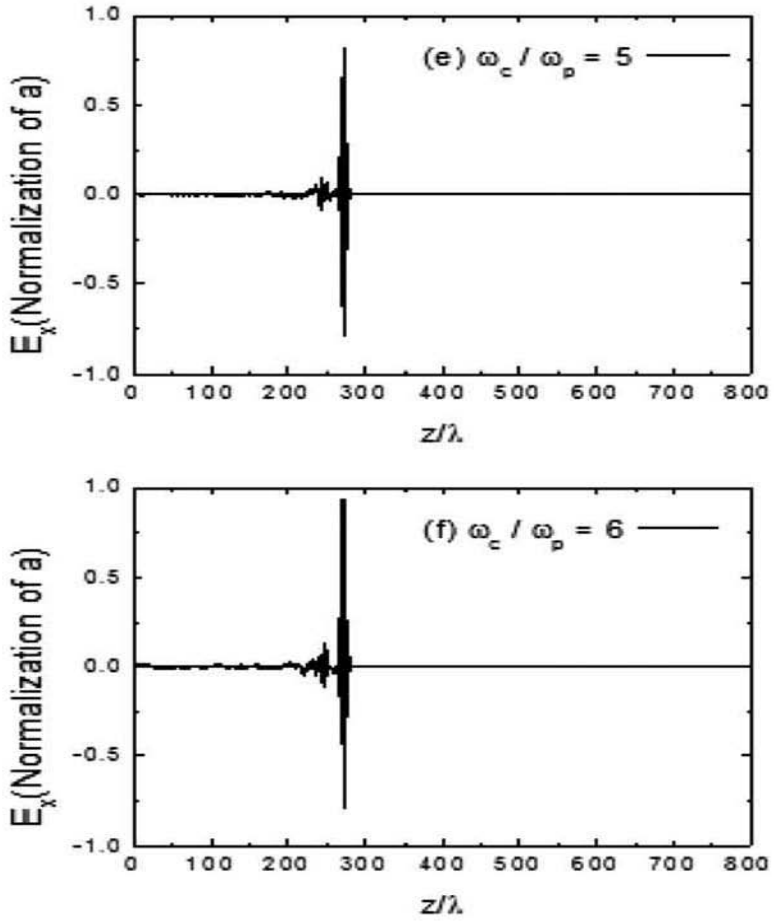

Figure 3.7: Spatial evolution of transverse wakefield along x-axis (E_x) for different magnetic field ratios ω_c/ω_p (a) 1.00, (b) 2.00 (c) 3.00, (d) 4.00, (e) 5.00 and (f) 6.00.

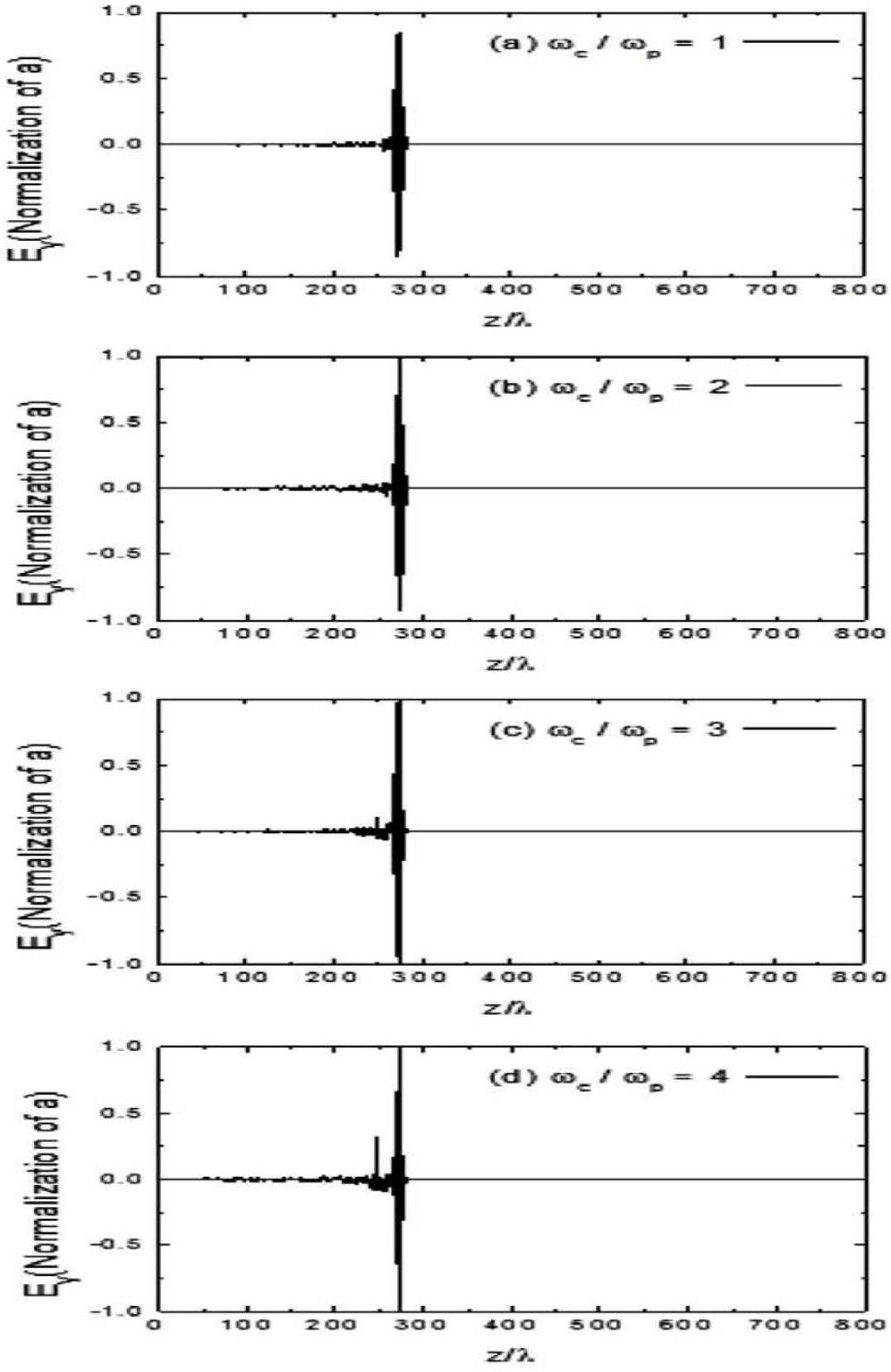
(a) ω_c / ω_p = 1
(b) ω_c / ω_p = 2
(c) ω_c / ω_p = 3
(d) ω_c / ω_p = 4
E_y (Normalization of a)
z/λ
1.0
0.5
0.0
-0.5
-1.0
0
100
200
300
400
500
600
700
800

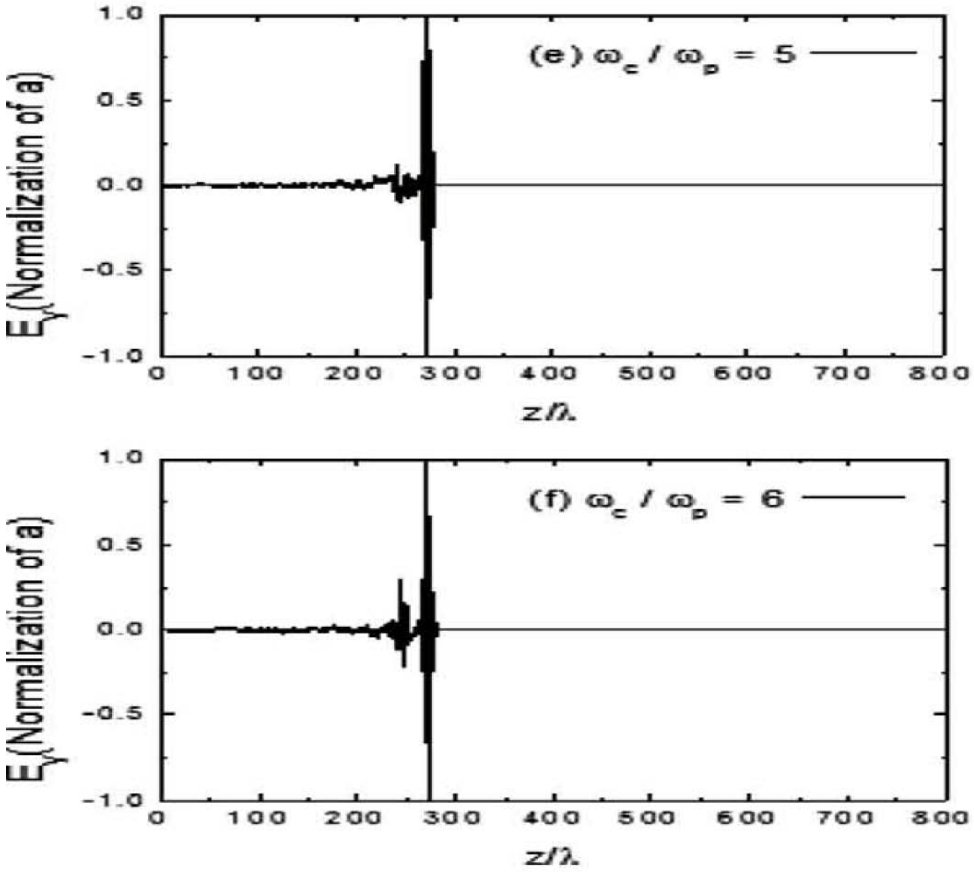

Figure 3.8: Spatial evolution of transverse wakefield along y-axis (E_y) for different magnetic field ratios ω_c/ω_p (a) 1.00, (b) 2.00 (c) 3.00, (d) 4.00, (e) 5.00 and (f) 6.00.

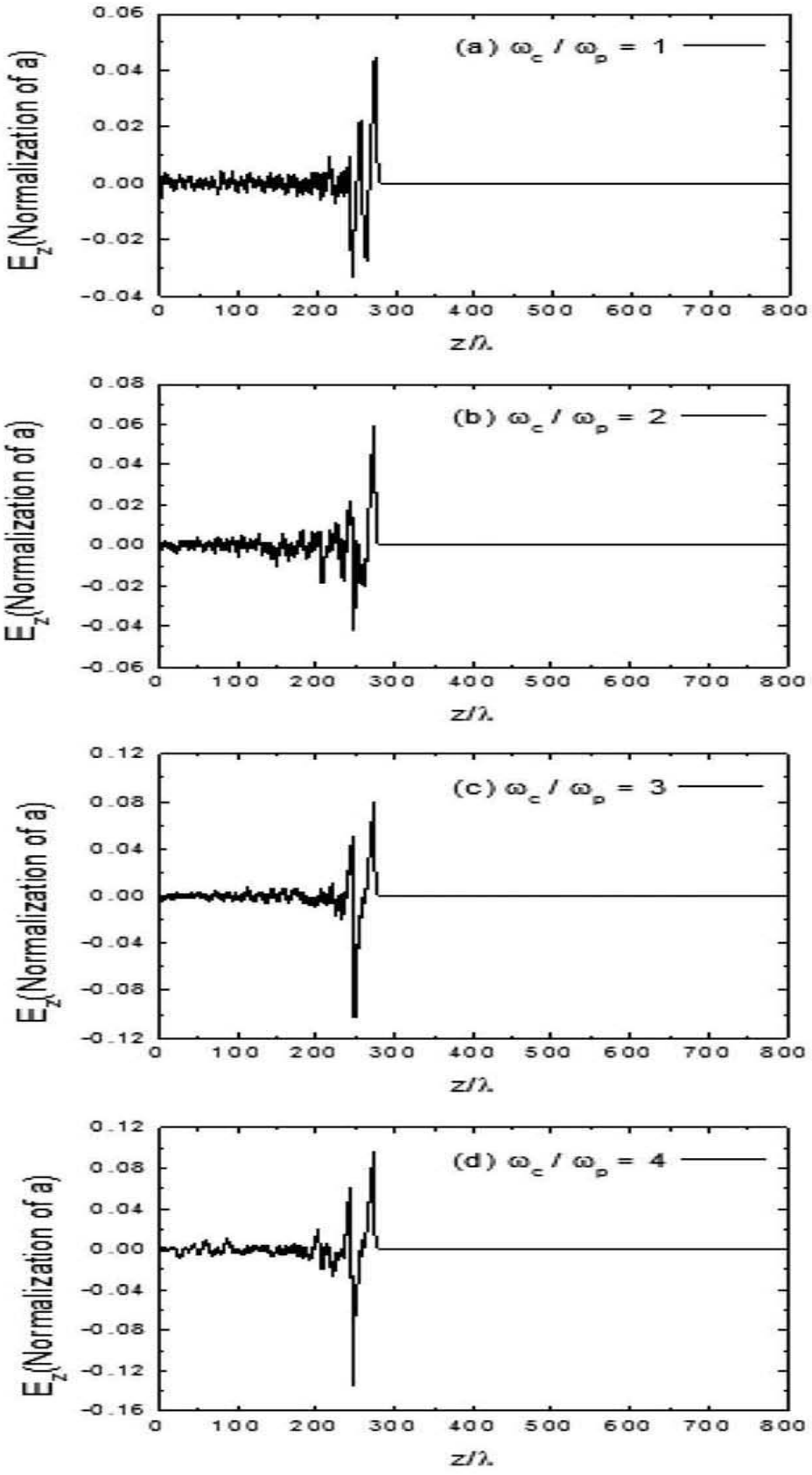
(a) ω_c / ω_p = 1
(b) ω_c / ω_p = 2
(c) ω_c / ω_p = 3
(d) ω_c / ω_p = 4
E_z (Normalization of a)
z/λ

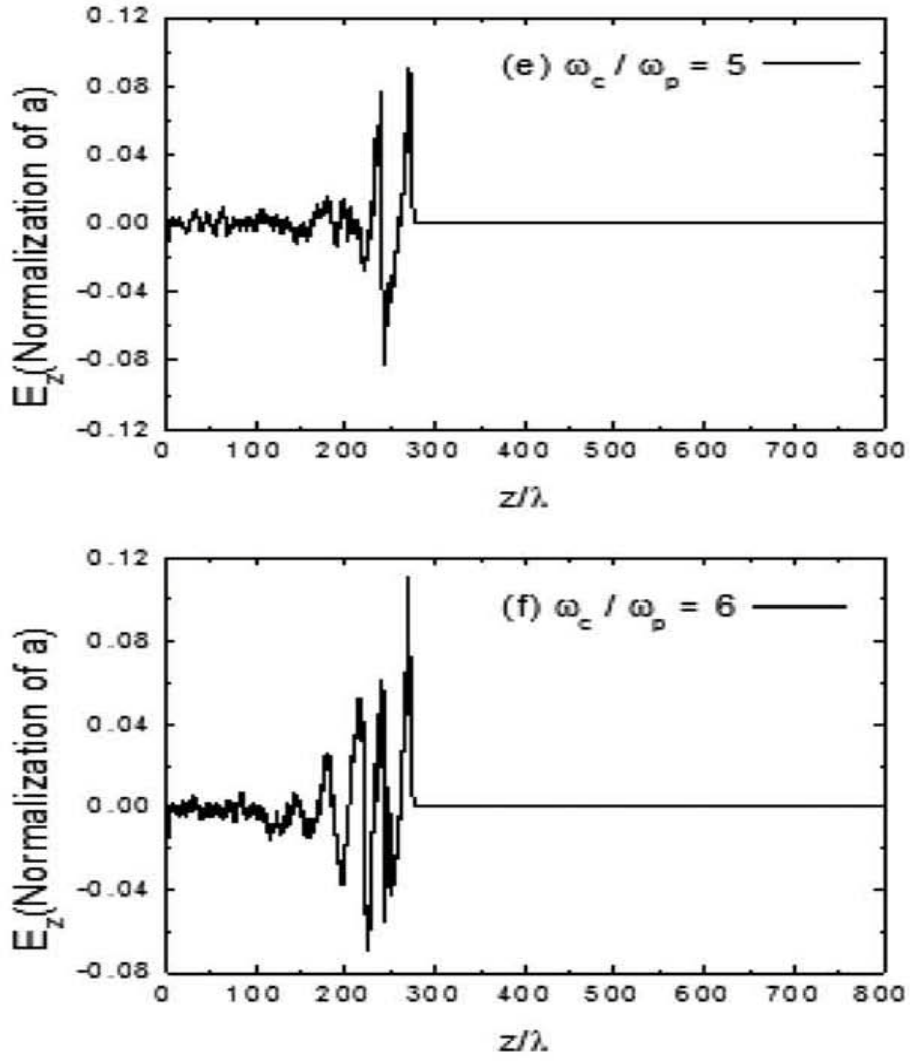

Figure 3.9: Spatial evolution of longitudinal wakefield (E_z) for different magnetic field ratios ω_c/ω_p (a) 1.00, (b) 2.00 (c) 3.00, (d) 4.00, (e) 5.00 and (f) 6.00.

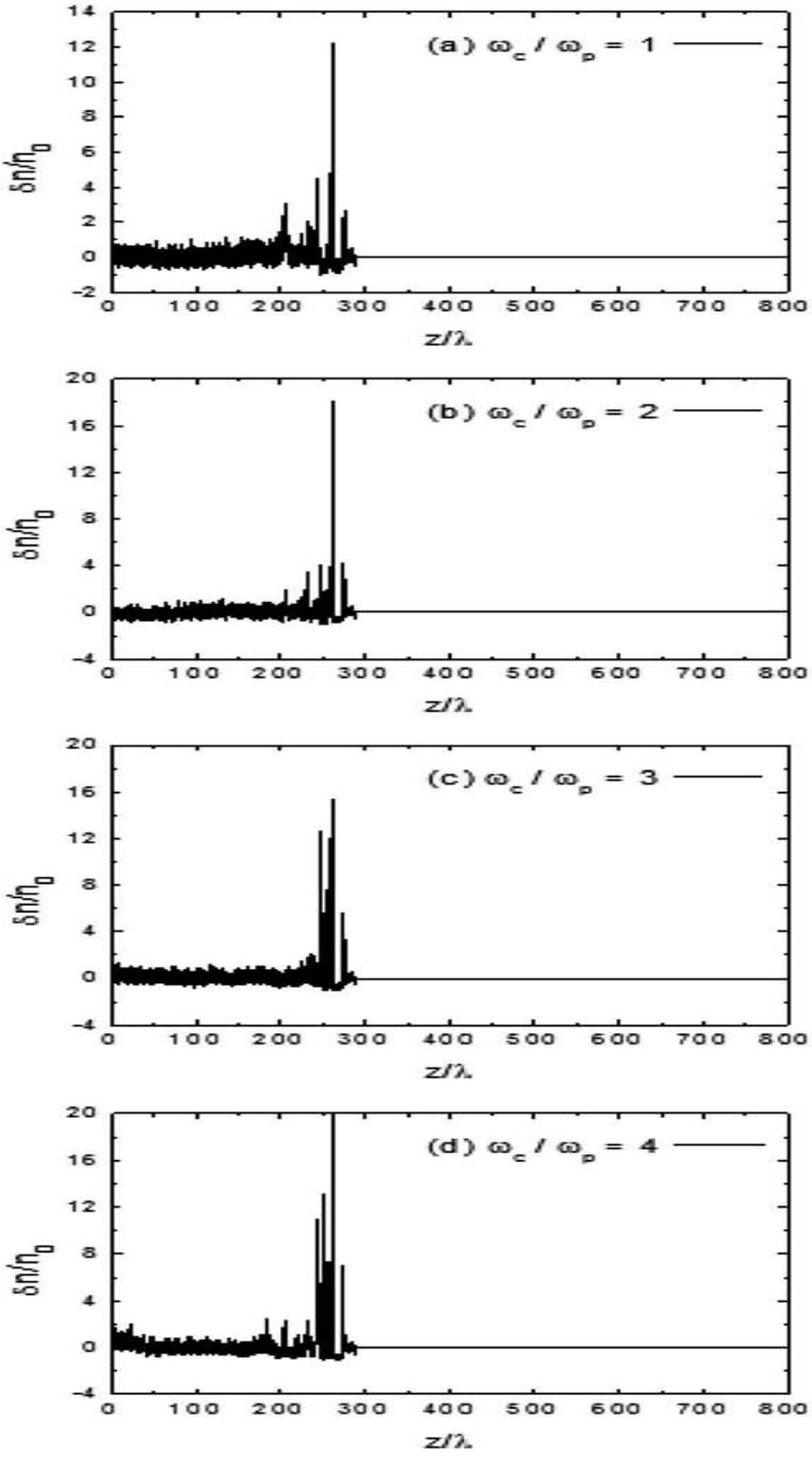
(a) ω_c / ω_p = 1
(b) ω_c / ω_p = 2
(c) ω_c / ω_p = 3
(d) ω_c / ω_p = 4
δn/n_0
z/λ_c

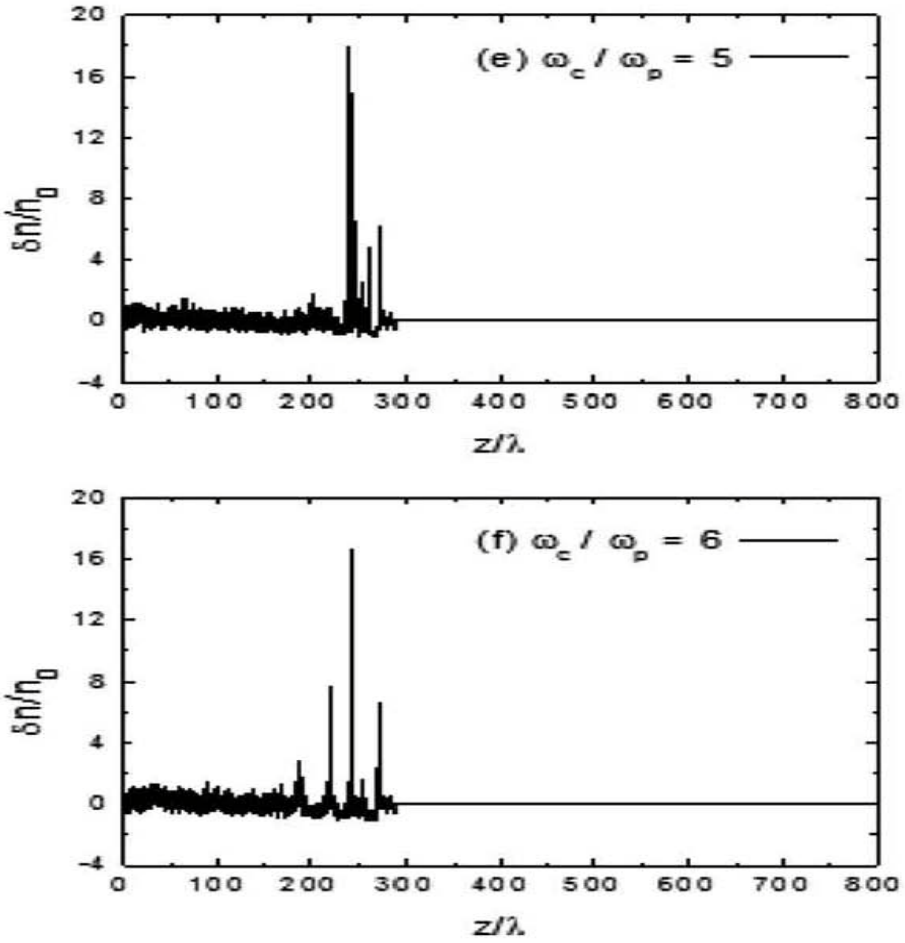

Figure 3.10: Spatial evolution of the normalized plasma density for different magnetic field ratios ω_c/ω_p (a) 1.00, (b) 2.00 (c) 3.00, (d) 4.00, (e) 5.00 and (f) 6.00.

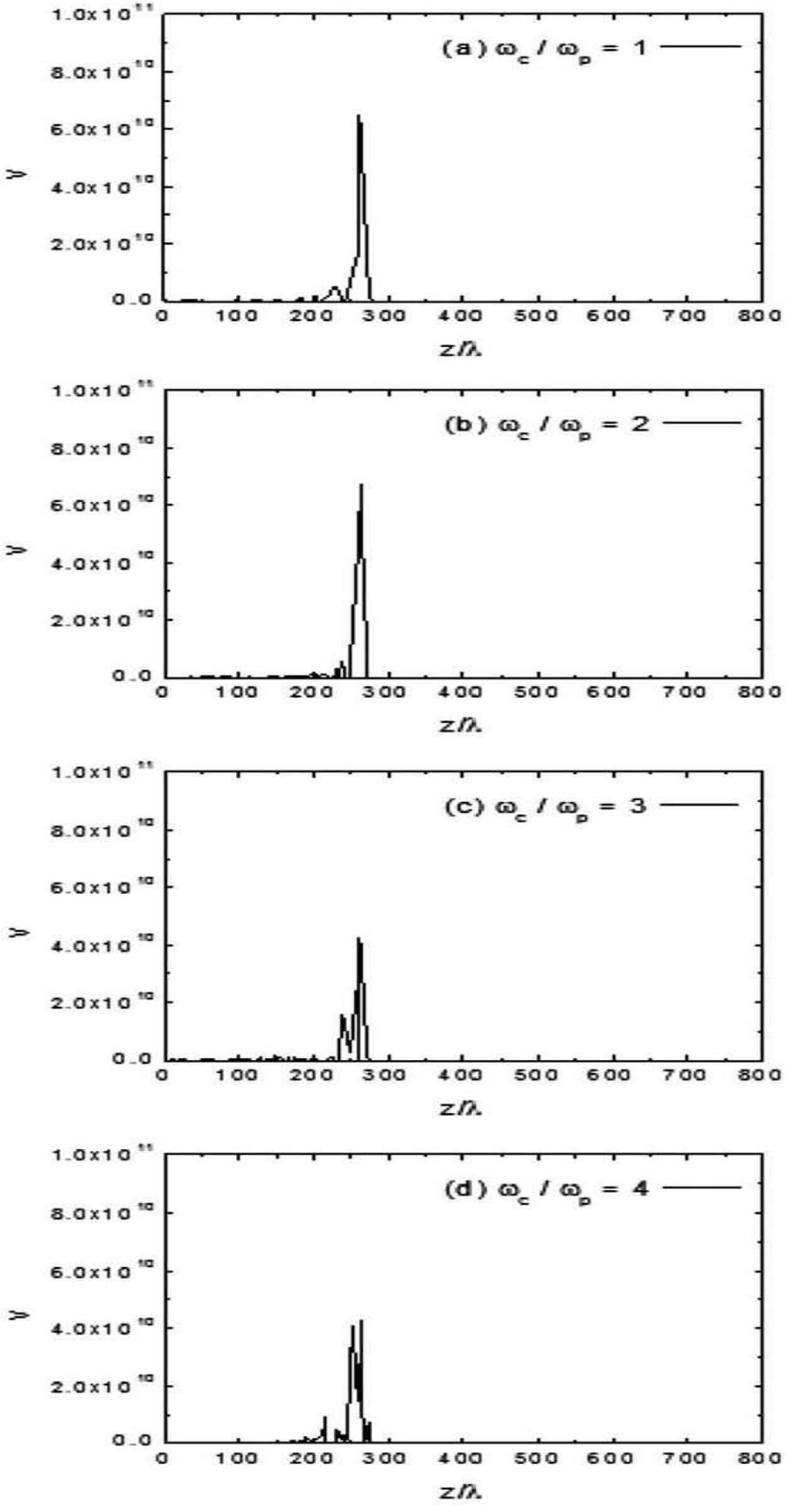
(a) ω_c / ω_p = 1
(b) ω_c / ω_p = 2
(c) ω_c / ω_p = 3
(d) ω_c / ω_p = 4
V
z/λ
0.0
2.0x10^10
4.0x10^10
6.0x10^10
8.0x10^10
1.0x10^11
0
100
200
300
400
500
600
700
800

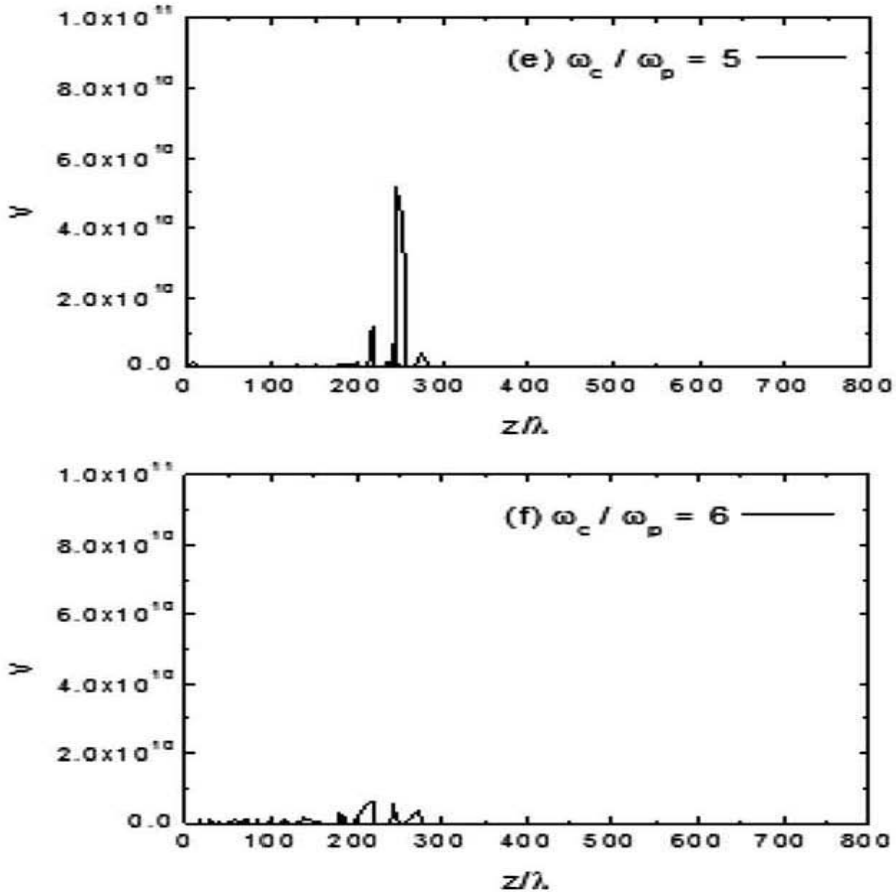

Figure 3.11: Spatial variation of relative velocity distribution of plasma wave for different magnetic field ratios ω_c/ω_p (a) 1.00, (b) 2.00 (c) 3.00, (d) 4.00, (e) 5.00 and (f) 6.00.

Figure 3.11 illustrates spatial profile distribution of the relative velocity between the electrons and the wave. It is concluded that the relative velocity distribution and its magnitude do not change in a proportionate manner with the magnetic field. Various relativistic nonlinear phenomena at different magnetic field ratios play the important role in the spatial profile distribution of the relative velocity.

3.6 Summary

The analysis of short nonparaxial laser pulse in the plasma channel has been carried out in this chapter. The excited wake has electrostatic as well as electromagnetic nature thus excitation of the wake in the plasma is nonlocal. Therefore, the algebraic decay of the fields due to the phase mixing of plasma oscillations with the spatially varying frequencies occurred in the plasma channel.

It has been found that the energy gain increases with increasing the magnetic field. However, the results illustrate the variable pattern of the energy gain for different magnetic field strengths. It was found that the channel radius decreases with magnetic field and increases with relativistic factor. Due to the presence of the collisionless damped hybrid (electromagnetic/electrostatic) modes of the transversely inhomogeneous plasma the channel radius changes significantly. The damped quasi-modes inside the plasma channel are excited.

Bibliography

[2] S.C. Wilks, W.L. Kruer, M. Tabak and A.B. Langdon, Phys. Rev. Lett. 69, 1383 (1992).

[6] T. Tajima and J.M. Dawson, Phys Rev. Lett. 43, 267 (1979).

[7] X. Wang *et al*., Phys Rev. Lett. 84(23), 5324-5327 (2000).

[12] A. Sharma and V.K. Tripathi, Phys. Plasmas 16, 043103 (2009).

[18] E. Esarey, P. Sprangle and J. Krall, IEEE J. Quant. Elect. 33(11), 1879-1914 (1997).

[24] P.K. Shukla, Phys. Scr. 52, 73 (1994).

[114] B.S. Sharma, Archna Jain, N.K. Jaiman, D.N. Gupta, D.G. Jang, H. Suk and V.V. Kulagin, Phys. Plasmas 21, 023108 (2014).

[137] E. Esarey, C. B. Schroeder and W. P. Leemans, Rev. Mod. Phys. 81, 1229 (2009).

[138] P. M. Nilson, S. P. D. Mangles, L. Willingale, M. C. Kaluza, A. G. R. Thomas, M. Tatarakis, R. J. Clarke, K. L. Lancaster, S. Karsch, J. Schreiber, Z. Najmudin, A. E. Dangor and K. Krushelnick, New J. Phys. 12, 045014 (2010).

[139] A. Pukhov and J. Meyer-ter-Vehn, Appl. Phys. B 74, 355 (2002).

[140] S. P. D. Mangles, C. D. Murphy, Z. Najmudin, A. G. R. Thomas, J. L. Collier, A. E. Dangor, E. J. Divall, P. S. Foster, J. G. Gallacher, C. J. Hooker, D. A. Jaroszynski, A. J. Langley, W. B. Mori, P. A. Norreys, F. S. Tsung, R. Viskup, B. R. Walton and K. Krushelnick, Nature 431, 535(2004).

[141] J. Faure, Y. Glinec, A. Pukhov, S. Kiselev, S. Gordienko, E. Lefebvre, J.-P. Rousseau, F. Burgy and V. Malka, Nature 431, 541 (2004).

[142] W. P. Leemans, B. Nagler, A. J. Gonsalves, C. Tóth, K. Nakamura, C. G. R. Geddes, E. Esarey, C. B. Schroeder and S. M. Hooker, Nat. Phys. 2,696 (2006).

[143] C. S. Liu and V. K. Tripathi, Phys. Rev. E 54, 4098 (1996).

[144] H. M. Milchberg, C. G. Durfee and J. Lynch, J. Opt. Soc. Am. B 12, 731(1995).

[145] D. N. Gupta and Chang-Mo Ryu, Phys. Plasmas 12, 053103 (2005).

[146] A. Sharma and V. K. Tripathi, Phys. Plasmas 12, 093109 (2005).

[147] R. P. Sharma and P. K. Chauhan, Phys. Plasmas 15, 063103 (2008).

[148] P. Gibbon, IEEE J. Quantum Electron. 33, 1915 (1997).

[149] H. Yang, J. Zhang, W. Yu, Y. J. Li and Z. Y. Wei, Phys. Rev. E 65,016406 (2001).

[150] C. Deutsch, H. Furukawa, K. Mima, M. Murakami and K. Nishihara, Phys. Rev. Lett. 77, 2483 (1996).

[151] E. Esarey, J. Krall and P. Sprangle, Phys. Rev. Lett. 72, 2887 (1994).

[152] W. Lu, M. Tzoufras, C. Joshi, F. S. Tsung, W. B. Mori, J. Vieira, R. A. Fonseca and L. O. Silva, Phys. Rev. ST Accel. Beams 10, 061301(2007).

[153] S. Kneip, S. R. Nagel, S. F. Martins, S. P. D. Mangles, C. Bellei, O. Chekhlov, R. J. Clarke, N. Delerue, E. J. Divall, G. Doucas, K. Ertel, F. Fiuza, R. Fonseca, P. Foster, S. J. Hawkes, C. J. Hooker, K. Krushelnick, W. B. Mori, C. A. J. Palmer, K. T. Phuoc, P. P. Rajeev, J. Schreiber, M. J. V. Streeter, D. Urner, J. Vieira, L. O. Silva and Z. Najmudin, Phys. Rev. Lett. 103, 035002 (2009).

[154] A. B. Borisov, A. V. Borovskiy, A. M. Prokhorov, O. B. Shiryae, X. M. Shi, T. S. Luk, A. McPherson, J. C. Solem, K. Boyer and C. K. Rhodes, Phys. Rev. Lett. 68, 2309 (1992).

[155] G. S. Sarkisov, V. Y. Bychenkov, V. N. Novikov, V. T. Tikhonchuk, A. Maksimchuk, S.-Y. Chen, R. Wagner, G. Mourou and D. Umstadter, Phys. Rev. E 59, 7042 (1999).

[156] J. E. Ralph, K. A. Marsh, A. E. Pak, W. Lu, C. E. Clayton, F. Fang, W. B. Mori and C. Joshi, Phys. Rev. Lett. 102, 175003 (2009).

[157] A. G. R. Thomas, S. P. D. Mangles, Z. Najmudin, M. C. Kaluza, C. D. Murphy, M. C. Kaluza and K. Krushelnick, Phys. Rev. Lett. 98, 054802(2007).

[158] A. G. R. Thomas, S. P. D. Mangles, C. D. Murphy, A. E. Dangor, P. S. Foster, J. G. Gallacher, D. A. Jaroszynski, C. Kamperidis, K.

Krushelnick, K. L. Lancaster, P. A. Norreys, R. Viskup and Z. Najmudin, Plasma Phys. Controlled Fusion 51, 024010 (2009).

[159] B. M. Luther, Y. Wang, M. C. Marconi, J. L. A. Chilla, M. A. Larotonda and J. J. Rocca, Phys. Rev. Lett. 92, 235002 (2004).

[160] C. G. R. Geddes, C. Toth, J. van Tilborg, E. Esarey, C. B. Schroeder, J. Cary and W. P. Leema, Phys. Rev. Lett. 95, 145002 (2005).

[161] A. J. Gonsalves, K. Nakamura, C. Lin, J. Osterhoff, S. Shiraishi, C. B. Schroeder, C. G. R. Geddes, C. Toth, E. Esarey and W. P. Leemans, Phys. Plasmas 17, 056706 (2010).

[162] C. G. R. Geddes, C. Toth, J. van Tilborg, E. Esarey, C. B. Schroeder, D. Bruhwiler, C. Nieter, J. Cary and W. P. Leemans, Nature 431, 538 (2004).

[163] E. Esarey, C. B. Schroeder, B. A. Shadwick, J. S. Wurtele and W. P. Leemans, Phys. Rev. Lett. 84, 3081 (2000).

[164] R. F. Hubbard, D. Kaganovich, B. Hafizi, C. I. Moore, P. Sprangle, A. Ting and A. Zigler, Phys. Rev. E 63, 036502 (2001).

[165] R. F. Hubbard, P. Sprangle and B. Hafizi, IEEE Trans. Plasma Sci. 28, 1159 (2000).

[166] P. Sprangle, E. Esarey, J. Krall and G. Joyce, Phys. Rev. Lett. 69, 2200 (1992).

[167] G. Shvets, J. S. Wurtele, T. C. Chiou and T. Katsouleas, IEEE Trans. Plasma Sci. 24, 351 (1996).

[168] C. G. R. Geddes, C. Toth, J. van Tilborg, E. Esarey, C. B. Schroeder, D. Bruhwiler, J. Cary and W. P. Leemans, AIP Conf. Proc. 737, 521 (2004).

[169] T. P. A. Ibbotson, N. Bourgeois, T. P. Rowlands-Rees, L. S. Caballero, S. I. Bajlekov, P. A. Walker, S. Kneip, S. P. D. Mangles, S. R. Nagel, C. A. J. Palmer, N. Delerue, G. Doucas, D. Urner, O. Chekhlov, R. J. Clarke, E. Divall, K. Ertel, P. S. Foster, S. J. Hawkes, C. J. Hooker, B. Parry, P. P. Rajeev, M. J. V. Streeter and S. M. Hooker, Phys. Rev. ST Accel. Beams 13, 031301 (2010).

[170] H. Y. Wang, C. Lin, Z. M. Sheng, B. Liu, S. Zhao, Z. Y. Guo, Y. R. Lu, X. T. He, J. E. Chen and X. Q. Yan, Phys. Rev. Lett. 107, 265002 (2011).

[171] A. Friou, E. Lefebvre and L. Gremillet, Phys. Plasmas 19, 022704 (2012).

[172] T. M. Antonsen and P. Mora, Phys. Fluids B 5, 1440 (1993).

[173] W. B. Mori and C. D. Decker, Phys. Rev. Lett. 72, 1482 (1994).

[174] Y. Ehrlich, C. Cohen, A. Zigler, J. Krall, P. Sprangle and E. Esarey, Phys. Rev. Lett. 77, 4186 (1996).

[175] P. Sprangle, J. Krall and E. Esarey, Phys. Rev. Lett. 73, 3544 (1994).

[176] N. E. Andreev, V. I. Kirsanov and L. M. Gorbunov, Phys. Plasmas 2, 2573 (1995).

[177] D. N. Gupta, Mamta Singh, B. S. Sharma, D. G. Jang and H. Suk, Simulation on laser wakefield generation in a parabolic magnetic-plasma channel, Proc. 5th Int. Particle Accelerator Conf. (IPAC'14), Dresden, Germany, paper TUPME075, pp 1528-1530, (2014).

[178] E. Esarey and W. P. Leemans, Phys. Rev. E 59, 1082 (1999).

[179] V. I. Karpman and H. Washimi, J. Plasma Phys. 18, 173 (1977).

[180] T. Katsouleas, Phys. Rev. A 33, 2056 (1986).

[181] W. P. Leemans, C. W. Siders, E. Esarey, N. E. Andreev, G. Shvets and W. B. Mori, IEEE Trans. Plasma Sci. 24, 331 (1996).

[182] W. P. Leemans, P. Volfbeyn, K. Z. Guo, S. Chattopadhyay, C. B. Schroeder, B. A. Shadwick, P. B. Lee, J. S. Wurtele and E. Esarey, Phys. Plasmas 5, 1615 (1998).

[183] R. Sadighi-Bonabi and M. Etehadi-Abari, Phys. Plasmas 17, 032101 (2010).

Chapter 4

Relativistic plasma mirror and attosecond pulse generation

4.1 Introduction

The interaction of an ultra-intense ultra-short laser pulse ($I \geq 10^{20}$ W/cm^2) with an optically reflecting metal surface generates a dense plasma that acts as a plasma mirror (PM). These mirrors spectacularly reflect the main part of the laser pulse and can be used as the active optical elements to manipulate the spatial and temporal properties of the high harmonics. The modification in the temporal contrast leads to generation of an intense attosecond extreme ultraviolet (XUV) or X-ray pulses of energy in the range 1-10 J through nonlinear harmonic upconversion of the laser pulse. However, pressure exerted by the laser pulse deforms the plasma mirror surface nonuniformlly. This results in the rotation of the plasma mirror that affects the spatial and temporal contrast of the reflected laser field and the high harmonics.

Plasma mirrors are routinely used at moderate light intensities ($10^{14} - 10^{16}$ W/cm^2) as ultrafast optical switches to enhance the temporal contrast of the femtosecond lasers. For intensities $I \geq 10^{16}$ W/cm^2, nonlinear response of the plasma mirrors to the laser field results in temporal modulations of the reflected field, associated to the high-order harmonic generation in its spectrum. These harmonics generated through various mechanisms are associated, in the time domain, to the attosecond pulses. For lasers with intensity $\geq 10^{18}$ W/cm^2, the key high-order harmonic generation results in the relativistic oscillating mirror where the laser driven oscillation of the plasma surface induces a periodic Doppler effect on the reflected laser field [4, 184-188] which further results in harmonic orders of several thousands. In these high intensity applications, laser field exerts such a high pressure on the plasma ($\approx$ 5 Gbar for $I \approx 10^{19}$ W/cm^2) inducing a significant motion of the plasma mirror surface even during a femtosecond laser

pulse. This leads to the spatial variation of intensity on the target giving rise to the deformation in the surface of the plasma mirror.

The work of this chapter is based on the deformation of the plasma mirror due to $\mathbf{E} \times \mathbf{B}$ drift. Deformation in the relativistic plasma mirror surface in the form of an elliptical curvature is considered which can affect the spatial and spectral properties of the reflected beam. This in turn rotates the plasma mirror which could bring a change in spatio-temporal coupling mechanism and the Doppler shift of the reflected laser field. The results of the harmonic generation and their dependence on the intensity of incident laser pulse have been presented. We have also studied the effect of the rotation on the wavefront of the reflected laser field and the effect of the phase divergence on the generation of the attosecond pulse. In section 4.2, theoretical model for attosecond pulse generation is presented. Spatial properties of reflected laser field in presence of plasma mirror are discussed in section 4.3. In section 4.4, spectral phase of attosecond pulses is described. Intensity dependence of generated harmonics is investigated in section 4.5. The summary of the work is presented in section 4.6.

4.2 Theoretical model for attosecond pulse generation

The presented model is based on quasi-instantaneous response of the electrons to the laser pulse in which it is assumed that the response time of electrons to the laser field is less than the optical period of the laser pulse. Qualitatively, when a high intense ultra-short laser beam ($I \approx 10^{18}$ W/cm^2) is incident on a highly polished surface of metal, it exerts a very high pressure of about 5 Gbar. Figure 4.1(a) shows the process in which electrons are pushed inside the metal with respect to the ion background. In each optical cycle electrons pulled outside with respect to ion background such that the response of electrons to laser field can be considered as a spring. When pulled outward, they form a relativistic electrons jet that are responsible for the relativistic oscillation of mirror (ROM) and generation of attosecond pulse as shown in Figure 4.1(b).

The process involves the following steps.

1. Electrons are pushed inside due to the tremendous pressure the laser exerts on the electrons; a high density spike is formed at the sharp surface of the electron distribution.

2. These fast electrons propagating in the dense part of the plasma form ultra-short bunches which impulsively excites plasma oscillations.

3. In the inhomogeneous part of the plasma formed by the density gradient at the vacuum-plasma interface, these collective oscillations radiate light at a different local plasma frequencies found in the gradient.

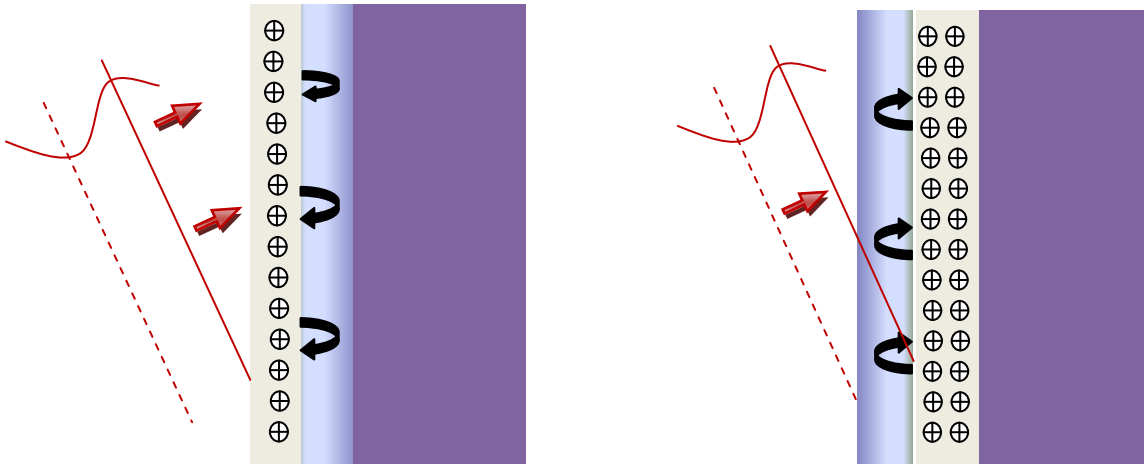

(a) (b)

Figure 4.1: Schematic representation of different processes (a) Electrons around n= n_c are pushed inside by the incident laser and (b) pulled outward because of inertia.

Let the laser beam incident on the target surface at an angle θ and compress the surface through a distance x(t) at time t. It is assumed that the electron density at the plasma mirror surface varies as $n(x) = n_0 \exp(x/L)$ for $n > n_0$, where n_0 is the electron density at the vacuum-plasma interface and L is the interaction length. Using the theory of balancing between the pushing force exerted by the laser pulse and the restoring force, it is obtained that

$$e\,E(x) = m\,\omega_p^{\,2}\,x, \tag{4.1}$$

where $\omega_p^{\,2} = 4\pi n_0 e^2/m$ is the plasma frequency for electron density n_0.

The reflected electric field from the moving surface of plasma mirror can be approximated as

$$E(x) \propto E_L\,(1 + \exp(x/L)), \tag{4.2}$$

where $E_L = m\omega c\alpha/e$ with $\omega = 2\pi c/\lambda$ is laser frequency and α is the normalized vector potential of the laser. For inward displacement at x = L, equation (4.1) leads to the following expression for the maximum inward excursion x_{max} of electrons in one optical cycle

$$x_{max} = L\,ln\,(1 + \frac{\lambda a n_c(1 + sin\,\theta)}{2\pi L n_0}). \tag{4.3}$$

The inward push depends on the laser strength parameter α and polarization state of the incident beam and x_{max} increases with interaction length L which depends on the intensity of the incident laser beam and the nature of the target surface.

To include the effect of the rotation of the plasma mirror due to $\mathbf{E} \times \mathbf{B}$ drift, we define the angular frequency Ω_r perpendicular to the plane of plasma mirror.

The velocity of the electrons due to $\mathbf{E} \times \mathbf{B}$ drift is defined as

$$\boldsymbol{v_d} = \boldsymbol{\Omega_r} \times \boldsymbol{r} = \frac{\boldsymbol{E} \times \boldsymbol{B}}{B^2}, \tag{4.4}$$

where we have assumed that rotation of the plasma mirror is considered as the rotation of the solid body.

This drift leads to an additional change in the spatial and temporal properties of the reflected electric field which affects the high-order harmonic generation (HHG) and attosecond pulse generation (ASG).

The electric field and magnetic field in the rotating frame can be written as [189]

$$\boldsymbol{E}' = \boldsymbol{E} + (\boldsymbol{\Omega_r} \times \boldsymbol{r}) \times \boldsymbol{B},$$

$$\boldsymbol{B}' = \boldsymbol{B} + \frac{m\boldsymbol{\Omega_r}}{e}. \quad (4.5)$$

It is assumed that a constant rotation to the plasma mirror and a constant shift in the attosecond pulse generation takes place. Including the effect of rotation per cycle of laser, the equation (4.3) is reduced to the following form

$$x_{max} = L\, ln\,(1 + \frac{\lambda a\, n_c(1+sin\ \theta)}{2\pi L n_0} + \frac{\pi \Omega_r L\, cos\ \theta}{\lambda\omega}), \quad (4.6)$$

where B << B_L, B_L and B are magnetic field of laser and the magnetic field arising due to the rotation of plasma mirror.

The rotational angular velocity Ω_r can be approximated as

$$\Omega_r = \sqrt{\left\{\frac{2\pi c^2 (1+a^2)^{\frac{1}{2}}}{L\lambda_p\left(1+\frac{\lambda}{\lambda_p}\right)}\right\}}. \quad (4.7)$$

This leads to the following expression for the maximum inward excursion x_{max} of electrons in a given optical period

$$x_{max} = L\, ln\,(1 + \frac{\lambda a\, n_c(1+sin\ \theta)}{2\pi L n_0} + \sqrt{\left\{\frac{\pi L (1+a^2)^{\frac{1}{2}}}{2\lambda_p\left(1+\frac{\lambda}{\lambda_p}\right)}\right\}}\, cos\ \theta), \quad (4.8)$$

where $\lambda_p(x)$ is space dependent plasma wavelength and is given by $\lambda_p(x) = \lambda_L\sqrt{(n_c/n_0)}$, where n_c and n_0 are critical and unperturbed plasma densities respectively.

From equation (4.8), it is obvious that the electron boundary displacement x_{max} depends on the normalized vector potential of the incident laser field. The higher the amplitude, the electrons get pushed further inside the target. This results in the more high-order harmonic generation (HHG) that can be isolated as attosecond pulse trains. The rotational effect in the plasma mirror further increase the boundary displacement of the electrons and provides greater denting in the plasma electron density surface. This result in the modification of the spatial envelope of plasma density that can be considered as a function of two

space coordinates as n(x, y) and is attributed to the spatially inhomogeneous ponderomotive force exerted by the laser field.

4.3 Spatial properties of reflected laser field

We consider that the spatial amplitude of the reflected beam is Gaussian and the spatial profile of the n^{th} harmonic is h_n in the plane of the plasma mirror such that

$$h_n \propto \exp(y'^2/2w_n^2), \tag{4.9}$$

where y' is the spatial coordinate and w_n is the beam size of n^{th} harmonic in the source plane z = 0.

Figure 4.2 shows the geometrical representation of the focusing of the harmonic beam by the plasma mirror. The parameter σ_n accounts for the effect of the plasma mirror curvature on the spatial properties of the harmonic beam. Following [190], the Rayleigh length of harmonic beam can be written as

$$z_{Rn} = \left(\frac{\pi w_n^2}{\lambda_n}\right) + \left(\frac{4\pi^2 \lambda_p^2 \Omega_r}{v_p}\right), \tag{4.10}$$

where $v_p \approx c$ is the phase velocity of the laser beam and λ_p is the plasma wave wavelength at some time t.

The focusing position of the n^{th} harmonic is given as

$$z_{n0} = z_{Rn} \frac{\sigma_n}{1+\sigma_n^2}, \tag{4.11}$$

where σ_n is the focusing parameter of the n^{th} harmonic.

The focusing parameter is a dimensionless quantity and is defined as

$$\sigma_n = \frac{2\pi}{\cos(\theta_n + \varphi_n)} \left(\frac{w_n}{w_f}\right)^2 \left(\frac{\rho_d}{\lambda_n}\right), \tag{4.12}$$

where w_n is the waist of n^{th} harmonic in the z = 0 plane and and w_f is the waist in the focal plane ($z = z_0$) respectively.

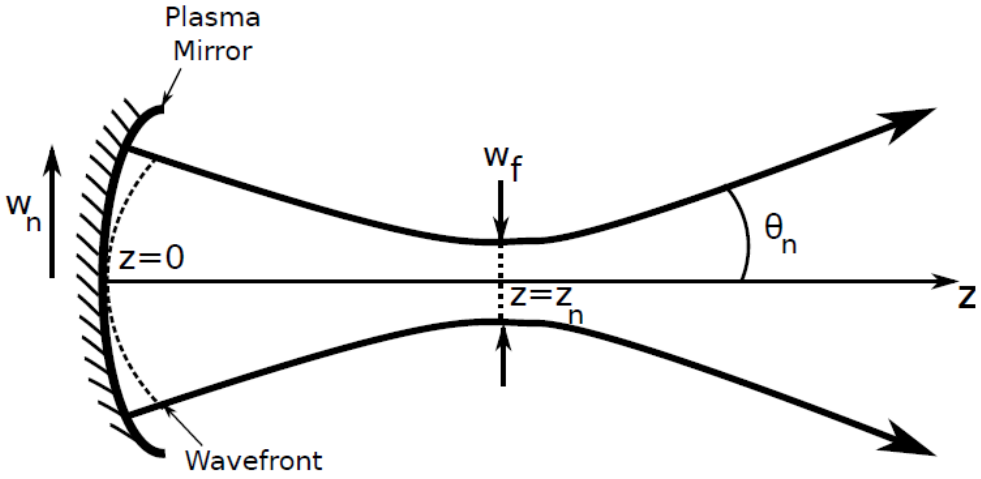

Figure 4.2: Focusing of the harmonic beam by the plasma mirror. The w_n is the harmonic beam size of n^{th} harmonics in the source plane z = 0 and z_n is the distance between the PM surface and harmonic's best focus.

φ_n is angle of rotation of the wavefront in the focal plane of the n^{th} harmonic and is defined as

$$\varphi_n = \sqrt{2\pi^2 nacx_{max}}/\omega L^2. \tag{4.13}$$

ρ_d is the denting parameter defined as

$$\rho_d = \frac{w_n^2}{2f_n}. \tag{4.14}$$

f_n is the focal length of the plasma mirror for n^{th} harmonic and is given as

$$f_n \approx w_f^2 \frac{\sin \varphi_n}{8\, L \cos^2(\theta_n + \varphi_n)}, \tag{4.15}$$

where θ_n is angle of divergence. This is one of the asymptotic focal length obtained from the electron dynamics only.

The rotating effect of plasma mirror due to $\mathbf{E} \times \mathbf{B}$ leads to the change in the value of w_f and w_n and decreases the divergence parameter of the reflected harmonics.

4.4 Relativistic oscillating mirror and spectral phase of attosecond pulses

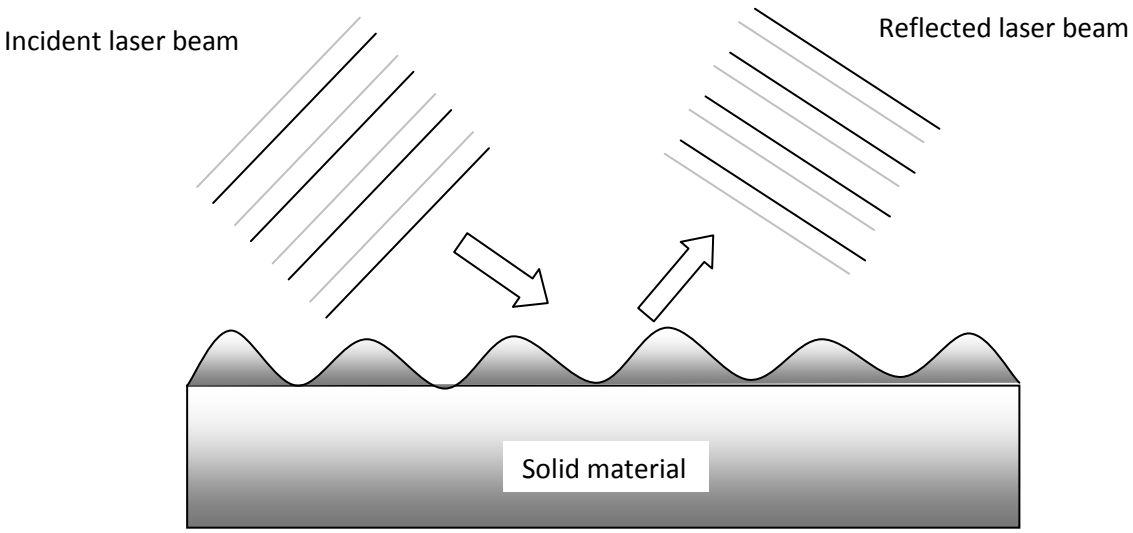

Figure 4.3: Schematic representation of the process involved in ROM.

The schematic representation of the relativistic oscillating mirror is shown in Figure 4.3. When high intense laser pulse is incident on a solid surface, the laser driven plasma surface becomes relativistic leading to the strong Doppler shifts of the laser light. As the oscillating surface rotates, it creates an additional phase shift and distortion in the field of the reflected harmonic beams.

As this phase distortion repeats itself with periodicity of the driving laser field leading to the more harmonics of the incident frequency appearing in the reflected beam as shown in Figure 4.4 in arbitrary unit (a.u.). The harmonic spectra associated with a train of attosecond pulses for different intensities are shown in Figure 4.5.

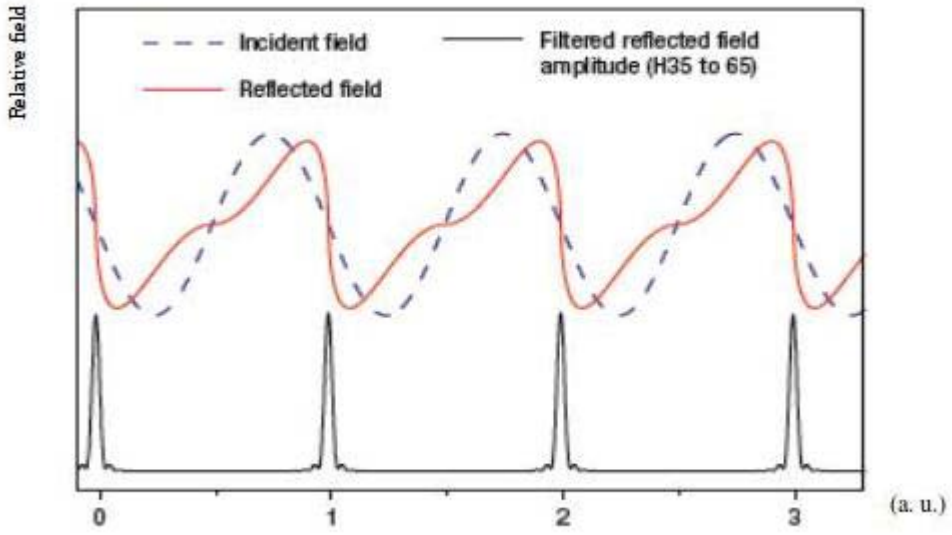

Figure 4.4: Electric field spectrum from the plasma mirror.

The harmonic divergence θ_n of n^{th} harmonic is given

$$\theta_n^2 = \left(\frac{\lambda_n}{\pi w_n}\right)^2 + \left(\frac{\lambda_n}{\pi w_n}\right)^2 (n\varphi_n)^2$$

$$\text{or } \theta_n = \theta_n^0 \sqrt{1 + (n\varphi_n)^2}, \qquad (4.16)$$

where $\theta_n^0 = \lambda_n/\pi w_n$ is the harmonic divergence for the source size w_n in the absence of plasma mirror curvature and rotational effect due to $\mathbf{E} \times \mathbf{B}$.

4.5 Intensity dependence

Figure 4.5 shows the intensity dependence of the harmonic spectrum from a metal surface. It is found that the wavetrain of the attosecond pulses can be observed when intensity of the laser beam exceeds to 10^{18} W/cm^2. It is further concluded that the rotation effect in relativistic oscillating plasma mirror changes the denting mechanism of the reflected laser field and the phase coherence in the attosecond pulses. The rotational effect of plasma mirror due to $\mathbf{E} \times \mathbf{B}$ changes the phase parameter of the harmonics and increases the value of f_h

leading to the high repetition rate for attosecond pulses with increased intensity. It is also observed that the intensity of the attosecond pulses depends on the harmonic phases.

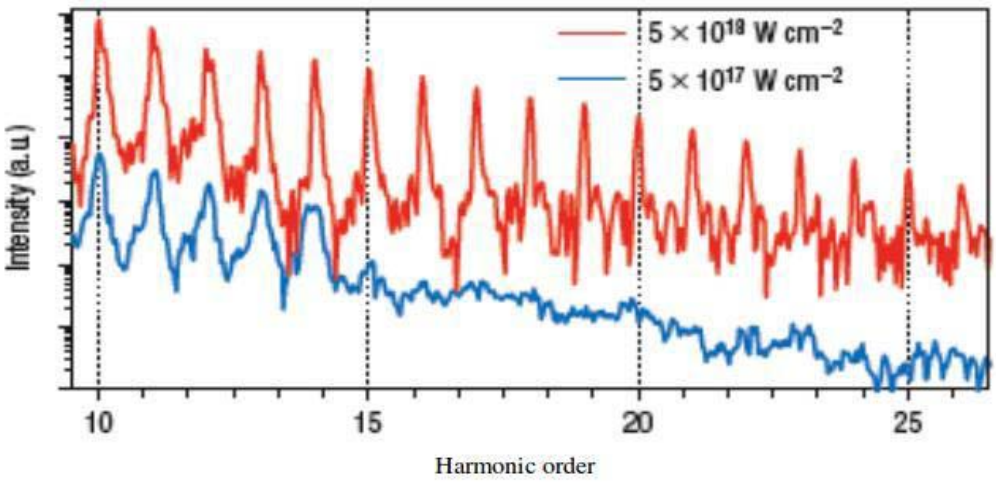

Figure 4.5: Harmonic spectra from the plasma mirror.

When an electromagnetic wave is reflected from an oscillating mirror, its frequency spectrum is extended to high frequency range and the wave breaks-up into the short waves.

In relativistic oscillating mirror, harmonics of much higher frequency are generated. The reflected wave's electric field from the oscillating mirror in a time t′ = t−x(t)/c is given as [4]

$$E_r = -\frac{1}{c}\frac{\partial A_L(t',x')}{\partial t'}, \qquad (4.17)$$

where x′ and t′ are the position and time of the reflected waves respectively in the observer's frame and A_L is the vector potential of the laser pulse. The oscillating mirror model implies that the tangential components of the vector potential are zero at the mirror surface. The component of reflected electric field from the oscillating plasma surface will be parallel to incident electromagnetic wave. As a result of it, if the oscillating mirror moves with relativistic factor γ_L » 1 towards

the laser pulse with oscillating frequency ω_{osc}, electric field $E_{\|}$ and duration τ_L, the reflected electric field will be given as [4]

$$E_r \propto \gamma_L^2 E_{\|}, \tag{4.18}$$

and the pulse duration will be [4]

$$\tau_L^{'} \propto \frac{\tau_L}{\gamma_L^2}. \tag{4.19}$$

The Fourier spectrum of the electric field of reflected beam at position x′ and time t′ is

$$E_r(\Omega_r) = \frac{mc\,\omega^2}{e\sqrt{2\pi}} \int a\left(t^{'}, x^{'}\right) e^{\left(-i\omega\left(t^{'}-\left(\frac{x^{'}}{c}\right)\right)\right)}\, e^{-i\varphi_r}\, dt^{'}, \tag{4.20}$$

where

$$t' - (x'/c) = t, \tag{4.21}$$

and φ_r is the phase of reflected wave and is given by

$$\varphi_r = \int \Omega_r(u) du = \omega[2t^{'}(u) - u], \tag{4.22}$$

where $u = t' - x'(t')/c$ and spatial position x′, time t′ and t′(u) can be obtained from the equation

$$t^{'}(u) = u + \frac{x^{'}\left(t^{'}(u)\right)}{c}. \tag{4.23}$$

Differentiating equation (4.22), we obtain

$$\frac{\partial \varphi_r^{'}}{\partial u} = \omega\left(1 + \frac{\beta^{'}(u)}{1-\beta^{'}(u)}\right), \tag{4.24}$$

where $\beta(u) = c^{-1}\, dx'(u)/dt'$ is the mirror velocity normalized by c. Using the exponential decay parts and properties of Array's function to analyze the spectrum modulation due to the **E** × **B** effect and equations (4.21-4.24), we obtain

$$E_r = \left(\frac{\omega}{n\,\Omega_r}\right)^{\frac{5}{2}} e^{\left(-\frac{16(\sqrt{5})\,\Omega_r^{\frac{5}{2}}}{5\left(\sqrt{n^3}\right)\omega\,\omega_p^{\frac{3}{2}}}\right)} \times Re\left(\frac{e^{i\,\Omega_r\,t\,-\,i\varphi_r'}}{\frac{10\sqrt{2}\omega_p}{5\left(\sqrt{n^3}\omega_p+i\omega\right)}}\right), \tag{4.25}$$

where Ω_r is the rotational frequency of the plasma mirror and n is harmonic order.

The amplitude of these reflected pulses decreases fast when Ω_r grow.

Using equation (4.25) to obtain the intensity of n^{th} harmonic as

$$I_n \propto \left(\frac{\omega}{n\,\Omega_r}\right)^5 \left(\frac{n^3\omega_p^2-\omega^2}{8\omega_p^2}\right) e^{\left(-\frac{32(\sqrt{5})\,\Omega_r^{\frac{5}{2}}}{5\left(\sqrt{n^3}\right)\omega\,\omega_p^{\frac{3}{2}}}\right)}. \tag{4.26}$$

The intensity of the reflected pulses decreases with higher harmonics and the plasma frequency.

Figure 4.5 shows the spectral representation of the intensity of reflected electric field of different attosecond pulses corresponding to two different intensities of the incident laser beam. It is observed that the intensity of the attosecond pulses depend on the harmonic phases. If v_r is the relativistic velocity of the reflected electric field of a particular harmonic at time t′(u), the maximum relativistic factor will be given as

$$\gamma_{max} = \frac{1}{\sqrt{\left(1-\frac{v_r^2\left(t'(u)\right)}{c^2}\right)}} \quad . \tag{4.27}$$

Consequently, for the surface γ factor during a relativistic spike, the highest harmonic will be generated over the time period

$$\Delta t \approx \frac{1}{\omega\gamma_{max}^3} \approx \frac{1}{\omega\left(\frac{n_c}{n_0}\right)^{\frac{3}{2}}}, \tag{4.28}$$

where n_c is the critical density of the plasma surface.

For this duration the reflected fields move with relativistic velocity in the direction of the emitted radiation.

The intensity variation over this time interval for nth harmonic can be written as

$$I_n \propto \left(\frac{\omega\, n_c}{n\, \Omega_r\, n_0}\right)^5 \left(\frac{n^3\omega_p^2 - \omega^2}{8\omega_p^2}\right) e^{\left(-\frac{32(\sqrt{5})\,\Omega_r^{\frac{5}{2}}}{5\left(\sqrt{n^3}\right)\omega\,\omega_p^{\frac{3}{2}}}\right)}. \quad (4.29)$$

Equation (4.29) shows a theoretical result of the temporal structure of the intensity of attosecond pulse trains produced on the plasma mirrors.

4.6 Summary

The chapter presents a simple analytical model for the generation of the attosecond pulse from the relativistic oscillating plasma mirror with $\mathbf{E} \times \mathbf{B}$ effect that leads to the rotation of the oscillating plasma mirror. The $\mathbf{E} \times \mathbf{B}$ effect changes the harmonic divergence which could change the pattern of extended ultra-broadband attosecond pulse spectrum and repetition rate. Also, it addresses the temporal characterization of the reflected electric field from plasma mirror with temporal resolution going down to the attosecond range. It is further observed that the harmonic number of the reflected laser field increases with the intensity of the incident laser beam.

Bibliography

[4] T. Baeva, S. Gordienko and A. Pukhov, Phys Rev. E 74, 046404 (2006).

[184] C. Thaury and F. Quéére, J. Phys. B 43, 213001 (2010).

[185] R. Licheters, J. Meyer-ter-Vehn, A. Pukhov, Phys. Rev. E 3, 3425 (1996).

[186] A.A. Gonoskov, A.V. Korzhimanvo, A.V. Kim, M. Marklund and A.M. Sergeev, Phys. Rev. E 84, 046403 (2011).

[187] B.Dromey et al., Nat. Phys. 2, 456 (2006).

[188] Michael Chini, Kun Zhao and Zenghu Chang, Nat. Photonics 8, 178-186 (2014).

[189] B. Lehnert, Dynamics of charged particles, Interscience Publishers, New York (1964).

[190] H. Vincenti , S. Monchoc , S. Kahaly , G. Bonnaud, P. Martin and F. Quéré, Nat. Communication (2014).

Chapter 5

High intense laser pulse propagation in an underdense magnetized plasma

5.1 Introduction

It has been about forty years since Tajima and Dawson [6] proposed the laser beams to excite plasma waves for the electron acceleration. In recent years, there has been tremendous progress in this field, both theoretical and experimental.

Plasma waves are generated through the displacement of plasma electrons by the ponderomotive force of a laser pulse. Electrons are trapped in large amplitude plasma waves. Under resonant condition, the trapped plasma electrons are accelerated to very high energies over very short distances by the longitudinal electric field of the waves. However, the laser plasma interaction distance is always less than or equal to the vacuum Rayleigh length due to the diffraction of the laser pulse in the plasma and hence, eliminates the advantage of ultrahigh gradient acceleration. The higher accelerations can be obtained only by maintaining the higher magnitudes of the wakefield amplitude as well as the laser plasma interaction length. Chen *et al*. [191] first investigated the plasma wakefield and Rosenzweig *et al*. [192, 193] reported the first experimental evidence followed by K. Nakajima *et al.* [194] for generation of plasma wakefield.

In laser plasma interactions, fast electrons are produced by the parametric instabilities such as the two plasmon decay near the quarter critical density and the Stimulated Raman Scattering (SRS) [195, 196] below the quarter critical density which have been extensively studied by the particle simulation in unmagnetized plasmas [197-202].

During the past few years there has been a great deal of theoretical and computational work on the propagation of high intensity short laser pulses through underdense plasmas [203-205] in which the pulse lengths less than the diffraction length, intensity approaching 10^{18} Wcm^{-2} for 1μm light and plasma

density of the order of 1% of the critical density is considered. At these high intensities the laser pulses, however, are susceptible to much collective phenomena which can cause the wave break up. One of these phenomena is the shock formation [39].

For the interaction of a high intense laser pulse and the plasma electrons, the electron density has an oscillatory component that modulates the phase of the electromagnetic wave effectively producing the wake. The magnetic effect modifies the localized conditions for the laser plasma interaction and hence the spatio-temporal properties of the accelerated particles. This also modifies the behavior of the plasma wave [206].

Propagation of a high intense ultra-short Gaussian laser pulse of normalized vector potential $\boldsymbol{\alpha}$ (= e$\mathbf{A}$/mc) in an underdense magnetized plasma of density 10^{-5} n_{cr} has been considered. The high intense ultra-short laser pulse evokes the wakefield excitation in the Rayleigh interaction length $z_R = \pi w_0^2/1.4\lambda_p$, where w_0 is the focal spot diameter which is equal to 8 μm and λ_p is electron plasma wavelength. The charge separation in the interaction region generates strong electric field of peak value $E = mc\alpha\omega/e$, where m, c, α, ω and e are the mass of an electron, speed of light, normalized vector potential, laser frequency and the charge of an electron respectively. In present analysis, electron acceleration by a Gaussian laser pulse in the presence of an axial magnetic field in a plasma has been studied.

In this chapter, the effect of magnetic field on the wakefield excitation for high intense ultra-short Gaussian laser pulse in an underdense magnetized plasma is analyzed. In section 5.2, relation between the generated electric field and the externally applied magnetic field has been obtained. In section 5.3, two dimensional particle-in-cell (2D PIC) simulation results are presented to give an insight into the the wakefield evolution. Finally, the summary of results and findings are presented in section 5.4.

5.2 wakefield analysis

Consider the propagation of a high intense ultra-short laser pulse in a low density plasma immersed in an axial magnetic field $\mathbf{B} = B_0\,\hat{\mathbf{z}}$.

The vector potential [108] of the high intense ultra-short laser pulse is given by

$$\boldsymbol{A} = A_0\, e^{-\frac{r^2}{w_0^2}}\, e^{-\frac{\xi^2}{2L^2}}\, e^{-i(\mathrm{kz}\,-\,\omega \mathrm{t})}, \tag{5.1}$$

where $\xi = z - ct$, L is laser pulse length equal to $c\,\tau_L$, $r = \sqrt{(x^2+y^2)}$ is the radial coordinate, k is the propagation constant, ω is the laser frequency and c is the speed of light.

The propagation constant [40] is given by

$$k = \frac{\omega}{c}\left(1 - \frac{\omega_p^2}{\omega(\gamma\omega - \omega_c)}\right)^{\frac{1}{2}}, \tag{5.2}$$

here $\omega_c = eB_0/m$ is the cyclotron frequency, $\omega_p = 4\pi n_0 e^2/m$ is the electron plasma frequency, n_0 is the unperturbed density of plasma and $\gamma = (1+a^2)^{1/2}$ is the relativistic factor.

The laser pulse propagates, in the rarefied plasma, almost with the speed of light c, spot size w_0 and length of the pulse remain almost unchanged during the propagation.

The response of underdense magnetized plasma to the high intense ultra-short laser pulse can be described by electron momentum equation

$$m\frac{d(\gamma \boldsymbol{v})}{dt} = -e\boldsymbol{E} - e(\boldsymbol{v}\times\boldsymbol{B}) - eB_0(\boldsymbol{v}\times\hat{\mathrm{z}}), \tag{5.3}$$

where electric field and magnetic field of the laser pulse are given in terms of the vector potential as

$$\boldsymbol{E} = -\frac{\partial \boldsymbol{A}}{\partial t}, \tag{5.4}$$

$$\boldsymbol{B} = \nabla \times \boldsymbol{A}. \tag{5.5}$$

For an axial symmetric geometry, we obtain from the equations (5.3-5.5)

$$m\frac{d(\gamma v_r)}{dt} = e\frac{\partial A}{\partial t} + ev_z\frac{\partial A}{\partial z} - eB_0 v_\varphi, \tag{5.6}$$

$$m\frac{d(\gamma v_\varphi)}{dt} = eB_0 v_r, \tag{5.7}$$

$$m\frac{d(\gamma v_z)}{dt} = -ev_r\frac{\partial A}{\partial z}. \tag{5.8}$$

Using equation (5.1) in equations (5.6-5.8), we obtain the axial component of the velocity of the electrons in the plasma as

$$v_z = \frac{c\alpha^2\xi^2}{1-\alpha^2\xi^2}, \tag{5.9}$$

where

$$\alpha^2 = \frac{c^2a^2}{L^4(\gamma^2\omega^2-\omega_c^2)}. \tag{5.10}$$

Here $a = \frac{eA}{mc}$ is the normalized vector potential of the laser pulse.

Since the wakefield is excited in the plasma during laser pulse plasma interaction, the value of axial electric field of the wake excited in the plasma is given by

$$-eE_z = m\frac{d\gamma v_z}{dt}.$$

Using equation (5.9), we have obtained the value of the axial electric field as

$$E_z = \frac{mc^2\gamma}{e}\frac{2\alpha^2\xi}{1-\alpha^2\xi^2}. \tag{5.11}$$

The density perturbation in the plasma due to the wake is

$$n = n_0\frac{2\gamma\alpha^2c^2}{\omega_p^2}\frac{1+3\alpha^2\xi^2}{(1-\alpha^2\xi^2)^3}. \tag{5.12}$$

The nonlinear current density in the plasma in presence of the laser pulse is obtained by using equation (5.9) and (5.12) as

$$. J = en_0 \frac{2\gamma c^3 \alpha^4 \xi^2}{\omega_p^2} \frac{1+3\alpha^2\xi^2}{(1-\alpha^2\xi^2)^4}. \quad (5.13)$$

$$J = en_0 \frac{2\gamma c^3 \alpha^4 \xi^2}{\omega_p^2} \frac{3\alpha^2\xi^2\left(1+\frac{1}{3\alpha^2\xi^2}\right)}{\alpha^8\xi^8\left(\frac{1}{\alpha^2\xi^2}-1\right)^4}.$$

Since $1 << \frac{1}{3\alpha^2\xi^2}$, hence the nonlinear current density is obtained as

$$J = en_0 \frac{2\gamma c^3}{\omega_p^2} \alpha^4\xi^2. \quad (5.14)$$

The expression of nonlinear current density offers an opportunity to further analysis of plasma such as instability etc.

The generation of the wakefield in a plasma is depending on the intensity of laser pulse and the laser pulse gets slightly modified with time.

5.3 PIC simulation results

Variation in the electron density due to the generation of the wakefield in the plasma is shown in Figure 5.1. Spatial profile of the electric field due to wake are plotted in Figures 5.2(a) and 5.2(b). It is shown that the evolution of the wakefield in a plasma depends on the magnitude of the external magnetic field. Figure 5.3 illustrated the spatial variation of the laser pulse propagating through a plasma which shows that the laser pulse gets slightly modified with time. Our results match that of the two dimensional PIC simulation of the propagation of a laser pulse, with the same typical set of parameters used earlier, in a magnetized plasma which gives an insight into the wakefield evolution.

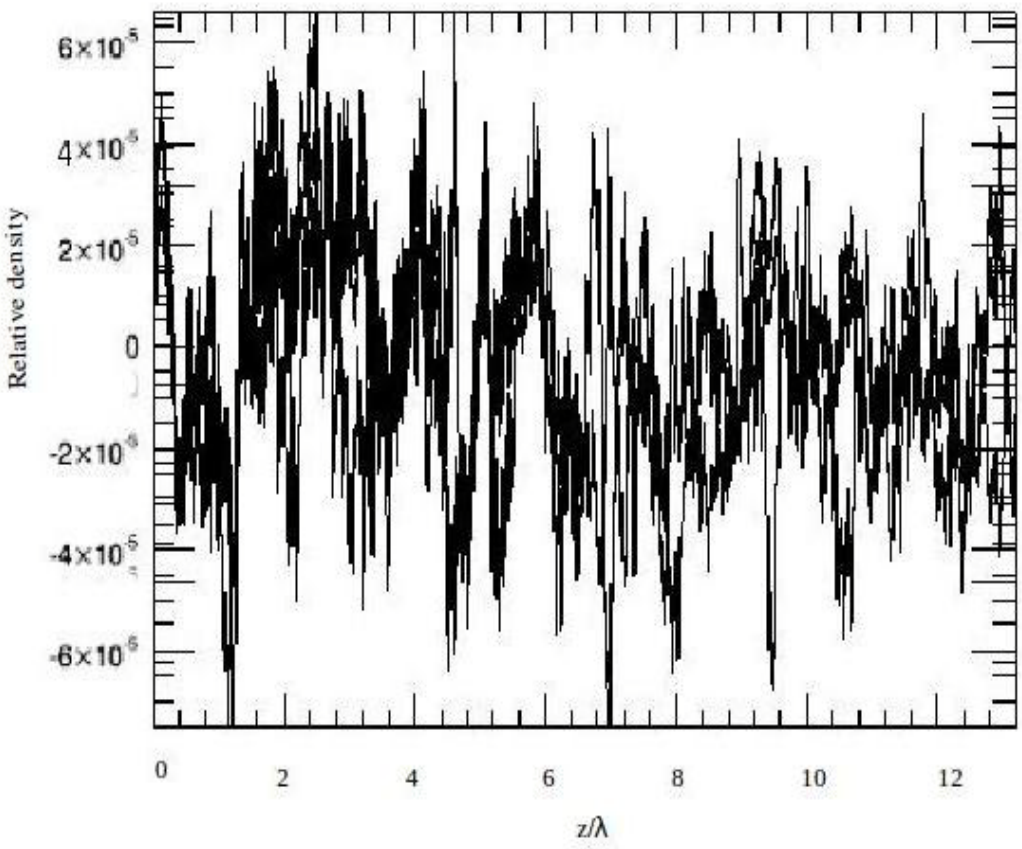

Figure 5.1: Spatial variation of the electron density relative to the critical density (i.e. on the scale of $\pm 6\times\mathbf{10}^{-5}$ n/n_{cr}).

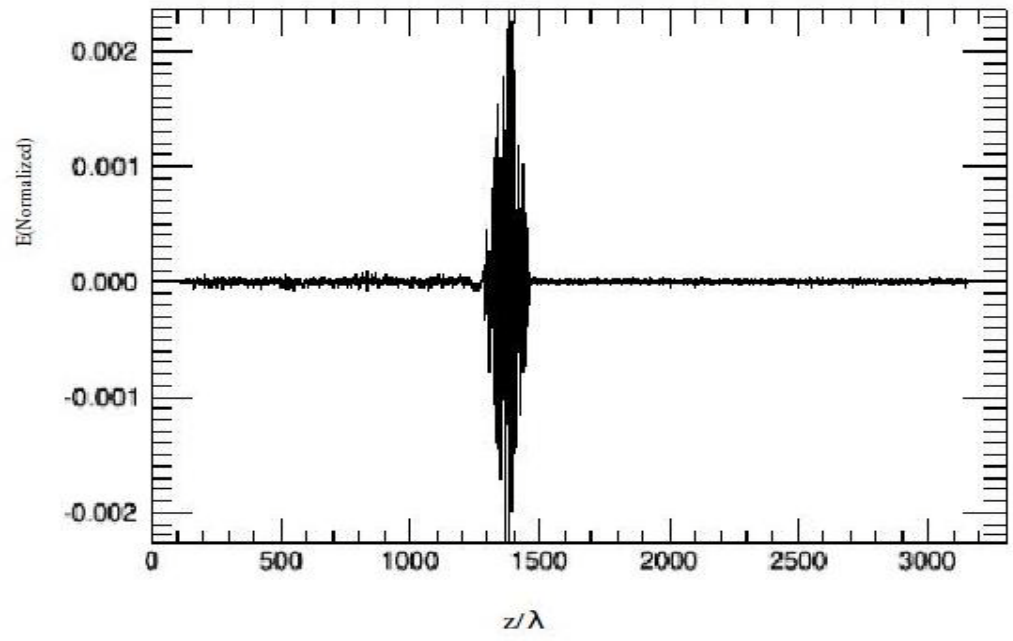

(a)

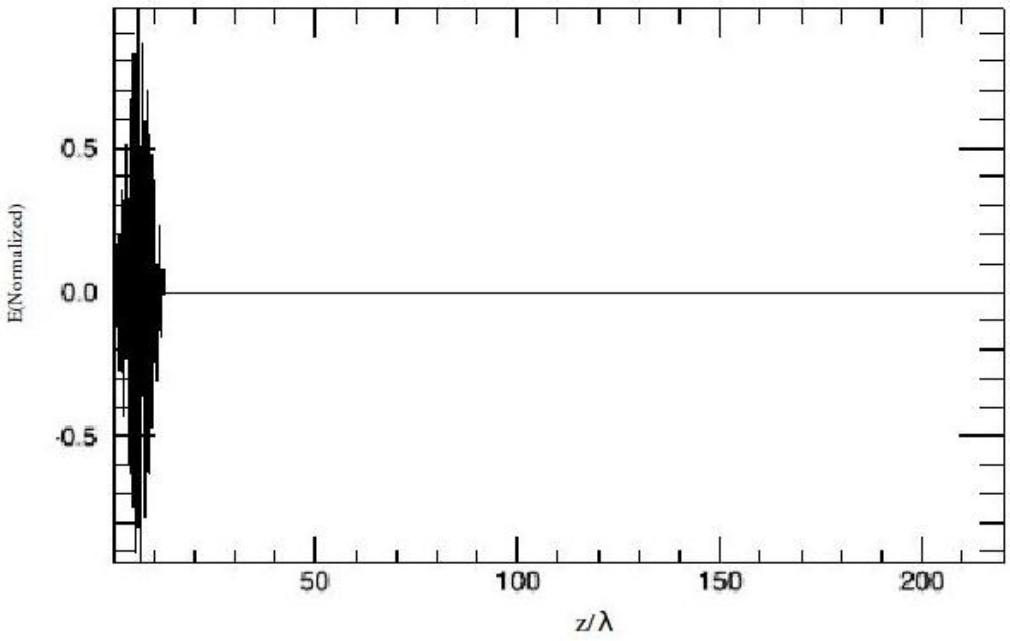

(b)

Figure 5.2: Spatial profile of normalized axial electric field at magnetic field ratios ω_c/ω_p (a) 0.31 (b) 1.57.

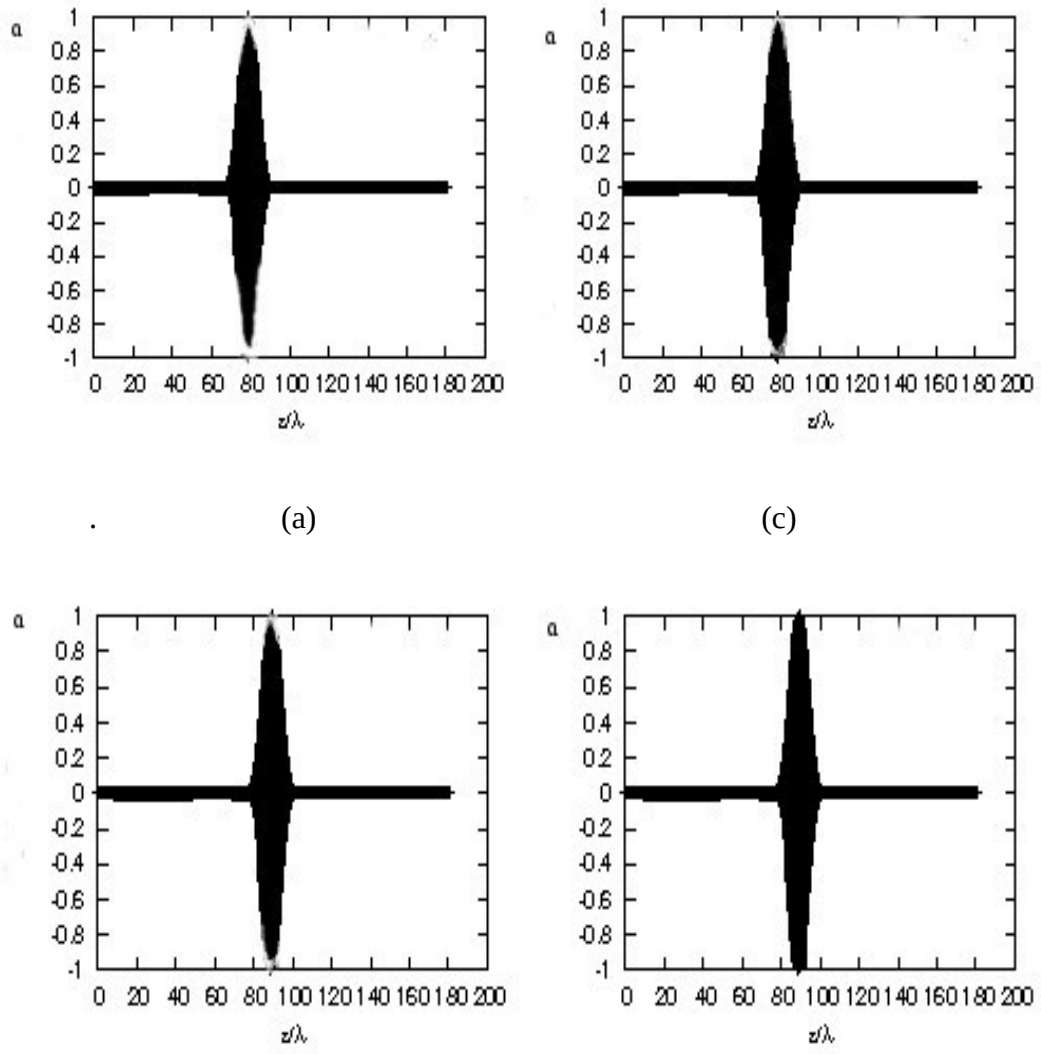

. (a) (c)

(b) (d)

Figure 5.3: Evolution of the laser pulse at time (a) 10 τ_L (b) 20 τ_L (c) 30 τ_L (d) 40 τ_L.

5.4 Summary

The generation of the wakefield in a plasma due to variation in the electron density depends on the magnitude of the external magnetic field. The energy exchange is more effective at the higher values of the magnetic field. It is also shown that the laser pulse gets slightly modified with time.

Bibliography

[6] T. Tajima and J.M. Dawson, Phys Rev. Lett. 43, 267 (1979).

[39] A. Sharma and V.K. Tripathi, Phys. Plasmas 12, 093109 (2005).

[40] R. Singh and V.K. Tripathi, Phys. Plasmas 16, 052108 (2009).

[108] E. Esarey, P. Sprangle, J. Krall and A. Ting, IEEE Trans. Plasma Sci. 24, pp.252-288 (1996).

[191] P. Chen, J. M. Dawson, R. W. Huff and T. Katsouleas, Phys. Rev. Lett. 54, 693 (1985).

[192] J. B. Rosenzweig, D. B. Cline, B. Cole, H. Figueroa, W. Gai, R. Konecny, J. Norem, P. Schoessow and J. Simpson, Phys. Rev. Lett. 61, 98 (1988).

[193] J. B. Rosenzweig, P. Schoessow, B. Cole, W. Gai, R. Koneey, J. Nora and J. Simpson, Phys. Rev. A 39, 1586 (1989).

[194] K. Nakajima *et al.*, Phys. Rev. Lett. 74, 4428 (1995).

[195] J. F. Drake et al., Phys. Fluids 17, 778 (1974).

[196] K. Estabrook and W. L. Kruer, Phys. Fluids 26, 1892 (1983).

[197] K. Estabrook, W. L. Kruer and B.F. Lasinki, Phys. Rev. Lett.45, 1399 (1980).

[198] D. W. Forslund, J. M. Kindel and E. L. Lindman, Phys. Rev. Lett. 30, 739 (1973).

[199] B. Sokri and A. R. Niknam, Phys. Plasmas 13, 113110 (2006).

[200] M. Y. Yu, Wei Yu, Z. Y. Chen et al., Phys. Plasma 16, 2468 (2003).

[201] A. Maksimchuk et al., Phys. Plasma 15, 056703 (2008).

[202] Z. Najmuddin, K. Krushellnick, E. L. Clark and C. Joshi, Journal of Modern Optics 50, 673 (2003).

[203] A. R. Niknam, M. Hashemzadeh, and B. Shokri, Phys. Plasma 16, 033105 (2009).

[204] J. R. Penano et al., Physical Review E 66, 036402 (2002).

[205] W. -T. Chen et al., Phy. Rev. Lett. 92, 075003 (2004).

[206] Khaleel Hassoon, Hyder Salih and V.K. Tripathi, Phys. Scr. 80, 065501 (2009).

Chapter 6

Conclusion and future work

In this thesis, we have presented an analytical model of orbital angular momentum transfer from and magnetic field generation by the relativistic Laguerre-Gaussian (LG) beam. Angular momentum transfer and magnetic field generation for both the linearly and circularly polarized Laguerre-Gaussian beams are presented in the relativistic domain. It is observed that generated magnetic field depend on the orbital angular momentum (OAM) transfer and mass correction of a photon in the relativistic limit. The effective mass of photons becomes more significant at higher Laguerre-Gaussian modes and larger plasma densities. The generated magnetic field depends on the Laguerre-Gaussian mode order, laser intensity, azimuthal angle and relativistic factor. It is found that the generated magnetic field increases with the laser intensity. It is observed that the generated axial magnetic field decreases on increasing the azimuthal angle when beam intensity is constant. The magnitude of the generated axial and azimuthal magnetic fields changes with both, the mode order of $LG_p^{|l|}$ and the azimuthal symmetry. Further, it is observed that excitation of magnetic fields are possible for both circularly and linearly polarized laser beams and for different azimuthal angles. The magnitude of generated magnetic field due to circularly polarized Laguerre-Gaussian beam of higher modes decreases with increasing azimuthal angle and is greater than that of the linearly polarized beam. It is also shown that the magnetic field generated due to the higher Laguerre-Gaussian modes is not quasistatic but change over some spatial distribution of the plasma.

The wakefield generation in an inhomogeneous magnetized plasma channel is also considered in the present work. The excited wake has an electrostatic as well as an electromagnetic nature and thus excitation of the wake in the plasma is nonlocal. Therefore, the algebraic decay of the fields due to the phase mixing of plasma oscillations with the spatially varying frequencies occurred in the plasma channel. Channel radius of the laser pulse changed significantly by the presence of the collisionless damped hybrid

(electromagnetic/electrostatic) modes of the transversely inhomogeneous plasma. It has been shown that the channel width decreases with increasing magnetic field ratio (ω_c/ω_p) and increases with relativistic factor ($\gamma(z)$). The results indicate that the propagation of an intense short circularly polarized laser pulse propagates over a significant extended distance. Furthermore, the laser pulse can have a much greater stability during propagation in the inhomogeneous magnetized plasma channel as compared with the homogeneous plasma channel. It is observed that the phase of the axial component of the wakefield increases linearly with magnetic field ratio (ω_c/ω_p) and also increases with relativistic factor ($\gamma(z)$). Thus, the phase shift of electrons with respect to the wakefield could be effectively controlled by an appropriate value of ω_c/ω_p. It is also observed that the dephasing length increases linearly up to the magnetic field ratio $\omega_c/\omega_p \leq 2.5$ and thereafter it becomes almost constant whereas the accelerating length increases with $\gamma(z)$ leading to the enhancement taking place in the combined focusing effects of the relativistic channel coupling with the nonlinearities and the wakefield. The results indicate that the decelerating length or the accelerating length can be increased by the external magnetic field and the relativistic factor $\gamma(z)$. Thus, the dephasing length can be enhanced over the conventional decelerating length by strong magnetic field. It has been found that the energy gain increases with increasing magnetic field. However, the simulation illustrates the variable pattern of the energy gain for different magnetic field strengths. It is predicted that an autoresonance condition is achieved at $\omega_c/\omega_p = 2$ where the energy gain is maximum. The wakefield gets longitudinal as well as transverse in the presence of the applied magnetic field. The transverse wakefield spectrum for different strengths of magnetic field predicted that the wake has maximum amplitude at $z \approx 270\lambda$, where z and λ are axial location and laser wavelength respectively. The transverse profile of the channel remains stable under the variation of applied magnetic field. The longitudinal wakefield profiles for different magnetic field strengths have shown that the wakefield has a maximum amplitude at $z \approx 270\lambda$. The density perturbation increases with the external magnetic field. Some undesired singularities and instabilities can be suppressed by the modulation in the plasma density changing the response of the relativistic

nonlinear regime. The relative velocity distribution and magnitude change, but, not proportionately, with the magnetic field when spatial profile distribution of the relative velocity is considered. Various nonlinear phenomena at different magnetic field ratios play an important role in the spatial profile distribution of the relative velocity.

The thesis also presents a simple analytical model for the generation of the attosecond pulse from the relativistic oscillating plasma mirror with $\mathbf{E} \times \mathbf{B}$ effect that leads to the rotation in the oscillating plasma mirror. The $\mathbf{E} \times \mathbf{B}$ effect changes the harmonic divergence which could change the pattern of an extended ultra-broadband attosecond pulse spectrum and repetition rate. It is further observed that the number of harmonics in the reflected laser field increases with the intensity of the incident laser beam and the electron plasma density. It is found that the wave train of the attosecond pulses can be observed when intensity of the laser beam exceeds 10^{18} W/cm^2. It is further concluded that the rotation effect in relativistic oscillating plasma mirror changes the denting mechanism of the reflected laser field and the phase coherence in the attosecond pulses. The rotation effect of plasma mirror due to $\mathbf{E} \times \mathbf{B}$ changes the phase parameter of the harmonics and increases the value of focal length of the plasma mirror leading to the high repetition rate for attosecond pulses with increased intensity.

The wakefield excitation and electron acceleration by a high intense ultra-short laser pulse in an underdense plasma in presence of an axial magnetic field has been studied. Also, the results of the PIC simulation have been compared with. It is demonstrated that the energy exchange is more effective at the higher values of the magnetic field and the laser pulse gets modified with time.

All these findings are relevant to self-focusing, wakefield acceleration, inertial confinement fusion and space plasmas etc.

In future, we are planning to establish these results with the help of 3D PIC simulation also in order to have better understanding of pulse plasma angular momentum transfer for different pulse shapes and intensities and other related nonlinear phenomena.

SUMMARY

The Chirped Pulse Amplification (CPA) technology has made it possible to have the high intense and ultra-short laser pulses; the nonlinear interaction of such pulses with plasma gives rise to several new phenomena which have not encountered so far in classical physics.

The nonlinearity can be produced either by the relativistic effects or through the modification of plasma by the ponderomotive force of high intense laser pulses. When a high intense ultra-short laser pulse propagates through a plasma, the wakefield is generated due to the high energy electron oscillations in the plasma. The quasistatic magnetic field generation due to various phenomena is one of the most significant nonlinear effects produced in the high intense ultra-short laser pulse plasma interaction.

This thesis is on the nonlinear interaction of an intense ultra-short pulse laser with a magnetized plasma. The research work presented in the thesis has been organized in six chapters.

In chapter 1, an introduction of the thesis and the concepts/phenomena such as Gaussian, Laguerre-Gaussian modes, high-order harmonic generation, attosecond pulses and other related topics have been briefly discussed.

In chapter 2, we have studied the nonlinear interaction of a linearly and circularly polarized Laguerre-Gaussian (LG) laser pulse with an inhomogeneous parabolic plasma channel, especially, the transfer of the orbital angular momentum (OAM) from the photons to the plasma electrons which results in the excitation of the magnetic field.

In a Laguerre-Gaussian laser pulse, the electric field is proportional to the product of the Gaussian function and associated Laguerre polynomial ($L_p^{|l|}$) and has an azimuthal angular dependence of exp ($\pm \iota |l| \varphi$), where $|l|$ and p are azimuthal and radial mode indices respectively. These modes are the eigen modes of the angular momentum operator carrying an angular momentum equal to $|l| \hbar$. Since the momentum has an azimuthal component, there is a finite longitudinal angular momentum of the laser pulse along the direction of propagation and is

proportional to ± |l|. The factor exp ± (ι |l| φ) is responsible for the plasma vorticity imparting the helicoidal motion to the photons.

We have used the Proca equation and calculated the effective mass of photons in plasma. A theory of interaction of the Laguerre-Gaussian laser beam with plasma is outlined and the governing equations for the transfer of orbital angular momentum and the effective mass of photons in a plasma are derived. The Laguerre-Gaussian laser pulse not only exerts the longitudinal force when it impinges on any dielectric medium but also exerts a transverse force in the radial and the azimuthal directions. The azimuthal force causes a torque on the plasma electrons with a corresponding transfer of the angular momentum from the beam to the plasma electrons leading to the rotation of the plasma electrons. The rotational motions of the electrons constitute a nonlinear current in the axial and the azimuthal directions resulting in the excitation of magnetic field. The interaction of a photon with a spatially structured plasma, e.g., vortex, etc., can be interpreted by an additional mass (effective mass) like term that appears in the Proca-Maxwell equations. The effective mass acquired by the photon in the spatially structured plasma couples with a plasmon to impart orbital angular momentum. The orbital angular momentum component on account of acquiring mass by the photon in a plasma may have significant role in various stimulated scattering processes and the magnetic field generation. The coupling of angular momentum to plasma for the different Laguerre-Gaussian modes (for various |l| values, e.g., |l| = 0, |l| = 1) and their effect on the magnetic field generation is analyzed. The analysis of the generation of magnetic fields B_z and B_φ for the different azimuthal angles and the beam intensities has been carried out.

These results match with the relativistic two dimensional (2D) PIC simulation for the normalized vector potential α (= eA/mc^2) which varies from α = 1.0 to 4.0, where A, c, e and m are vector potential, speed of light, charge and mass of the electron respectively. We have taken the typical set of parameters for a laser pulse, e. g., intensity ranging from 1.0×10^{18} -1.3×10^{19} W/cm^2, central wavelength λ = 1 μm, spot size w_0 = 50 μm and pulse duration 33 fs. We have considered the profile of the plasma density as $n = n_0 \left(1 + \frac{\Delta n}{n_0}\frac{r^2}{r_0^2}\right)$, where the

unperturbed plasma density is $n_0 \approx 10^{19}$ cm^{-3}, r is radial distance and r_0 is the channel radius. The dimensions of the simulation box are 400 × 200 μm^2. The simulation box moves and scans 8000 × 400 cells with five particles per cell.

It has been observed that the generated magnetic field depends on the orbital angular momentum (OAM) transfer and mass correction of a photon in the relativistic limit. The generated magnetic field depends on the Laguerre-Gaussian mode order, laser intensity, azimuthal angle and the relativistic gamma factor. It is found that the generated magnetic field increases with the laser intensity.

The strength of the magnetic field also depends on the polarization state of a laser field. It is shown that the excitation of the magnetic fields for both linearly and circularly polarized laser beams depends on the azimuthal angle. The magnitude of generated magnetic field due to circularly polarized Laguerre-Gaussian beam of higher modes decreases with increasing azimuthal angle and is greater than that of the linearly polarized beam. It is further observed that the magnetic field generated due to the higher Laguerre-Gaussian modes is not quasistatic but changes with the spatial distribution of the plasma.

In chapter 3, the nonlinear interaction of a circularly polarized Gaussian laser pulse with the intensity $I \approx 1.3\times10^{19}$ Wcm^{-2}, central wavelength ≈ 1.0 μm and pulse duration ≈ 33 fs is considered. The laser pulse propagates through a preformed inhomogeneous plasma channel generated by an ultra-relativistic laser pulse ($\alpha \approx 3$). The externally applied magnetic field is taken along the pulse propagation direction, i. e., along z-axis.

The plasma channel profile has been considered to be parabolic. The analysis of short nonparaxial laser pulse in plasma channel has been carried out. The electron energy gain in the wake of the laser pulse at different magnetic field strengths is determined. The effects of magnetic field on the wakefield structure, channel radius and accelerating length have been analyzed.

It has been found that the energy gain increases with increasing magnetic field. However, the result illustrates the variable pattern of the energy gain for different magnetic field strengths. It is predicted that the autoresonance condition is achieved at $\omega_c/\omega_p = 2$, where the energy gain is maximum. The variations of the channel width as a function of magnetic field ratio ω_c/ω_p for different relativistic factors have shown that the channel width decreases with increasing ω_c/ω_p and increases with relativistic gamma factors. This result shows that the laser gets self focused and hence there is a possibility of propagation of an intense short circularly polarized laser pulse over a significant extended distance. Our results match with the relativistic 2D PIC simulation for the laser pulse propagated in the inhomogeneous plasma channel for different values of the magnetic field ranging from $B_0 = 10^3$ T ($\omega_c = 17.8\times10^{13}$ rad/s) to 7×10^3 T ($\omega_c = 12.5\times10^{14}$ rad/s). The dimensions etc of simulation box are same as earlier.

It has been observed that the excited wake has electrostatic as well as electromagnetic nature and thus excitation of the wake in the plasma is nonlocal. The transverse wakefield spectrum for different strengths of magnetic field predicted that the wake has maximum amplitude at $z \approx 270\lambda$, where z and λ are axial location and laser wavelength respectively. The transverse profile of the channel remains stable under variation of applied magnetic field. The longitudinal wakefield profiles for different magnetic field strengths have shown that the wakefield has a maximum amplitude at $z \approx 270\lambda$. We also find that the density perturbation increases with the external magnetic field. The phase of the axial component of the wakefield increases linearly with magnetic field and increases with the relativistic gamma factor and thus the phase shift of electrons with respect to the wakefield could be effectively controlled by an appropriate value of the magnetic field strength.

Since the wake propagates with the group velocity of the laser, the accelerated electrons will eventually outrun the wake and therefore they will slip into the decelerating phase over a distance called the dephasing length. It has been shown that the dephasing length increases linearly up to the ratio $\omega_c/\omega_p \leq 2.5$ and thereafter it becomes almost constant. The results indicate that the decelerating length or the accelerating length can be increased by the external

magnetic field and the relativistic gamma factor. Thus, the dephasing length can be enhanced over the conventional decelerating length by the strong magnetic field. Since the dephasing length increases with decreasing density, hence, the low plasma densities are required for longer acceleration lengths.

In chapter 4, we have presented a simple analytical model for generation of an attosecond pulse from the relativistic oscillating plasma mirror with **E** × **B** effect that leads to the rotation in the oscillating plasma mirror.

The interaction of an ultra-intense ultra-short laser pulse with an optically reflecting metal surface generates a dense plasma that acts as a plasma mirror (PM). These mirrors reflect the main part of the laser pulse and can be used as the active optical elements to manipulate the spatial and temporal properties of the high harmonics. The relativistic PM with **E** × **B** drift leads to the rotation in the oscillating PM. The drift results in a modification in the temporal contrast giving rise to an intense attosecond extreme ultraviolet (XUV) or X-ray pulses of energy in the energy range 1-10 J through nonlinear harmonic upconversion of the laser pulse. However, an intense laser pulse exerts high pressure on the plasma ($\approx$ 5 Gbar for I $\approx 10^{19}$ W/cm^2) that induces a significant motion of the plasma mirror surface, even during a femtosecond laser pulse. This leads to the spatial variation of intensity on the target giving rise to the deformation in the surface of the plasma mirror. Deformation in the relativistic plasma mirror surface in the form of an elliptical curvature can affect the spatial and spectral properties of the reflected beam. This in turn rotates the plasma mirror which could bring a change in spatio-temporal coupling mechanism and the Doppler shift of the reflected laser field. The rotational effects in the plasma mirror further increase the boundary displacement of the electrons and provide greater denting in the plasma electron density surface. As the oscillating surface rotates it creates an additional phase shift and distortion in the field of the reflected harmonic beams. This phase distortion repeats itself with periodicity of the driving laser field leading to the more harmonics of the incident frequency.

The **E** × **B** effect changes the harmonic divergence which could change the pattern of an extended ultra-broadband isolated attosecond pulse spectrum

and repetition rate. We have studied the effect of the rotation on the wavefront of the reflected laser field and the effect of the phase divergence on the generation of the attosecond pulse. The results of the harmonic generation and their dependence on the intensity of incident laser pulse have been presented. Also, the number of harmonics in the reflected laser field increases with the intensity of the incident laser beam. The wave train of the attosecond pulses can be observed when intensity of the laser beam exceeds 10^{18} W/cm^2. It is further found that the rotational effect in relativistic oscillating plasma mirror changes the denting mechanism of the reflected laser field and the phase coherence in the attosecond pulses. The rotational effect of plasma mirror due to $\mathbf{E} \times \mathbf{B}$ changes the phase parameter of the harmonics and increases the value of the focal length of the plasma mirror leading to the high repetition rate for attosecond pulses with increased intensity. It is also observed that the intensity of the attosecond pulses depends on the harmonic phases.

In chapter 5, the effect of magnetic field on the wakefield excitation for high intense ultra-short laser pulse in underdense magnetized plasma is analyzed.

Plasma waves are generated through the displacement of plasma electrons by the ponderomotive force of a laser pulse. Electrons are trapped in large amplitude plasma waves. Under resonant condition, the trapped plasma electrons are accelerated to very high energies over very short distances by the longitudinal electric field of the waves. However, the laser plasma interaction distance is always less than or equal to the vacuum Rayleigh length due to the diffraction of the laser pulse in a plasma and hence eliminates the advantage of ultrahigh gradient acceleration. The higher accelerations can be obtained only by maintaining the higher magnitudes of the wakefield amplitude as well as the laser plasma interaction length.

The relation between the generated electric field and the externally applied magnetic field has been obtained. It is observed that the generation of the wakefield in the plasma due to the variation in the electron density depends on the external magnetic field. The magnitude of the wakefield increases with

magnetic field strength. The energy exchange is more effective at the higher values of the magnetic field. Our results match with the relativistic two dimensional PIC simulation of the propagation of a laser pulse in a magnetized plasma which gives an insight into the wakefield evolution. We use a laser pulse with the same typical set of parameters used earlier.

In conclusion, this thesis presents the study of nonlinear interaction of an intense ultra-short pulse laser with a magnetized plasma, especially, the mechanism of the generation of magnetic field, excitation of the wake and the effect of magnetic field on it and generation of an attosecond pulse. The analytical results obtained agree well to the PIC simulation results. C**hapter 6** summarizes the work presented in the thesis and also the scope for the future work.

Bibliography

[1] N. Kumar and V.K. Tripathi, Phys. Plasmas 14, 103108 (2007).

[2] S.C. Wilks, W.L. Kruer, M. Tabak and A.B. Langdon, Phys. Rev. Lett. 69, 1383 (1992).

[3] S.V. Bulanov, N.M. Naumova and F. Pagoraro, Phys. Plasmas 1, 745 (1994).

[4] T. Baeva, S. Gordienko and A. Pukhov, Phys Rev. E 74, 046404 (2006).

[5] S.L. Anisimov and B.S. Lukyanchuk, Phys. Usp. 45, 293 (2002).

[6] T. Tajima and J.M. Dawson, Phys Rev. Lett. 43, 267 (1979).

[7] X. Wang *et al*., Phys Rev. Lett. 84(23), 5324-5327 (2000).

[8] M.E. Dieckmann, B. Aliasson and P.K. Shukla, Phys Rev. E 70, 036401 (2004).

[9] Sandeep kumar and Hitendra K. Malik, J. Plasma Phys., 72(6), 983-987 (2006).

[10] K. Schmid *et al.*, Phys Rev. Lett. 102,124801 (2009).

[11] V.B. Krasovitskii, V.G. Dorofeenko, V.I. Sotnikov and B. S. Bauer, Phys. Plasmas 11(2), 724-742 (2004).

[12] A. Sharma and V.K. Tripathi, Phys. Plasmas 16, 043103 (2009).

[13] M. Kumar and V. K. Tripathi, Phys Plasmas 17, 053103 (2010).

[14] P. Polynkin, M. Kolesik, J.V .Moloney, G.A. Siviloglou, D.N. Christodoulides, science 324,229-232 (2009).

[15] A. Proulx, A. Talebpour, S. Petit, S.L. Chin, Opt. Commun. 174, 305 (2000).

[16] C. D'Amico *et al*., Phys. Rev. Lett. 98, 235002 (2007).

[17] J. Kasparian *et al*., Opt.Express, 16, 5757 (2008).

[18] E. Esarey, P. Sprangle and J. Krall, IEEE J. Quant. Elect. 33(11), 1879-1914 (1997).

[19] A. Modena, Z. Najmudin, A. E. Dangor, C. E. Clayton, K. A. Marsh, C. Joshi, V. Malka, C.B. Darrow and C. Danson, IEEE Trans.Plasma Sci., 24,289 (1996).

[20] C.E. Max, J. Arons and A.B. Langdon, Phys. Rev. Lett., 33, 209 (1974).

[21] M.S. Wei *et al*., Phys Rev. Lett. 93, 155003 (2004).

[22] A. Pukhov *et al.*, Phys. Plasmas 6, 2847 (1999).

[23] G.D. Tsakiris, C. Gahn and V.K. Tripathi, Phys. Plasmas 7, 3017 (2000).

[24] P.K. Shukla, Phys. Scr. 52, 73 (1994).

[25] G. Berdin and J. Lundberg, Phys. Rev. E 57, 7041 (1998).

[26] U. Wagner *et al*., Phys Rev. E 70, 026401 (2004).

[27] A. Pukhov and J. Meyer-terVehn, Phys Rev. Lett. 76, 3975 (1996).

[28] Z. Najmudin *et al*., Phys Rev. Lett. 87, 215004 (2001).

[29] B. Qiao, X.T. He, S. Zhu, C.Y. Zheng, Phys. Plasmas 12,083102 (2005).

[30] H.Y. Niu, X.T. He, B. Qiao and C.T. Zhou, Laser Part. Beam 26, 51 (2008).

[31] C.Y. Zheng, X.T. He and S.P. Zhu, Phys. Plasmas 12,044505 (2005).

[32] B. Qiao, S. Zhu, C.Y. Zheng and X.T. He, Phys. Plasmas 12, 053104 (2005).

[33] C. Grebogi and C.S. Liu, Phys. Fluids 23, 1330 (1980).

[34] H.C. Barr *et al*., Phys. Fluids 27, 2730 (1984).

[35] H. Liu, X.T. He and S.G. Chen, Phys. Rev. E 69, 066409 (2004).

[36] W. Yu *et al*., Phys. Rev. E 66, 036406 (2003).

[37] X. He *et al*., Phys. Rev. E 68, 056501(2003).

[38] C.S. Liu and V.K. Tripathi, Phys. Plasmas 12, 043103 (2005).

[39] A. Sharma and V.K. Tripathi, Phys. Plasmas 12, 093109 (2005).

[40] R. Singh and V.K. Tripathi, Phys. Plasmas 16, 052108 (2009).

[41] L. Allen, M.J. Padgett and M. Babiker, Prog. Opt.34, 291 (1999).

[42] S. Franke-Arnold, L. Allen and M.J. Padgett, Laser and Photon. Rev. 2, 299 (2008).

[43] J.P. Torres and L. Torner, Eds., *Twisted Photons* (Willey-VCH, 2011).

[44] J. Zhou, J. Peatross, M.M. Murnane, H.C. Kapteny and Christov, Phys. Rev. Lett. 76, 752 (1996).

[45] G. Mourou, Z. Chang, Maksimhuk, J. Nees, S.V. Bulanov, V. Y. Bychenkov, T.Z. Esirkepov, N.M. Naumova, F. Pegorero and H. Ruhl, Plasma Phys. Rep. 28, 12 (2002).

[46] S.V. Bulanov, T.Z. Esirkepov, N.M. Naumova and I.V. Sokolov, Phys. Rev. E. 67, 016405 (2003)

[47] I.P. Christov, M.M. Murnane and H.C. Kapteyn, Phys. Rev. Lett. 78, 1251-1254 (1997).

[48] M.V. Frolov, N.L. Manakov, T.S. Sarantseva and A.F. Starace, J. Phys. B: At. Mol. Opt. Phys. 42, 035601 (2009).

[49] F. Quéré, C. Thaury, P. Monot, S. Dobosz and P. Martin, Phys. Rev. Lett. 96, 125004 (2006).

[50] K. Eidmann, T. Kawachi, A. Marcinkevicius, R. Bartlome, G.D. Tsakiris and K. Witte, Phys. Rev. E 72, 036413 (2005).

[51] H. Yang, J. Zhang, J. Zhang, L.Z. Zhao, Y.J. Li, H. Teng, Y.T. Li, Z.H. Wang, Z.L. Chen, Z.Y. Wei, J.X. Ma, W. Yu and Z.M. Sheng, Phys. Rev. E 67, 015401 (2003).

[52] G. Zeng, B. Shen, W. Yu and Z. Xu, Phys Plasmas 3(11), 4220-4224 (1996).

[53] L. Allen and M.J. Padgett, Optics Communications 184, 67-71 (2000).

[54] L. Allen, M.W. Beijersbergen, R.J.C. Spreeuw and J.P. Woerdman, Phys. Rev. A 45(11), 8185-8189 (1992).

[55] O. Buneman, Phys. Rev. 115, 503-17 (1959).

[56] J.M. Dawson, Phys. Fluids 5, 445-59 (1962).

[57] C.K. Birdsall and A.B. Langdon, Plasma Physics via Computer Simulation, Mc-Graw Hill, Newyork (1985).

[58] R.W. Hockney and J.W. Eastwood, Computer Simulation Using Particles, Mc-Graw Hill, Newyork (1981).

[59] V. Vehadi and M. Surendra, Comput. Phys. Commun. 87, 179-98 (1995).

[60] J.P. Verboncoeur, A.B. Langdon and N.T. Gladd, Comput. Phys. Commun. 87, 199-211 (1995).

[61] J. Yoo *et al*., Comp. Phys. Commun. 177, 93-94 (2007).

[62] Y. Chen and S.E.Parker, Phys. Plasmas 16, 052305 (2009).

[63] S. Morsed, T. M. Antonsen and J. P. Palastro, Phys. Plasmas 17, 063106 (2010).

[64] N. Nasari, S. G. Bochkarev and W. Rozemus, Phys. Plasmas 17, 033107 (2010).

[65] D. Strickland and G. Mourou, Opt. Commun. 56, 219 (1985).

[66] M.D. Perry and G. Mourou, Science 264, 917 (1994).

[67] P. Gibbon and E. Forster, Plasma Phys. Control Fusion 38, 769 (1996).

[68] S. Backus, C.G. Durfee III, M.M. Murname and H.C. Kapteyn, Rev. Sci. Instrum. 69, 1207 (1998).

[69] Shalom Eliezer, The Interaction of High Power Lasers with Plasmas, Institute of Physics Publishing, Bristol (2002).

[70] Enrique J. Galvez, Gaussian Beams, Colgate University (2009), (http://www.colgate.edu/portaldata/imagegallerywww/98c178dc-7e5b-4a04-b0a1-a73abf7f13d5/imagegallery/gaussian-beams.pdf).

[71] A. T. O'Neil, I. MacVicar, L. Allen, M. J. Padgett, Phys. Rev. Lett. 88, 053601 (2002).

[72] N. B. Simpson, K. Dholakia, L. Allen, M.J. Padgett, Opt. Lett. 22, 52-54 (1997).

[73] C. Winterfeldt and G. Gerber, Rev. Mod. Phys.80, 117 (2008).

[74] D.V. Linde, Applied Phys. B 68, 315-319 (1999).

[75] S. Nuzzo, M. Zarcone, G. Ferrante and S. Basile, Laser and Particle beams 18, 483-487 (2000).

[76] P. Villoresi, P. Barbiero, L. Poletto, M. Nisoli, G. Cerullo, E. Priori, S. Stagira, C. De, R. Bruzzese and C. Altucci, Laser and Particle beams 19, 41-45 (2001).

[77] A. Pukhov, Rep. Prog. Phys. 65, R1-R55 (2002).

[78] M. Nisoli, G. Sansone, S. Stagira, S.D. Silverstri, C. Vozzi, M. Pascolini, L. Poletto, P. Villoresi and G. Tondello, Phys. Rev. Lett 91, 2139051-54 (2003).

[79] I.B. Foldes, G. Kocsis, E. Racz, S. Szatmari and G. Veres, Laser and Particle beams 21, 517-521 (2003).

[80] T. Baeva, S. Gordienko and A. Pukhov, Phys. Rev. E 74, 046404(1-11) (2006).

[81] A.S. Pirozkov, S.V. Bulanov, T.Z. Esirkepov, A.S. Mori and H. Daido, Phys. Plasmas 13, 013107(1-12) (2006).

[82] R.A. Ganeev, Physics –Uspekhi. 52, 55-77 (2009).

[83] U. Teubner and P. Gibbon, Rev. Mod. Phys. 81, 445-479 (2009).

[84] B. Dromey, M. Zepf, A. Gopal, K.Lancaster, M.S. Wei, K. Krushelnick, M. Tatarakis, N. Vakakis, S. Moustaizis, R. Kodama, M. Tampo, C. Stoeckl, R. Clarke, H. Habara, D. Neely, S. Karsch and P. Norreys, Nature Phys. 2, 456 (2006).

[85] R. Lichters, J. Meyer-ter-vehn and A. Pukhov, Phys. Plasmas 3, 3425-3437 (1996).

[86] D. Von der Linde and K. Rzazewski, Applied Phys. B 63, 499 (1996).

[87] Vinita Jain, An analytical and numerical investigation of generation of high order optical Harmonics as a result of the interaction of intense laser pulses with solid surfaces/gaseous medium (Doctoral Thesis), University of Kota, Kota, India (2014).

[88] G.D. Tsakiris, K. Eidmann, J. Meyer-ter-vehn and F. Krausz, New J. Phys. 8, 19 (2006).

[89] A.S. Pirozhkov, S.V. Bulanov, T.Z. Esirkepov, M. Mori, A. Sagisaka and H. Daido, Phys. Rev. Lett. A 349, 256-263 (2006).

[90] T.Z. Esirkepov, S.V. Bulanov, M. Kando, A.S. Pirozhkhov and A.G. Zhidkov, Proc. of Spie vol. 7359, 735909-1-735909-11 (2009).

[91] S.V. Bulanov, T.Z. Esirkepov, M. Kando, J.K. Koga, A.S. Pirozhkov, N.N. Rosanov and A.G. Zhidkov, AIP Conf. 1032, 221 (2011).

[92] V.A. Vshivkov, N.M. Naumova, F. Pegarero and S.V. Bulanov, Phys. Plasmas 5, 2727-2741 (1998).

[93] S.V. Bulanov, T.Z. Esirkepov and T. Tajima, Phys. Rev. Lett. 91, 085001 (2003).

[94] S. Gordienko, A. Pukhov, O. Shorokhov and T. Baeva, Phys. Rev. Lett. 93, 115002 (2004).

[95] S.V. Bulanov, I.N. Inovenkov, V.I. Kirsanov, N.M. Naumova and A.S. Sakharov, Phys. Fluids B 4, 1935-1942 (1992).

[96] A.D. Bandrauk, F. Krausz and A.F. Starace, New J. Phys. 10, 025004 (2008).

[97] E. Goulielmakis, M. Uiberackar, R. Kienberger, A. Baltuska, V. Yakovlev, A. Scrinzi, T. Westerwalbesloh, U. Kleineberg, U. Heinzmann, M. Drescher and F. Krausz, Science 305, 1267 (2004).

[98] A.L. Cavalieri, N. Müllar, T. Uphues, V.S. Yakovlev, A. Baltuska, B. Horvath, B. Schmidt, L. Blumel, R. Hozwarth, S. Hendel, M. Drescher, U. Kleineberg, P.M. Echenique, R. Kienberger, F. Krausz and U. Heizmann, Nature 449, 1029 (2007).

[99] M. Uiberacker, T. Uphues, M. Schultze, A.J. Verhoef, V. Yakovlov, M.F. Kling, J. Rauschenberger, N.M. Kabachnik, H. Schröder, M. Lezius, K.L. Kompa, H.G. Mullar, M.J.J. Vrakking, S. Hendel, U. Kleineberg, U. Heinzmann, M. Drescher and F. Krausz, Nature 446, 627 (2007).

[100] M. Lewenstein, P. Balcou, M. Y. Ivanov, A. L'Huillier and P.B. Corkum, Phys. Rev. A 49, 2117 (1994).

[101] P.B. Corkum, Phys. Rev. Lett. 71, 1994 (1993).

[102] T.W. Hansch, Opt. Commun. 80, 71 (1990).

[103] S. Kohlweyer, G.D. Tsakiris, C.G. Wahlstrom, C. Tillman and L. Mercer, Opt. Commun. 117, 431 (1995).

[104] P.A. Norreys, M. Zepf, S. Moustaizis, A.P. Fews, J. Zhang, P. Lee, M. Bakarezos, C.N. Danson, A. Dyson, P. Gibbon, P. Loukakos, D. Neely, F.N. Walsh, J.S. Wark and D.A.E., Phys. Rev. Lett. 76, 1832 (1996).

[105] M. Zepf, G.D. Tsakiris, G. Pretzler, I. Watts, D.M. Chambers, P.A. Norreys, U. Andiel, A.E. Dangor, K. Eidmann, C. Gahn, A. Machacek, J.S. Wark and K. Witte, Phys. Rev. E 58, R5253 (1998).

[106] P. Sprangle, E. Esarey and A. Ting, Phys. Rev. A 41, 4463 (1990).

[107] Philip Sprangle and Eric Esarey, 67, 2021 (1991).

[108] E. Esarey, P. Sprangle, J. Krall and A. Ting, IEEE Trans. Plasma Sci. 24, pp.252-288 (1996).

[109] P. Yadav, D.N. Gupta and K. Avinash, Discharges and Electrical Insulation in Vacuum (ISDEIV), International Symposium, pp. 657-659 (2014).

[110] H. Hamster, A. Sullivan, S. Gordon, W. White and R.W. Falcone, Phys. Rev. Lett. 71, 2725 (1993).

[111] K.P. Singh, D.N. Gupta, V.K. Tripathi and V.L. Gupta, Phys. Rev. E 69, 046406 (2004).

[112] Palavi Jha, Akanksha Saroch, Rohit Kumar Mishra and Ajay Kumar Upadhyay, Phys. Rev. ST Accel. Beams 15, 081301 (2012).

[113] M. Moshkelgosha and R. Sadighi-Bonabi, IEEE Trans. Plasma Sci. 41, pp. 1570-1574 (2013).

[114] B.S. Sharma, Archna Jain, N.K. Jaiman, D.N. Gupta, D.G. Jang, H. Suk and V.V. Kulagin, Phys. Plasmas 21, 023108 (2014).

[115] D.A. Tidman and L.L. Burton, Phys. Rev. Lett. 37, 1397 (1976).

[116] Partrick Mora and Rene Pellat, Phys. Fluids 24, 2219 (1981).

[117] R.J. Kingham and A.R. Bell, Phys. Rev. Lett. 88, 045004 (2002).

[118] Bin Qiao, X.T. He and Shao-ping Zhu, Phys. Plasmas 13, 053106 (2006).

[119] N. Naseri, V. Yu. Bychenkov and W. Rozmus, Phys. Plasmas 17, 083109 (2010).

[120] Bhuvana Srinivasan and Xian-Zhu Tang, Phys. Plasmas 19, 082703 (2012).

[121] Hong-bo Cai, Wei Yu, Shao-ping Zhu and Cang-tao Zhou, Phys. Rev. E. 76, 036403 (2007).

[122] J. Briand, V. Adrian, M. E. Tamer, A. Gomes, Y. Quemener, J.P. Dinguirard and J.C. Kieffer, Phys. Rev. Lett.54, 38 (1985).

[123] P. Auvray, J. Larour, S.D. Moustaizis, 2009 IET European Pulsed Power Conference, pp. 1-8 (2009).

[124] R.N. Sudan, Phys. Rev. Lett. 70, 3075 (1993).

[125] V.K. Tripathi and C.S. Liu, Phys. Plasmas 1, 990 (1994).

[126] Z.M. Sheng and J. Meyer-ter-Vehn, Phys. Rev. E 54, 1833 (1996).

[127] L.M. Gorbunov and R.R. Ramazashvili, J. Exp. Theor. Phys. 87, 461 (1998).

[128] M.G. Haines, Phys. Rev. Lett. 87, 135005 (2001).

[129] E. Kolka, S. Eliezer and Y. Pais, Phys. Lett. A 180, 132 (1993).

[130] M. Borghesi, A.J. MacKinnon, A.R. Bell, R. Gaillard and O. Willi, Phys Rev. Lett. 81, 112 (1998).

[131] L.M. Gorbunov, P. Mora and T.M. Antonsen, Phys. Plasmas 4, 4358 (1997).

[132] F. Tamburini, A. Sponselli, B. Thide and J. T. Mendonca, EPL 90, 45001 (2010).

[133] S. Ali, J.R. Davies and J.T. Mendonca, 37th EPS conference on Plasma Physics P5.211, 1952 (2010).

[134] Enrique J. Galvez, Am. J. Phys. 74, 355 (2006).

[135] P.W. Anderson, Phys. Rev. 130, 439 (1963).

[136] R.A.Beth, Phys. Rev. 50, 115 (1936).

[137] E. Esarey, C. B. Schroeder and W. P. Leemans, Rev. Mod. Phys. 81, 1229(2009).

[138] P. M. Nilson, S. P. D. Mangles, L. Willingale, M. C. Kaluza, A. G. R. Thomas, M. Tatarakis, R. J. Clarke, K. L. Lancaster, S. Karsch, J. Schreiber, Z. Najmudin, A. E. Dangor and K. Krushelnick, New J. Phys. 12, 045014 (2010).

[139] A. Pukhov and J. Meyer-ter-Vehn, Appl. Phys. B 74, 355 (2002).

[140] S. P. D. Mangles, C. D. Murphy, Z. Najmudin, A. G. R. Thomas, J. L. Collier, A. E. Dangor, E. J. Divall, P. S. Foster, J. G. Gallacher, C. J. Hooker, D. A. Jaroszynski, A. J. Langley, W. B. Mori, P. A. Norreys, F. S. Tsung, R. Viskup, B. R. Walton and K. Krushelnick, Nature 431, 535(2004).

[141] J. Faure, Y. Glinec, A. Pukhov, S. Kiselev, S. Gordienko, E. Lefebvre, J.-P. Rousseau, F. Burgy and V. Malka, Nature 431, 541 (2004).

[142] W. P. Leemans, B. Nagler, A. J. Gonsalves, C. Tóth, K. Nakamura, C. G. R. Geddes, E. Esarey, C. B. Schroeder and S. M. Hooker, Nat. Phys. 2,696 (2006).

[143] C. S. Liu and V. K. Tripathi, Phys. Rev. E 54, 4098 (1996).

[144] H. M. Milchberg, C. G. Durfee and J. Lynch, J. Opt. Soc. Am. B 12, 731(1995).

[145] D. N. Gupta and Chang-Mo Ryu, Phys. Plasmas 12, 053103 (2005).

[146] A. Sharma and V. K. Tripathi, Phys. Plasmas 12, 093109 (2005).

[147] R. P. Sharma and P. K. Chauhan, Phys. Plasmas 15, 063103 (2008).

[148] P. Gibbon, IEEE J. Quantum Electron. 33, 1915 (1997).

[149] H. Yang, J. Zhang, W. Yu, Y. J. Li and Z. Y. Wei, Phys. Rev. E 65,016406 (2001).

[150] C. Deutsch, H. Furukawa, K. Mima, M. Murakami and K. Nishihara, Phys. Rev. Lett. 77, 2483 (1996).

[151] E. Esarey, J. Krall and P. Sprangle, Phys. Rev. Lett. 72, 2887 (1994).

[152] W. Lu, M. Tzoufras, C. Joshi, F. S. Tsung, W. B. Mori, J. Vieira, R. A. Fonseca and L. O. Silva, Phys. Rev. ST Accel. Beams 10, 061301(2007).

[153] S. Kneip, S. R. Nagel, S. F. Martins, S. P. D. Mangles, C. Bellei, O. Chekhlov, R. J. Clarke, N. Delerue, E. J. Divall, G. Doucas, K. Ertel, F. Fiuza, R. Fonseca, P. Foster, S. J. Hawkes, C. J. Hooker, K. Krushelnick, W. B. Mori, C. A. J. Palmer, K. T. Phuoc, P. P. Rajeev, J. Schreiber, M. J. V. Streeter, D. Urner, J. Vieira, L. O. Silva and Z. Najmudin, Phys. Rev. Lett. 103, 035002 (2009).

[154] A. B. Borisov, A. V. Borovskiy, A. M. Prokhorov, O. B. Shiryae, X. M. Shi, T. S. Luk, A. McPherson, J. C. Solem, K. Boyer and C. K. Rhodes, Phys. Rev. Lett. 68, 2309 (1992).

[155] G. S. Sarkisov, V. Y. Bychenkov, V. N. Novikov, V. T. Tikhonchuk, A. Maksimchuk, S.-Y. Chen, R. Wagner, G. Mourou and D. Umstadter, Phys. Rev. E 59, 7042 (1999).

[156] J. E. Ralph, K. A. Marsh, A. E. Pak, W. Lu, C. E. Clayton, F. Fang, W. B. Mori and C. Joshi, Phys. Rev. Lett. 102, 175003 (2009).

[157] A. G. R. Thomas, S. P. D. Mangles, Z. Najmudin, M. C. Kaluza, C. D. Murphy, M. C. Kaluza and K. Krushelnick, Phys. Rev. Lett. 98, 054802 (2007).

[158] A. G. R. Thomas, S. P. D. Mangles, C. D. Murphy, A. E. Dangor, P. S. Foster, J. G. Gallacher, D. A. Jaroszynski, C. Kamperidis, K. Krushelnick, K. L. Lancaster, P. A. Norreys, R. Viskup and Z. Najmudin, Plasma Phys. Controlled Fusion 51, 024010 (2009).

[159] B. M. Luther, Y. Wang, M. C. Marconi, J. L. A. Chilla, M. A. Larotonda and J. J. Rocca, Phys. Rev. Lett. 92, 235002 (2004).

[160] C. G. R. Geddes, C. Toth, J. van Tilborg, E. Esarey, C. B. Schroeder, J. Cary and W. P. Leema, Phys. Rev. Lett. 95, 145002 (2005).

[161] A. J. Gonsalves, K. Nakamura, C. Lin, J. Osterhoff, S. Shiraishi, C. B. Schroeder, C. G. R. Geddes, C. Toth, E. Esarey and W. P. Leemans, Phys. Plasmas 17, 056706 (2010).

[162] C. G. R. Geddes, C. Toth, J. van Tilborg, E. Esarey, C. B. Schroeder, D. Bruhwiler, C. Nieter, J. Cary and W. P. Leemans, Nature 431, 538 (2004).

[163] E. Esarey, C. B. Schroeder, B. A. Shadwick, J. S. Wurtele and W. P. Leemans, Phys. Rev. Lett. 84, 3081 (2000).

[164] R. F. Hubbard, D. Kaganovich, B. Hafizi, C. I. Moore, P. Sprangle, A. Ting and A. Zigler, Phys. Rev. E 63, 036502 (2001).

[165] R. F. Hubbard, P. Sprangle and B. Hafizi, IEEE Trans. Plasma Sci. 28, 1159 (2000).

[166] P. Sprangle, E. Esarey, J. Krall and G. Joyce, Phys. Rev. Lett. 69, 2200 (1992).

[167] G. Shvets, J. S. Wurtele, T. C. Chiou and T. Katsouleas, IEEE Trans. Plasma Sci. 24, 351 (1996).

[168] C. G. R. Geddes, C. Toth, J. van Tilborg, E. Esarey, C. B. Schroeder, D. Bruhwiler, J. Cary and W. P. Leemans, AIP Conf. Proc. 737, 521 (2004).

[169] T. P. A. Ibbotson, N. Bourgeois, T. P. Rowlands-Rees, L. S. Caballero, S. I. Bajlekov, P. A. Walker, S. Kneip, S. P. D. Mangles, S. R. Nagel, C. A. J. Palmer, N. Delerue, G. Doucas, D. Urner, O. Chekhlov, R. J. Clarke, E. Divall, K. Ertel, P. S. Foster, S. J. Hawkes, C. J. Hooker, B. Parry, P. P. Rajeev, M. J. V. Streeter and S. M. Hooker, Phys. Rev. ST Accel. Beams 13, 031301 (2010).

[170] H. Y. Wang, C. Lin, Z. M. Sheng, B. Liu, S. Zhao, Z. Y. Guo, Y. R. Lu, X. T. He, J. E. Chen and X. Q. Yan, Phys. Rev. Lett. 107, 265002 (2011).

[171] A. Friou, E. Lefebvre and L. Gremillet, Phys. Plasmas 19, 022704 (2012).

[172] T. M. Antonsen and P. Mora, Phys. Fluids B 5, 1440 (1993).

[173] W. B. Mori and C. D. Decker, Phys. Rev. Lett. 72, 1482 (1994).

[174] Y. Ehrlich, C. Cohen, A. Zigler, J. Krall, P. Sprangle and E. Esarey, Phys. Rev. Lett. 77, 4186 (1996).

[175] P. Sprangle, J. Krall and E. Esarey, Phys. Rev. Lett. 73, 3544 (1994).

[176] N. E. Andreev, V. I. Kirsanov and L. M. Gorbunov, Phys. Plasmas 2, 2573 (1995).

[177] D. N. Gupta, Mamta Singh, B. S. Sharma, D. G. Jang and H. Suk, Simulation on laser wakefield generation in a parabolic magnetic- plasma channel, Proc. 5th Int. Particle Accelerator Conf. (IPAC'14), Dresden, Germany, paper TUPME075, pp 1528-1530, (2014).

[178] E. Esarey and W. P. Leemans, Phys. Rev. E 59, 1082 (1999).

[179] V. I. Karpman and H. Washimi, J. Plasma Phys. 18, 173 (1977).

[180] T. Katsouleas, Phys. Rev. A 33, 2056 (1986).

[181] W. P. Leemans, C. W. Siders, E. Esarey, N. E. Andreev, G. Shvets and W. B. Mori, IEEE Trans. Plasma Sci. 24, 331 (1996).

[182] W. P. Leemans, P. Volfbeyn, K. Z. Guo, S. Chattopadhyay, C. B. Schroeder, B. A. Shadwick, P. B. Lee, J. S. Wurtele and E. Esarey, Phys. Plasmas 5, 1615 (1998).

[183] R. Sadighi-Bonabi and M. Etehadi-Abari, Phys. Plasmas 17, 032101 (2010).

[184] C. Thaury and F. Quéére, J. Phys. B 43, 213001 (2010).

[185] R. Licheters, J. Meyer-ter-Vehn, A. Pukhov, Phys. Rev. E 3, 3425 (1996).

[186] A.A. Gonoskov, A.V. Korzhimanvo, A.V. Kim, M. Marklund and A.M. Sergeev, Phys. Rev. E 84, 046403 (2011).

[187] B.Dromey et al., Nat. Phys. 2, 456 (2006).

[188] Michael Chini, Kun Zhao and Zenghu Chang, Nat. Photonics 8, 178-186 (2014).

[189] B. Lehnert, Dynamics of charged particles, Interscience Publishers, New York (1964).

[190] H. Vincenti , S. Monchoc , S. Kahaly , G. Bonnaud, P. Martin and F. Quéré, Nat. Communication (2014).

[191] P. Chen, J. M. Dawson, R. W. Huff and T. Katsouleas, Phys. Rev. Lett. 54, 693 (1985).

[192] J. B. Rosenzweig, D. B. Cline, B. Cole, H. Figueroa, W. Gai, R. Konecny, J. Norem, P. Schoessow and J. Simpson, Phys. Rev. Lett. 61, 98 (1988).

[193] J. B. Rosenzweig, P. Schoessow, B. Cole, W. Gai, R. Koneey, J. Nora and J. Simpson, Phys. Rev. A 39, 1586 (1989).

[194] K. Nakajima *et al.*, Phys. Rev. Lett. 74, 4428 (1995).

[195] J. F. Drake, P. K. Kaw, Y. C. Lee, G. Schmidt, C. S. Liu and M. N. Osenbluth, Phys. Fluids 17, 778 (1974).

[196] K. Estabrook and W. L. Kruer, Phys. Fluids 26, 1892 (1983).

[197] K. Estabrook, W. L. Kruer and B.F. Lasinki, Phys. Rev. Lett.45, 1399 (1980).

[198] D. W. Forslund, J. M. Kindel and E. L. Lindman, Phys. Rev. Lett. 30, 739 (1973).

[199] B. Sokri and A. R. Niknam, Phys. Plasmas 13, 113110 (2006).

[200] M. Y. Yu, Wei Yu, Z. Y. Chen et al., Phys. Plasma 16, 2468 (2003).

[201] A. Maksimchuk, S. Reed, S.S. Bulanor et al., Phys. Plasma 15, 056703 (2008).

[202] Z. Najmuddin, K. Krushellnick, E. L. Clark and C. Joshi, Journal of Modern Optics 50, 673 (2003).

[203] A. R. Niknam, M. Hashemzadeh, and B. Shokri, Phys. Plasma 16, 033105 (2009).

[204] J. R. Penano, B. Hafizi, P. Sprangle, R. F. Hubbard and A. Ting, Physical Review E 66, 036402 (2002).

[205] W. -T. Chen, T. -Y. Chien, C. -H. Lee et al., Phy. Rev. Lett. 92, 075003 (2004).

[206] Khaleel Hassoon, Hyder Salih and V.K. Tripathi, Phys. Scr. 80, 065501 (2009).

[207] B. S. Sharma and Arachna Jain, Phys. Scr. 87, 025501(2013).

IOP Conf. Series: Journal of Physics: Conf. Series **836** (2017) 012022 doi:10.1088/1742-6596/836/1/012022

Attosecond pulse generation from relativistic plasma mirror

B S Sharma[1,a], R C Dhabhai[1], A Sharma[2] and N K Jaiman[3]

[1] Department of Physics, Govt College Kota, Kota-324001, India.
[2] Department of Electrical Engineering and Photonics, IIT Kanpur-208016.
[3]Department of Pure and Applied Physics, University of Kota, Kota-324010, India.

E-mail: [a)]bs_phy@yahoo.com

Abstract. When an intense relativistic short laser pulse incident on an optically polished surface, it generates a high density plasma that acts as a relativistic plasma mirror. As this mirror reflects the intense laser field, its space time characterization changes due to high nonlinear response of the field. This lead to the phase variation both temporally and spatially that could affect the generation of high harmonics of the laser and attosecond pulses. The present theoretical study address the issues of the intensity dependent space-time characteristics on the generation of attosecond pulses from relativistic plasma mirror.

1. Introduction

The interaction of ultrashort-ultraintense laser ($I \geq 10^{20} W/m^2$) pulse with an optically reflected metal surface generates a dense plasma that acts as a plasma mirror(PM). These mirrors specularly reflect the main part of the laser pulse and can be used as an active optical elements to manipulate the spatial and temporal properties of the high harmonics. The modification in the temporal contrast lead to generate an intense attosecond extreme ultraviolet(XUV) or X-ray pulses of energy in the range 1-10 J through nonlinear harmonic up-conversion of the laser pulse. However, pressure exerted by the laser pulse deformed the PM surface non-uniformly This results in the rotation of the PM that effect the spatial and temporal contrast of the reflected laser field and the high harmonics.

PMs are routinely used at moderate light intensities ($10^{14} - 10^{16} W/cm^2$) as ultrafast optical switches, to enhance the temporal contrast of the femtosecond lasers. For intensities $I \geq 10^{16} W/cm^2$, nonlinear response of the PMs to the laser field results in sub-cycle temporal modulations of the reflected field , associated to the high harmonic generation in its spectrum (HHG).These harmonics generated through various mechanism are associated in the time domain to the attosecond pulses.For lasers with intensity $\geq 10^{18} W/cm^2$, the key HHG results in the relativistic oscillating mirror where the laser driven oscillation of the plasma surface induces a periodic Doppler effect on the reflected laser field [1, 2, 3, 4, 5, 8],which can result in harmonic orders of several thousands. In these high intensity applications, laser field exerts such a high pressure on the plasma ($\cong 5 Gbar for I \approx 10^{19} W/cm^2$) that it induces a significant motion of the PM surface, even during a femtosecond laser pulse. This leads spatial variation of intensity on the target and hence the deformation in the surface of the PM.

Our present work is based on the spatiotemporal coupling (STC) to the generation of isolated attosecond pulse. We consider deformation in the relativistic plasma mirror surface in the form of an elliptical curvature-which can affect the spatial and spectral properties of the reflected beam.

The intensity dependence of the harmonic spectrum and the attosecond pulse are described in section 2. Conclusions are presented in section 3.

2. Intensity Dependence

It is observed that the wave train of the attoseond pulses can be observed when intensity of the laser beam exceeds to $10^{18} W/cm^2$. It is further concluded that the rotation effect in relativistic oscillating plasma mirror change the denting mechanism of the reflected laser field and phase coherence in the attosecond pulses. The rotation effect of plasma mirror due to $E \times B$ changes the phase parameter of the harmonics and increases the value of f_h. This leads high repetition rate for attosecond pulses with increased intensity.

When an electromagnetic wave reflected from an oscillating mirror, its frequency spectrum extended to high frequency range and the wave breaks-up in the short waves. In relativistic oscillating mirror, harmonics of much higher frequency are generated. The reflected wave's electric field from the oscillating mirror in a reflection time $t' = t - x(t)/c$ is given as

$$\mathbf{E_r} = -\frac{\mathbf{1}}{\mathbf{c}} \frac{\partial \mathbf{A_L}(\mathbf{t}', \mathbf{x}')}{\partial \mathbf{t}'} \tag{1}$$

where x' and t' are the position and time of the reflected waves in observer's frame. The oscillating mirror model implies that the tangential components of the vector potential are zero at the mirror surface. The component of reflected electric field from the oscillating plasma surface will be parallel to incident electromagnetic wave. As a result of it,if the oscillating mirror moves with $\gamma_L \gg 1$ towards the laser pulse with oscillating frequency ω_{osc} and electric field $E_{\|}$, and duration τ_L, the reflected electric field of the n^{th} harmonics will be given as

$$E_r \propto n\gamma_L^2 E_l \tag{2}$$

and the pulse duration will be

$$\tau_L' \propto \frac{\tau_L}{n\gamma_L^2} \tag{3}$$

The Fourier spectrum of the electric field of reflected beam at position x' and time t' is

$$E_r(\Omega_r) = \frac{mc\omega}{e\sqrt{2\pi}} \int_{-\infty}^{\infty} \mathbf{a_L}(\mathbf{t}', \mathbf{x}') \times \exp -\iota\omega_L t' - \iota\omega_L (x'/c) \exp(-\iota\phi_r) \tag{4}$$

where

$$t' - x(t')/c = t \tag{5}$$

and ϕ_r is the phase of reflected wave and is given by

$$\phi_r = \int_0^u \Omega_r(u) du = \omega_L [2t'(u) - u] \tag{6}$$

where $u = t' - x'(t')/c$ and spatial position x' and time t' and t'(u) can be obtained from the equation

$$t'(u) = u + x'(t'(u))/c \tag{7}$$

Differentiating above equation, we obtain

$$\phi_r' = \omega_L \frac{1 + \beta'(u)}{1 - \beta'(u)} \tag{8}$$

where $\beta'(u) = dx'(u)/cdt'$ is the mirror velocity normalized by c. Using both power law and the exponential decay parts, and properties of Array's function to analyze the spectrum modulation due to the $E \times B$ effect, we use Eq.(4-6) in Eq(2) to obtain

$$E_r = \left(\frac{\omega_L}{\Omega'_r n}\right)^{5/2} \exp\left(\frac{-16\sqrt{5}\Omega'_r}{5\sqrt{n^3}\omega_L\omega_p^{3/2}}\right) \times Re\frac{\exp(\iota\Omega'_r t - \iota\psi'_r)}{10\sqrt{2}/(5\sqrt{n^3}\omega_p) + \iota\omega_L} \tag{9}$$

where $\Omega'_r = \Omega_r + \Omega_{rot}$.
The amplitude of these reflected pulses decreases fast when Ω_r grows. However, the pulse duration does not depend on Ω_r. Since the fundamental frequency grows as Ω_r, the pulses obtained with an above cut-off filter are filled with electric field oscillations. We use Eq.(9) to obtain the intensity of n^{th} harmonics as

$$I_{rn} \propto \left(\frac{\omega_L}{\Omega'_r n}\right)^5 \exp\left(\frac{-32\sqrt{5}\Omega'^{5/2}_r}{5\sqrt{n^3}\omega_L\omega_p^{3/2}}\right) \times \frac{\left(n^3\omega_p^2 - \omega_L^2\right)}{8\omega_p^2} \tag{10}$$

The intensity of the reflected pulses decreases with higher harmonics and plasma frequency. However the pulse repetition rate increases when Ω_r grows. It is observed that the intensity of the attosecond pulses depend on the harmonic phases. if v_r is the ultra relativistic velocity of the reflected electric field of a particular harmonics at time $t'(u)$, than the maximum relativistic factor will be given as

$$\gamma_{max} = \frac{1}{\sqrt{1 - \frac{v_r(t'(u))^2}{c^2}}} \tag{11}$$

Consequently, for the surface γ factor during a relativistic spike, the highest harmonic will be generated over the time period

$$\Delta t \approx \frac{1}{\omega_L\gamma_{max}^3} \approx \frac{1}{\omega_L n_{cr}^{3/2}} \tag{12}$$

where n_{cr} is the critical density of plasma surface.
For this duration the reflected fields move with ultra-relativistic velocity in the direction of the emitted radiation. The intensity variation over this time interval for n^{th} harmonic can be written as

$$I_n \propto \left(\frac{n_{cr}}{n^3\Omega'_r}\right)^5 \exp\left(\frac{-32\sqrt{5}\Omega'^{5/2}_r}{5\sqrt{n^3}\omega_L\omega_p^{3/2}}\right) \times \frac{\left(n^3\omega_p^2 - \omega_L^2\right)}{8\omega_p^2} \tag{13}$$

Eq.(13) shows a theoretical result of temporal structure of the intensity of attosecond pulse trains produced on plasma mirrors. The harmonic spectra associated with a train of attosecond pulses

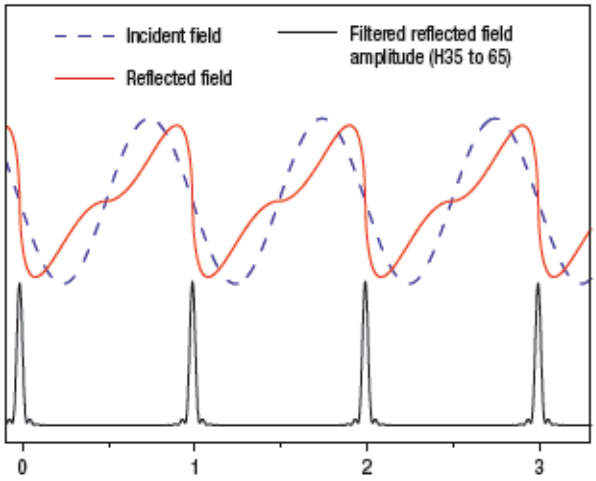

Figure 1. Harmonic spectra from plasma mirror

for different intensities is shown in the figure(1) The harmonic divergence θ_n of n^{th} harmonics is given

$$\theta_n^2 = \left(\frac{\lambda_n}{\pi w_n}\right)^2 + \left(\frac{\lambda_n}{\pi w_n}\right)^2 (n\phi_L)^2$$
$$\theta_n = \theta_n^0 \sqrt{1 + (n\phi_L)^2} \tag{14}$$

where $\theta_n^0 = \lambda_n/\pi w_n$ is the harmonic divergence for the source size w_n, in the absence of PM curvature and rotational effect due to $E \times B$.

3. Conclusions

We have presented a simple analytical model for the generation of the attosecond pulse from the relativistic oscillating plasma mirror with $E \times B$ effect that leads rotation in the oscillating plasma mirror. The $E \times B$ effect changes the harmonic divergence which could change the pattern of extended ultra-broadband isolated attosecond pulse spectrum and repetition rate. We have also addressed the temporal characterization of the reflected electric field from plasma mirror, with temporal resolution going down to the attosecond range. It is further observed that the number of harmonics in the reflected laser field increases with intensity of the incident laser beam and electron plasma density.

References

[1] Thaury C.and F.Quéére, J. Phys. B, **43**,213001(2010).
[2] Licheters R., Meyer-ter-Vehn J., Pukhov.A, Phys. Rev. E **3**,3425(1996).
[3] Baeva T., Gordienko S., Pukhov A., Phys. Rev. **74**,046404(2006).
[4] Gonoskov,A.A., Korzhimanvo A.V.,Kim A.V.,Marklund M. and Sergeev A.M, Phys. Rev. E **84**, 046403(2011).
[5] Dromey B. *et al* . Nat. Phys. **2**,456(2006).
[6] Lehnert B., Dynamics of charged particles (New York: Interscience Publishers, (1964).
[7] Vincenti H. , Monchoc S. , Kahaly S. , Bonnaud G., Martin Ph. and Quéré F., Nat. Communication, (2014).
[8] Chini Michae, Zhao Kun and Chang Zenghu Nat. Photonics, **8**,178-186(2014).

IOP Conf. Series: Journal of Physics: Conf. Series **836** (2017) 012031 doi:10.1088/1742-6596/836/1/012031

Semi-Classical theory of Nonlinear interaction of circularly polarized optical vortex beam with plasma channel

B.S.Sharma[1,a], R.C. Dhabhai[1], A.Sharma [2], and N.K.Jaiman[3]

[1] Department of Physics, Govt. College Kota, Kota-324001, India.
[2]Department of Electrical Engineering, Indian Institute of Technology Kanpur, Kanpur-208016,India.
[3]Department of Pure and Applied Physics, University of Kota, Kota-324010, India.

E-mail: [a)]bs_phy@yahoo.com

Abstract. A semiclassical approach of nonlinear interaction of intense circularly polarized optical vortex Laguerre-Gaussian (LG) beam modes with a plasma channel is analyzed theoretically and numerically. We study an exchange of angular momentum between the vortex beam and plasma channel. The transfer of angular momentum and the generated magnetic field are calculated. We have observed that both the generated magnetic field and angular momentum transfer depend on beam mode, intensity, and the polarization state of beam mode.

1. Introduction

It is now well understood that light beam with helical phase front carries orbital angular momentum (OAM) along their direction of propagation in addition to spin angular momentum that describe their polarization. Photons in a light beam have spin $\sigma_z\hbar$, where $\sigma_z = \pm 1$ refers to the left and right circular polarization states respectively. For linear polarized beam,$\sigma_z = 0$ in the direction of propagation. In polarized light, spin of photons align in the direction of propagation and contribute to a net spin angular momentum. The helical wavefront exists when the wave vectors spiral around the beam axis and constitute to the OAM [1].

The current understanding of transfer of spin and orbital angular momentum suggest that any beam with an amplitude distribution $u(r, \phi, z) = u_0(r, \phi, z) \exp \iota\ell\phi$, carries angular momentum about the beam optical axis. These laser beams carry total angular momentum much greater than that associated with the circularly polarized Gaussian laser beam. This problem was addressed recently in plasma physics where its effect on various phenomenon of laser-plasma interaction were taken into account. Cormier-Michel *et al* [6] and Stupakov *et al* [7] has recently studied the excitation of quasi-magnetic field due to the interaction of LG higher modes with plasma. Ali *et al* [4] pointed out that a linearly polarized beam in OAM state could also generate magnetic field in plasma. The propagation of higher laser modes in plasma channel was studied by York *et al* and has explained direct acceleration of electrons in a corrugated plasma channel [8]. Nesterov *et al* [9] has analyzed the importance of transfer of OAM by CPVBs to inhomogeneous plasma. Andersen *et al* [10] has demonstrated the coherent transfer of the orbital angular momentum of a photon to an atom in quantized units of $\hbar$ using a 2-photon stimulated Raman process with Laguerre-Gaussian beams to generate an atomic vortex state in the Bose-Einstein condensation of sodium atoms. Kyosuke Sakai *et al* [11] has recently studied the excitation of multipole plasmons by an optical vortex beam and explained the transfer of angular momentum between photons and plasmons.

In the present work, we have proposed a model that allow transfer of OAM of LG_p^ℓ modes and magnetic field generation in plasma channel at relativistic limit. We have theoretically examined

that a normal incident CPVBs with a specific azimuthal mode can excite the magnetic field and couple to the plasmons of spiraling plasma electrons which results into the transfer of angular momentum of CPVBs to plasma electrons. We have demonstrated that the transfer of OAM and magnetic field generation depend on the mode and the polarization states of the vortex beam.

The paper is organized as follows: In section 2, the governing Equations of the angular momentum transferred to plasma electrons is derived using semiclassical approach. The conclusions are presented in section 3.

2. The Model

The OAM of LG_p^ℓ modes impart helicoidal motion to the plasma electrons and form vortices like structure in a plane perpendicular to the direction of beam propagation. Evolution of these structures result into the excitation of asymmetric quasi-static magnetic fields which depend on the order of beam mode and an axial phase velocity $v_{ph,z} = c(1 - 1/k(\partial\theta_{lp}/\partial z))$. Hence, the average torque received by electrons per unit volume also be depend on the beam mode.
An Equation for the average rate of change of angular momentum of the electrons per unit volume is given as

$$m_e n \frac{d(rv_\phi)}{dt} = -enr(E_\phi + v_z B_r - v_r B_z) - \frac{dM_z}{dt}, \tag{1}$$

where E_ϕ is the azimuthal electric field, B_r and B_z are respectively radial and axial magnetic fields. And M_z is the axial angular momentum density of photons per unit wavelength. The term $m_e v_\phi r$ is the angular momentum of electrons in the z direction and dM_z/dt refers to the pressure like term of quasi-static magnetic field. The relation for E_ϕ is given by

$$E_\phi \simeq \frac{-1}{e\omega L}\frac{\partial I}{\partial r} \tag{2}$$

We observed that the total angular momentum is non-zero for the plane polarized light ($\sigma_z = 0$). Following [**?**] and Faraday's law, the time derivative of the generated axial magnetic field is given as

$$\frac{\partial B_z}{\partial t} = \frac{1}{enr_{ch}^3 L}\frac{d}{dt}\left(\frac{1}{2\omega c}\frac{\partial}{\partial r}\Big(r\frac{\partial I(r,z,\phi)}{\partial r}\Big)\times (\ell_{pz} + p \pm \sigma_z)\hbar\cos\theta_{lpz}\right). \tag{3}$$

Integrating Eq.(6) within the time limit t=0 and t and assuming that the damping rate of the laser energy over this period is almost negligible, the generated magnetic field in plasma channel turns out to be of the following form

$$B_z = \frac{\eta(r)}{enr_{ch}^3\omega Lc}\left(\frac{\partial}{\partial r}\left(r\frac{\partial I}{\partial r}\right)\times (\ell_{pz} + p \pm \sigma_z)\hbar\cos\theta_{lpz}\right), \tag{4}$$

It is important to note here that for linearly polarized light B_z is nonzero.

To estimate B_z in Mega Gauss (MG), we assume $\partial/\partial r = 1/r_{ch}$. Thus Eq.(7) can be written as

$$B_z = \eta(r)\left(\frac{\lambda^2}{r_{ch}^2}\right)\left(\frac{n_c}{n}\right)\left[(\ell_{pz} + p \pm \sigma_z)\hbar\cos\theta_{lpz}\right]\left(\frac{I(r,\phi)\lambda^2}{7.3\times 10^{22} W m^{-2}(\mu m)^2}\right), \tag{5}$$

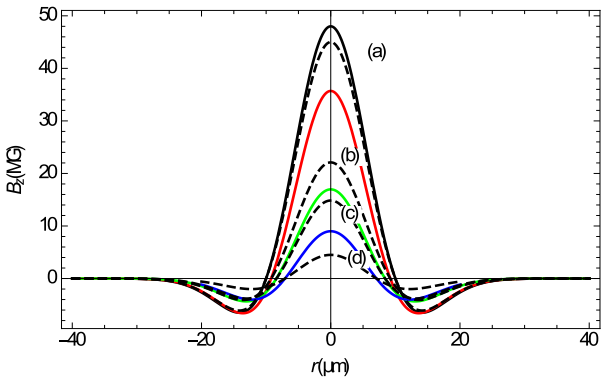

Figure 1. The generated axial magnetic field B_z of mode LG_0^1 at different values of the phase shifts $(a)\theta_{lpz} = 0(b)\theta_{lpz} = \pi/3$ (c) $\theta_{lpz} = \pi/4$ and (d)$\theta_{lpz} = \pi/6$. The continuous and dashed lines respectively refers to the variation right circular and left circular polarized beam.

where λ is wavelength of the laser beam, n_c is critical density (which is approximately $1.1 \times 10^{15} m^{-3}$).

The intensity profile of LG beam modes in the focal plane (z=0) is given as

$$I(r,\phi) = I_0 \frac{(-1)^{2\ell} p!}{(\ell+p)!} \exp(-\rho^2) \times (\sqrt{2}\rho)^{2\ell} \times L_p^{\ell}(\rho^2) \cos^2(\theta_{lpz}), \tag{6}$$

where $I_0 = a_0^2(4\omega^2/k^2\pi^2)(1/(w_0^2(1+\delta_{0\ell}^2))$ is the maximum intensity of LG beam. It is clear from Eqs.(8-9) that the generated axial magnetic field depends on the beam mode, plasma density, channel width, the phase shift θ_{lpz}, and polarization state of the beam. The generated axial magnetic field for the mode $LG_0^0(\ell = 0, p = 0)$ can be obtained via Eq.(8) and Eq.(9) and read as

$$B_z \approx \frac{I_0 \eta(r) \cos\theta_{pl}}{e n r_{ch}^3 \omega c} \left[\sigma_z \hbar \cos\theta_{lpz} \exp(-\rho^2) \right], \tag{7}$$

for $LG_0^1(\ell_{pz} \approx 1$ and $p = 0)$, we have

$$B_z \approx \frac{I_0 \eta(r)}{e n r_{ch}^3 \omega c} \left[(1 \pm \sigma_z)(1-\rho^2) \hbar \cos\theta_{lpz} \right] \exp(-\rho^2), \tag{8}$$

Figure 1 shows the variation of the generated magnetic field as a function of r for different values of beam phase transfer and polarization states for right and circularly polarized beams of LG_0^1 mode. The continuous and broken curves show the variation for right circular and left circular polarized beams respectively. We have observed that the magnitude of the generated magnetic field for right circular polarized beam mode is higher than the left circularly polarized beam.

Figure 2 shows the variation of an angular momentum density M_z of the plasma electrons as a function of r for the different beam modes LG_0^0, LG_0^1, and LG_0^2. It is observed that the angular momentum density transfer increases with increasing mode order and also depends on the polarization state of the beam modes.

3. Conclusion

In the present work, we have examined theoretically and numerically the effect of polarization states on the transfer of angular momentum and the generated magnetic field of CPVBs in the

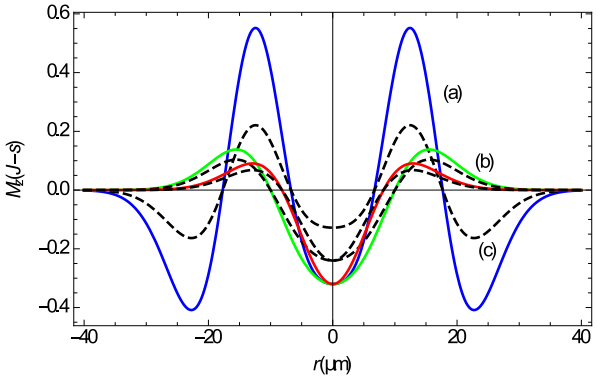

Figure 2. The variation of orbital angular momentum density M_z as a function of r for different modes (a)LG_0^2(b)LG_0^1, and (c) LG_0^0..The continuous and broken curve refers to the variation of right circular and left circular polarized beam respectively.

plasma channel using a semi-classical approach. We note that both the generated magnetic field and the angular momentum transfer depends on the LG_p^ℓ mode order, polarization state of beam and the intensity of beam. The present study may be useful in various context of laser plasma interaction such as in angular dependent wake fields, various laser acceleration schemes, laser fusion research, generation of electron vortex beams and in photonic science.

References

[1] Allen L, Beijersbergen M W, Spreeuw R J C and Woerdman J P 1992 Orbital angular momentum of light and the transformation of Laguerre-Gaussian laser modes *Phys. Rev. A* **45** 8185
[2] Marrucci L, Manzo C and Paparo D 2006 Optical spin-to-orbital angular momentum conversion in inhomogeneous anisotropic media *Phys. Rev. Lett.* **96** 1639305
[3] Leach J, Padgett M J, Barnett S M, Franke-Arnold S and Courtial J 2002 Measuring the orbital angular momentum of a single photon *Phys. Rev. Lett.* **88** 257901
[4] Ali S, Davies J R, and Mendonca J T 2010 Inverse Faraday Effect with Linearly Polarized Laser Pulses *Phys. Rev. Lett.* **105** 035001
[5] Mendonca J T, Thide B, Bergman J E S, Mohamadi S M, Eliasson B, Baan W and Then H 2008 Photon orbital angular momentum in a plasma vortex *arXiv:0804.3221v3.* Najmudin Z, Tatarakis M, Pukhov A, Clark E L, Clarke R J, Dangor A E, Faure J, Malka V, Neely D, Santala M I K and Krushelnick K 2001 Measurements of the Inverse Faraday Effect from Relativistic Laser Interactions with an Underdense Plasma *Phys. Rev. Lett.* **87** 215004
[6] Cormier-Michel E, Esarey E, Geddes C G R,Schroeder C B, Paul K, Mullowney P J, Cary J R and Leemans W P 2011 Control of focusing fields in laser-plasma accelerators using higher-order modes *Phys. Rev. ST Accel. Beams* **14** 031303.
[7] Stupakov G V and Zolotorev M S 2001 Ponderomotive Laser Acceleration and Focusing in Vacuum for Generation of Attosecond Electron Bunches *Phys. Rev. Lett.* **86** 5274.
[8] York A G, Milchberg H M, Plastro J P, and Antonsen T M 2008 Direct Acceleration of Electrons in a Corrugated Plasma Waveguide *Phys. Rev. Lett.* **100** 195001
[9] Nesterov A N and Niziev V.G 2000 Laser beams with axially symmetric polarization *Journal of Phys. D:Applied Phys.* **33** 1817.
[10] Andersen M F, Ryu C, Clade Pierre, Natarajan, Vazir A, Helmerson K, and Phillips W D 2006 Quantized Rotation of Atoms from Photons with Orbital Angular Momentum *Phys. Rev. Lett.* **97** 170406.
[11] Sakai Kyosuke, Nomura Kensuke, Yamamoto Takeaki, and Sasaki Keiji 2015 Excitation of multipole plasmons by optical vortex beams *Scientific Reports* **5** Article 8431 .